

DEVELOPMENT & OPTIMIZATION OF A RULE-BASED ENERGY  
MANAGEMENT STRATEGY FOR FUEL ECONOMY IMPROVEMENT  
IN HYBRID ELECTRIC VEHICLES

A Dissertation

Presented in Partial Fulfillment of the Requirements for the

Degree of Doctorate of Philosophy

with a

Major in Mechanical Engineering

in the

College of Graduate Studies

University of Idaho

by

Mostafa Asfoor

JULY 2014

Major Professor: Steven W. Beyerlein, Ph.D.

## Authorization to Submit Thesis

This dissertation of Mostafa Asfoor, submitted for the degree of Doctorate of Philosophy with a major in Mechanical Engineering and titled "Development & Optimization of A Rule-Based Energy Management Strategy for Fuel Economy Improvement in Hybrid Electric Vehicles," has been reviewed in final form. Permission, as indicated by the signatures and dates given below, is now granted to submit final copies to the College of Graduate Studies for Approval.

Major

Professor: \_\_\_\_\_ Date: \_\_\_\_\_  
Steven W. Beyerlein, Ph.D.

Committee

Members: \_\_\_\_\_ Date: \_\_\_\_\_  
Edwin M. Odom, Ph.D., P.E.

\_\_\_\_\_ Date: \_\_\_\_\_  
Karen Den Braven, Ph.D.

\_\_\_\_\_ Date: \_\_\_\_\_  
Ahmed Abdel-Rahim, Ph.D., P.E.

Department

Administrator: \_\_\_\_\_ Date: \_\_\_\_\_  
John Crepeau, Ph.D., P.E.

Discipline's

College Dean: \_\_\_\_\_ Date: \_\_\_\_\_  
Larry Stauffer, Ph.D., P.E.

Final Approval and Acceptance by the College of Graduate Studies:

\_\_\_\_\_ Date: \_\_\_\_\_  
Jie Chen, Ph.D.

## Abstract

The gradual decline of oil reserves and the increasing demand for energy over the past decades has resulted in automotive manufacturers seeking alternative solutions to reduce the dependency on fossil-based fuels for transportation. A viable technology that enables significant improvements in the overall energy conversion efficiencies is the hybridization of conventional vehicle drive systems.

This dissertation builds on prior hybrid powertrain development at the University of Idaho. Advanced vehicle models of a passenger car with a conventional powertrain and three different hybrid powertrain layouts were created using GT-Suite. These different powertrain models were validated against a variety of standard driving cycles. The overall fuel economy, energy consumption, and losses were monitored, and a comprehensive energy analysis was performed to compare energy sources and sinks. The GT-Suite model was then used to predict the formula hybrid SAE vehicle performance. Inputs to this model were a numerically predicted engine performance map, an electric motor torque curve, vehicle geometry, and road load parameters derived from a roll-down test. In this case study, the vehicle had a supervisory controller that followed a rule-based energy management strategy to insure a proper power split during hybrid mode operation. The supervisory controller parameters were optimized using discrete grid optimization method that minimized the total amount of fuel consumed during a specific urban driving cycle with an average speed of approximately 30 [mph]. More than a 15% increase in fuel economy was achieved by adding supervisory control and managing power split. The vehicle configuration without the supervisory controller displayed a fuel economy of 25 [mpg]. With the supervisory controller this rose to 29 [mpg].

Wider applications of this research include hybrid vehicle controller designs that can extend the range and survivability of military combat platforms. Furthermore, the GT-Suite model can be easily accommodated to simulate propulsion systems that store regenerative power when braking, making it available for acceleration and off-road maneuvering.

## Acknowledgments

First of all, I'd like to thank my advisor Prof. Beyerlein for his continued support, encouragement and guidance. He helped shape the course of my research and spent countless hours editing and improving my analysis. It was a great pleasure and I feel incredibly fortunate for the opportunity to work with you. Also, I am grateful to Prof. Karen Den Braven, Prof. Edwin Odom and Dr. Ahmed Abdel-Rahim who have contributed to this work with numerous suggestions. I feel very privileged to have had you on my committee.

I would like to acknowledge the Egyptian Ministry of Defense for the extended financial support to this work. A special word of thanks goes to the GT Senior Engineer Mike Arnett who greatly illuminated valuable aspects to me about GT-Suite modeling.

I also feel fortunate for having met during my school years many people that had a profound impact on my life: my elementary school teacher, Enaam, who gave an injection of confidence to a shy kid; my science teacher in middle school, Mohamed Farghaly, who made me appreciate the beauty of mathematics and science; my master's thesis advisor, Prof. Mohamed Elhadad, who has always believed in me, and my formal Egyptian advisor, Dr. Sharaf, who made me a rational person and transmitted me his love for knowledge.

I truly enjoyed the times I spent with many great friends whom I got the chance to meet with over the years here at Idaho Engineering Works. Kysen Palmer, Dan Mathew and Curtis Bower to name only a few. Special thanks to all the University of Idaho Formula Hybrid SAE team generations. Dan Cordon, Sam Wos, Chris Eacker, & Rory Lilley. Thanks to Amos Bartlow & David Arnett for code development and data acquisition setup.

I saved the last spot for the persons who deserve this degree as much as I do. They raised me up and helped me through my whole life. Mom & Dad, I cannot thank you enough for everything, for being always so close to me despite the geographical distance. I could not make it without your support.

*I would like to thank my wife for her endless support and taking care of our kids, Mazen and Yara, while pursuing my*

*Ph.D.*

# Table of Contents

Authorization to Submit Thesis.....	ii
Abstract.....	iii
Acknowledgments.....	iv
Table of Contents.....	vi
List of Figures .....	x
List of Tables .....	xiv
Abbreviations.....	xv
Nomenclature .....	xvii
Chapter 1. Introduction .....	1
1.1 Overview .....	1
1.2 Problem Statement .....	4
1.3 Research Objectives .....	4
1.4 Dissertation Organization .....	5
Chapter 2. Literature Review.....	6
2.1 Introduction.....	6
2.2 History of Hybrid Electric Vehicle.....	6
2.3 Hybrid Electric Vehicle Architectures.....	10
2.3.1 Series Hybrid Configuration .....	12
2.3.2 Parallel Hybrid Configuration.....	15
2.3.3 Series-Parallel Hybrid Configuration.....	17
2.3.4 Complex Hybrid Configuration .....	19
2.4 Control Levels in HEVs.....	20
2.4.1 Supervisory Control Level .....	21
2.4.2 Component Control Level .....	22
2.5 Vehicle Energy Management .....	23
2.5.1 Energy Management in Hybrid Electric Vehicles.....	24
2.5.2 Rule-Based Energy Management Strategies .....	25
2.5.3 Optimization-Based Energy Management Strategies.....	27

2.5.4	Energy Management as an Optimization Problem.....	28
2.6	HEV Powertrain Modeling and Simulation.....	30
2.6.1	General Concepts.....	31
2.6.2	Forward facing models .....	32
2.6.3	Backward facing models .....	34
2.6.4	Modeling Tools.....	35
2.7	Driving Cycles .....	37
2.7.1	United States (US) light-duty vehicle driving cycles .....	38
2.7.2	European Union light-duty vehicle driving cycle .....	39
2.8	Summary .....	40
Chapter 3.	HEV Powertrain Modeling .....	41
3.1	Overview .....	41
3.2	Conventional ICE Vehicle Model .....	43
3.3	Hybrid Vehicle Model.....	46
3.3.1	Series HEV Model.....	48
3.3.2	Parallel HEV Model .....	49
3.3.3	Series-Parallel HEV Model .....	50
3.3.4	Selection of Driving Cycles .....	54
3.4	Model Governing Equations.....	54
3.5	Simulation Results.....	56
3.5.1	FTP Driving Cycle Outputs.....	56
3.5.2	HWY Driving Cycle Outputs.....	59
3.5.3	US06 Driving Cycle Outputs .....	62
3.5.4	NEDC Driving Cycle Outputs .....	65
Chapter 4.	Model Results & Validation .....	68
4.1	Overview .....	68
4.2	Fuel Economy .....	68
4.3	Energy Analysis.....	70
4.3.1	Energy Depleted and Stored.....	71

4.3.2	Energy Losses .....	77
Chapter 5.	University of Idaho FHSAE Case Study.....	82
5.1	Overview .....	82
5.2	Current Developments.....	83
5.3	Platform Design & Implementation .....	84
5.3.1	Current Powertrain Development .....	85
5.3.2	High Voltage Battery Pack.....	86
5.3.3	Supervisory Controller Implementation .....	88
5.3.4	Hybrid Mode Energy Management .....	90
5.3.5	Drive-by-Wire.....	91
5.4	Case Study Model.....	93
5.4.1	Engine Performance Map .....	94
5.4.2	Traction Motor Torque Characteristics .....	95
5.4.3	Battery Pack Model.....	96
5.4.4	Supervisory Control Strategy .....	96
5.4.5	Model Driving Cycle .....	98
Chapter 6.	Supervisory Controller Optimization .....	100
6.1	GT-Suite Optimization Tools .....	100
6.1.1	Direct Optimization Tool.....	100
6.1.2	Design of Experiments Tool .....	101
6.2	Case Study Optimization .....	102
6.2.1	Discrete-Grid Optimization Set-up.....	102
6.2.2	Optimization Problem Outputs.....	105
6.3	Model Outputs .....	107
6.3.1	Without A Supervisory Controller.....	107
6.3.2	With Optimized EMS.....	109
6.3.3	With EMS & Regenerative Energy .....	110
6.3.4	Model Results Comparative Analysis.....	112
6.3.5	Energy Analysis .....	113



6.4	Testing .....	114
Chapter 7.	Conclusions and Recommendations.....	116
7.1	Conclusions.....	116
7.2	Recommendations .....	118
References	.....	120
Appendix A:	Vehicle Specifications.....	127
Appendix B:	Supervisory Controller Code.....	130

## List of Figures

Figure 1: Energy Management Control Role in HEV .....	3
Figure 2: Ferdinand Porsche’s First Hybrid Vehicle (1900) .....	7
Figure 3: Classifications of HEVs. ....	12
Figure 4: Series Hybrid Configuration .....	14
Figure 5: Series Hybrid Operating Modes .....	14
Figure 6: Parallel Hybrid Configuration.....	15
Figure 7: Parallel Hybrid Operating Modes.....	17
Figure 8: Series-Parallel Hybrid Configuration.....	18
Figure 9: Control Levels in a HEV .....	20
Figure 10: HEV Energy Management Control Strategies.....	25
Figure 11: The FTP-75 Driving Cycle.....	38
Figure 12: The Highway Fuel Economy (HWY) Driving Cycle .....	39
Figure 13: The New European Driving Cycle (NEDC) .....	39
Figure 14: ICE Performance Map .....	44
Figure 15: Conventional Power Plant Model .....	45
Figure 16: Series HEV Power Plant Model .....	49
Figure 17: Parallel HEV Power Plant Model.....	50
Figure 18: Series-Parallel HEV Power Plant Model .....	51
Figure 19: Series Mode Strategy .....	53
Figure 20: Parallel Mode Strategy.....	53
Figure 21: Conventional Vehicle Undergoing FTP Driving Cycle.....	57
Figure 22: Series HEV Undergoing FTP Driving Cycle.....	57
Figure 23: Parallel HEV Undergoing FTP Driving Cycle .....	57
Figure 24: Series-Parallel HEV Undergoing FTP Driving Cycle .....	57
Figure 25: FTP: Power Demand and Power Production in Conventional Vehicle .....	58
Figure 26: FTP: Power Demand and Power Production in Series HEV .....	58
Figure 27: FTP: Power Demand and Power Production in Parallel HEV .....	58

Figure 28: FTP: Power Demand and Power Production in Series-Parallel HEV .....	58
Figure 29: Conventional Vehicle Undergoing HWY Driving Cycle.....	60
Figure 30: Series HEV Undergoing HWY Driving Cycle.....	60
Figure 31: Parallel HEV Undergoing HWY Driving Cycle .....	60
Figure 32: Series-Parallel HEV Undergoing HWY Driving Cycle .....	60
Figure 33: HWY: Power Demand and Power Production in Conventional Vehicle .....	61
Figure 34: HWY: Power Demand and Power Production in Series HEV .....	61
Figure 35: HWY: Power Demand and Power Production in Parallel HEV .....	61
Figure 36: HWY: Power Demand and Power Production in Series-Parallel HEV .....	61
Figure 37: Conventional Vehicle Undergoing US06 Driving Cycle .....	63
Figure 38: Series HEV Undergoing US06 Driving Cycle .....	63
Figure 39: Parallel HEV Undergoing US06 Driving Cycle.....	63
Figure 40: Series-Parallel HEV Undergoing US06 Driving Cycle.....	63
Figure 41: US06: Power Demand and Power Production in Conventional Vehicle.....	64
Figure 42: US06: Power Demand and Power Production in Series HEV.....	64
Figure 43: US06: Power Demand and Power Production in Parallel HEV .....	64
Figure 44: US06: Power Demand and Power Production in Series-Parallel HEV .....	64
Figure 45: Conventional Vehicle Undergoing NEDC Driving Cycle .....	66
Figure 46: Series HEV Undergoing NEDC Driving Cycle .....	66
Figure 47: Parallel HEV Undergoing NEDC Driving Cycle .....	66
Figure 48: Series-Parallel HEV Undergoing NEDC Driving Cycle .....	66
Figure 49: NEDC: Power Demand and Power Production in Conventional Vehicle .....	67
Figure 50: NEDC: Power Demand and Power Production in Series HEV .....	67
Figure 51: NEDC: Power Demand and Power Production in Parallel HEV.....	67
Figure 52: NEDC: Power Demand and Power Production in Series-Parallel HEV .....	67
Figure 53: Fuel Economy of Different Powertrain models .....	69
Figure 54: FTP: Depleted ICE Energy in Conventional Vehicle.....	72
Figure 55: FTP: Depleted and Stored Energy in Series HEV .....	72
Figure 56: FTP: Depleted and Stored Energy in Parallel HEV.....	72

Figure 57: FTP: Depleted and Stored Energy in Series-Parallel HEV.....	72
Figure 58: HWY: Depleted ICE Energy in Conventional Vehicle .....	73
Figure 59: HWY: Depleted and Stored Energy in Series HEV.....	73
Figure 60: HWY: Depleted and Stored Energy in Parallel HEV .....	73
Figure 61: HWY: Depleted and Stored Energy in Series-Parallel .....	73
Figure 62: US06: Depleted ICE Energy in Conventional Vehicle .....	75
Figure 63: US06: Depleted and Stored Energy in Series HEV .....	75
Figure 64: US06: Depleted and Stored Energy in Parallel HEV .....	75
Figure 65: US06: Depleted and Stored Energy in Series-Parallel HEV .....	75
Figure 66: NEDC: Depleted ICE Energy in Conventional Vehicle .....	76
Figure 67: NEDC: Depleted and Stored Energy in Series HEV.....	76
Figure 68: NEDC: Depleted and Stored Energy in Parallel HEV .....	76
Figure 69: NEDC: Depleted and Stored Energy in Series-Parallel HEV .....	76
Figure 70: Energy Losses during FTP Driving Cycle .....	78
Figure 71: Energy Losses during HWY Driving Cycle .....	79
Figure 72: Energy Losses during US06 Driving Cycle .....	80
Figure 73: Energy Losses during NEDC Driving Cycle.....	81
Figure 74: UI First Pre-transmission Parallel Hybrid Powertrain Render .....	85
Figure 75: UI New Post-transmission Parallel Hybrid Powertrain Render .....	86
Figure 76: The Battery Pack .....	86
Figure 77: EMUS Current Sensor.....	87
Figure 78: Current Sensor Location in the Battery Box .....	87
Figure 79: Supervisory Controller / Vehicle Mode Selection Layout.....	89
Figure 80: Overall Supervisory Controller Layout.....	90
Figure 81: Throttle Pedal Potentiometers Render.....	92
Figure 82: Post-transmission Powertrain Model .....	93
Figure 83: YZ250F Predicted BSFC map .....	94
Figure 84: Traction Motor Torque Curve .....	95
Figure 85: Supervisory Control Strategy Model.....	96

Figure 86: Mode Selector Inputs/Outputs Variables .....	97
Figure 87: Mode Selector Actions and Conditions .....	98
Figure 88: ARTEMIS Urban Driving Cycle .....	99
Figure 89: Discrete-Grid Optimization Method Set-up .....	103
Figure 90: Independent Variable Parameters Ranges .....	103
Figure 91: Optimization Problem Constraints Set-up .....	104
Figure 92: Optimum VehSpdThresh Parameter Value .....	105
Figure 93: Optimum Power Split % Parameter Value .....	105
Figure 94: Optimum Min. Battery SOC Parameter Value .....	106
Figure 95: Optimum Fuel Consumption Amount .....	106
Figure 96: Power Required & Supplied Without EMS .....	108
Figure 97: Power Supplied During the First 200 sec. Without EMS .....	108
Figure 98: Avg. Fuel Consumption Rate & Avg. Battery SOC, Without EMS .....	108
Figure 99: Power Required & Supplied Using Optimized EMS Factors .....	109
Figure 100: Power Supplied During the First 200 sec., Optimized EMS .....	109
Figure 101: Avg. Fuel Consumption Rate & Avg. Battery SOC , Optimized EMS .....	110
Figure 102: Power Required, Supplied, & Regenerated in Optimized EMS & Regen .....	111
Figure 103: Power Supplied During the First 200 sec., Optimized EMS & Regen .....	111
Figure 104: Avg. Fuel Consumption Rate & Avg. Battery SOC, Optimized EMS & Regen ...	111
Figure 105: Without EMS .....	113
Figure 106: With Optimized EMS .....	113
Figure 107: With EMS & Regen .....	113
Figure 108: Testing Track .....	114

## List of Tables

Table 1: Comparison of Different Driving Test Cycles .....	40
Table 2: Conventional ICE and Vehicle Specifications .....	45
Table 3: HEV Model Specifications .....	47
Table 4: Different Models Fuel Economy Outputs .....	69
Table 5: Different Models Energy Analysis Outputs .....	70
Table 6: Different Powertrain Energy Losses in [KJ] during Different Driving Cycles .....	77
Table 7: Lynch D135RAGS DC Traction Motor Specifications .....	95
Table 8: Model Driving Cycle Characteristics .....	99
Table 9: Comparative Analysis of Model Results .....	112
Table 10: Comparison of ICE only Test Results With and Without DBW System .....	115
Table 11: Endurance Event Energy Allotment .....	118
Table 12: Endurance Event Energy Predictions .....	118

## Abbreviations

ADVISOR	Advanced Vehicle Simulator
BATT	Battery
BMS	Battery Management System
BSFC	Brake Specific Fuel Consumption
CAE	Computer Aided Engineering
CAFE	Corporate Average Fuel Economy
DDP	Deterministic Dynamic Programming
DOE	Department of Energy
DP	Dynamic Programming
EESS	Electrical Energy Storage System
EM	Electric Motor
EV	Electric Vehicle
ECU	Engine Control Unit
EFI	Electronic Fuel Injection
EMS	Energy Management Strategy/System
EPA	Environmental Protection Agency
ECMS	Equivalent Consumption Minimization Strategy
EUDC	Extra Urban Driving Cycle
FE	Fuel Economy
FHSAE	Formula Hybrid Society of Automotive Engineering
FTP	Federal Test Procedure
GM	General Motors
GTI	Gamma Technologies Incorporation
GUI	Graphical User Interface

HE-VESIM	Hybrid Electric Vehicle Simulation Tool
HIL	Hardware In the Loop
HV	Hybrid Vehicle
HWY	Highway Fuel Economy Driving Schedule
ICE	Internal Combustion Engine
IEMA	Intelligent Energy Management Agent
HEV	Hybrid Electric Vehicle
NEDC	New European Driving Cycle
PCB	Printed Circuit Board
PNGV	Partnership For a New Generation of Vehicles
PPS	Peaking Power Source
PSAT	Powertrain System Analysis Toolkit
RESS	Rechargeable Energy Storage System
RB	Rule-Based
SIL	Software In the Loop
SIMPLEV	Simple Electric Vehicle Simulation
SOC	Battery State of Charge
UDC	Urban Driving Cycle
UDDS	Urban Dynamometer Driving Schedule
UI	University of Idaho
US	United States
WOT	Wide Open Throttle



## Nomenclature

Variable	Description	Unit
$\rho$	Ambient air density	$\text{Kg/m}^3$
$C_D$	Vehicle drag coefficient	---
$A_f$	Vehicle frontal Area	$\text{m}^2$
$V$	Vehicle Velocity	$\text{Km/hr.}$
$C_R$	Vehicle Rolling Resistance Coefficient	----
$M_V$	Vehicle Weight	$\text{Kg}$
$\theta$	Road Grade Angle	Degree
$g$	Gravitational Acceleration	$\text{m/s}^2$
$P(t)$	Tractive Power Demand/Road Power	$\text{KW}$
$v(t)$	Time dependent vehicle velocity	$\text{Km/h}$
$E_{RL}$	Road load energy	$\text{KJ}$
$\Delta t$	Time step	$\text{sec}$
$\Delta KE$	Change in kinetic energy	$\text{KJ}$
$E_{\text{Inertia}}$	Rotational inertia energy losses	$\text{KJ}$
$I$	Mass moment of inertia	$\text{Kgm}^2$
$\alpha(t)$	Angular acceleration	$\text{rad/s}^2$
$E_{\text{Ovral}}$	Overall energy requirement	$\text{KJ}$
$E_{KE}$	Kinetic Energy	$\text{KJ}$
$E_{\text{PTL}}$	Powertrain energy losses	$\text{KJ}$
$\eta_{\text{fuel}}$	Fuel conversion efficiency	---
$Q_{\text{HV}}$	Fuel lower heating value	$\text{MJ/Kg}$
$m_f$	Fuel mass	$\text{g}$

## Chapter 1. Introduction

### 1.1 Overview

The word “hybrid” describes the combination of attributes of two separate entities working to achieve one desired end goal. This concept has existed for many years in biology, Greek mythology, music, culture, and transportation. Manufacturers in several countries across the world now build highly efficient hybrid locomotives. Gantry cranes that lift rail cars on and off ships now utilize a generator to recover energy while the load is lowered. Boeing Company is investigating hybrid packages for Auxiliary Power Units (APU) in their next generation 737. The military is conducting research on parallel hybrids to support stealth operations and rapid acceleration in their Humvees. The most significant achievement in mass produced hybrid technology is perhaps the Toyota Prius. Since the Toyota Prius hit the automobile market in 1997, Toyota’s hybrid vehicles have continued to set record sales year in and year out.

Hybrid electric vehicles (HEVs) offer the promise of higher energy efficiency and reduced emissions when compared with conventional vehicles, but they can also be designed to overcome the range limitations inherent in a purely Electric Vehicle (EV) by utilizing two distinct energy sources for propulsion. In hybrid vehicles, energy is stored as a petroleum fuel and in an electrical storage device, such as a battery pack, and is converted to mechanical energy by an internal combustion engine (ICE) and Electric motor (EM) respectively. The EM is used to improve energy efficiency and vehicle emissions while the ICE provides extended range capability. Though many different arrangements of power sources and converters are possible in a hybrid power plant, the generally accepted classifications are series, parallel, and series-parallel or combined.

The presence of two alternative power sources, the ICE and the battery, in a HEV poses the problem of determining the optimal power split among them for a given driver’s request in order to achieve minimum fuel consumption. The determination of the optimal power split among the available power sources is the key issue for achieving a high fuel economy by an Energy Management System (EMS).

Energy management in HEVs involves in deciding the amount of power delivered at each instant by the energy sources present in the vehicle. It is sometimes called *supervisory control*, in contrast to *low-level* or *component-level* control, which is used to drive single components so that they behave as dictated by the driver. However, the terms energy management and supervisory control are not synonyms. In fact, the supervisory controller is a layer above the energy management; the energy management is used to split the power demand between the powertrain actuators while the supervisory controller has the task of deciding when such power split algorithm can be applied, or whether a special behavior should be forced in response to specific situations. Thus, in the past decade, a variety of EMSs for HEVs have been developed from control and optimization perspectives. Most of these strategies were evaluated using standard driving cycles.

In a conventional vehicle, there is no need for an EMS: the driver decides the instant speed and the instant power delivery using the brake and accelerator pedals, and, in manual transmission vehicles, decides what gear is engaged at each time. The driver's desires are translated into action by low-level controllers: for example, the engine control unit (ECU) determines the amount of fuel to be injected given the accelerator input; the automatic transmission controller decides when to shift gear based on engine conditions and vehicle speed, etc. In HEVs, there is an additional decision that must be taken: how much power is delivered by each of the energy sources present on the vehicle. In principle, this could be delegated to the driver (for example, providing two separate accelerator commands); but it is much easier, and efficient if a computer takes care of it, leaving to the driver only the decision on how much total power is needed. This is why all hybrid vehicles must possess an EMS, which can be seen as an additional layer between the driver and the component controllers. As mentioned before, the scope of an EMS in a HEV is to determine the optimal power split between the energy sources present on board. What to consider optimal depends on the specific application. In most cases, the strategies tend to minimize the fuel consumption, but the objective could also include the minimization of pollutant emissions, the maximization of power delivery, or a compromise among all these goals.

The role of the energy management in HEVs is represented as in Figure 1. The outer layer is the speed control, which is the human driver in a real vehicle and a driver model (typically a PI controller) in simulation. The speed controller decides the total power request  $P_{req}(t)$  that the powertrain must deliver in order to follow the prescribed speed profile. The inner layer is the EMS. The separation of the two control layers considers only the Battery State of Charge (SOC) in the EMS, while the vehicle speed does not need to be treated as a state of the system, since it is controlled independently by the driver.

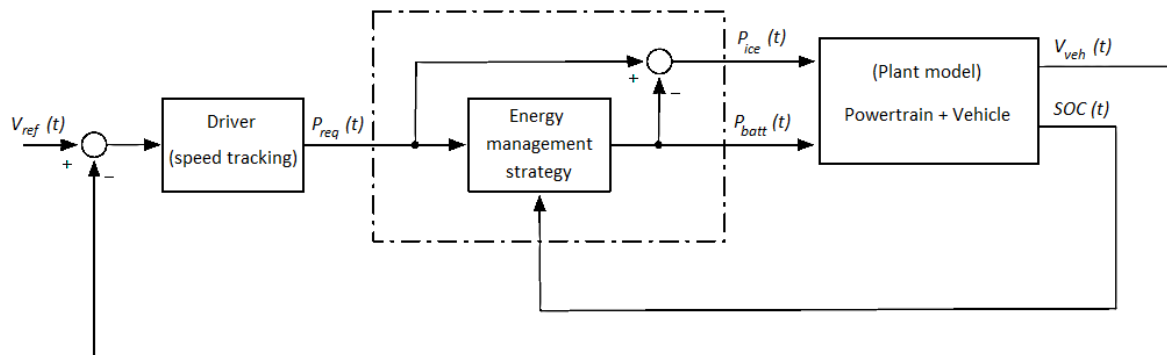


**Figure 1: Energy Management Control Role in HEV**

In general, the main reason for using a hybrid electric architecture is the additional degree of freedom due to the presence of an additional energy source beside the fuel tank; this implies that, at each instant of time, the required power can be provided by either one of these sources, or by a combination of the two. Choosing the correct combination is usually a complex problem and imposes some sort of dilemma, which is basically the supervisory controller's role. At the same time, the answer to this question depends on several variables. The important aspect to consider is the actual objective of hybridization, which in general, could be defined as the minimization of a given cost function, representing fuel consumption, emissions, or a sum of both. The minimization should ideally take place over the entire life cycle of the vehicle, but in practical cases the optimization horizon is finite and usually coincides with a short trip or section of a trip. So, once a suitable optimization horizon and cost function has been decided, the control problem in HEVs consists in minimizing the total cost using a sequence of instantaneous actions, which is a typical optimal control problem. [1], [2]

## 1.2 Problem Statement

The increased global energy demand and environmental concerns are challenging the automobile industry. Under this background, the energy management function of vehicles must be carefully designed to fully realize the potential of vehicle powertrains to meet the above challenges.

The old method of control in the University of Idaho Formula Hybrid racecar (UI-FHSAE) is based on throttle position, where the required torque is split passively between the ICE and the EM, meaning that no information about previous or future operating points determines the torque split. The implication of this system is that the rate at which throttle position demands torque is the only method of adjusting the load between the systems, and no higher level controller is used to determine the torque demand or the proper power split between the two power systems. In the previous vehicle, if the driver turns the acceleration pedal for maximum acceleration, the EM and ICE will produce as much torque as they can. However, in this situation, the ICE operating point would not be in the most efficient condition for a period of time. A new EMS that will coordinate the overall powertrain and determine the proper power split between the electrical and thermal energy sources to satisfy the required performance target is required. This is especially important in light of the new endurance event distance, 44 km from the previous 22 km, in addition of tight restrictions on the total amount of energy that can be used.

## 1.3 Research Objectives

The goals of the research described in this dissertation are the following:

- Create GT-Suite advanced models for a conventional powertrain and three different HEV powertrain layouts.
- Validate the different powertrain models against four standard driving cycles (Federal Test Procedure (FTP), the Highway driving cycle (HWY), the high aggressive acceleration driving schedule (US06), and the New European Driving Cycle (NEDC)).

- Select and compile metrics for comparing different HEV powertrain layouts under different driving cycles.
- Forecast fuel consumption of the current FHSAE vehicle with open-loop energy management.
- Propose an achievable Supervisory vehicle controller that incorporates rule-based energy management for the UI-FHSAE vehicle.
- Forecast fuel consumption with the proposed supervisory controller and the rule-based energy management system using GT-Suite model, accounting for energy depleted from major vehicle components.
- Implement the supervisory controller along with the rule-based energy management system on the vehicle that will compete in the 2015 FHSAE competition.

#### **1.4 Dissertation Organization**

This dissertation documents and details the work carried through to design and develop an energy management control strategy for a HEV. Chapter 1 gives an overview on the vehicle energy management and its theory, problem statement and research objectives. Chapter 2 briefly overviews the HEV architectures and gives a literature survey on different aspects related to the HEV technology. Chapter 3 describes deeply the powertrain model development in GT-Suite and some of the output results for different standard driving cycles. Chapter 4 presents validation of the model results through a fuel economy and energy usage comparative analysis. Chapter 5 presents the dissertation case study, design and implementation of a Supervisory controller for the University of Idaho Formula hybrid car, including both powertrain modeling and hardware implementation. Chapter 6 presents the supervisory controller optimization using GT-Suite discrete grid method, then three case scenarios will be presented to validate the optimized controller along with experimental testing. Chapter 7 gives the conclusion and some future recommendations.

## **Chapter 2. Literature Review**

### **2.1 Introduction**

HEVs have existed since before 1900, but interest in these vehicles has grown substantially only in the last 20 years. The main reason for this interest is the expectation that HEVs represent a short-term approach for improving fuel efficiency and reducing pollutant emissions. It is commonly known that, a hybrid vehicle comprises two or more power sources in the drivetrain. There are many different layouts of HEVs, but only the gasoline-electric hybrids are currently commercially available. HEVs could be classified according the arrangement of input power as: Series, Parallel and Series-Parallel HEV. Each of these configurations has different operating modes where power flow is controlled through a vehicle supervisory controller. These operating modes differ from electric only, engine only, electric power assist, battery charging and regenerative braking modes.

Surprisingly, the concept of HEVs is almost as old as the automobile itself. The primary purpose, however, was not so much to lower the fuel consumption but rather to assist the ICE to provide an acceptable level of performance. Indeed, in the early days, ICE engineering was less advanced than EM engineering.

HEVs combine a conventional combustion engine propulsion system with one or more electric propulsion systems. The presence of the electric powertrain is for the purpose of achieving better fuel economy than conventional vehicle. The control strategies of HEVs are more complicated than those of conventional vehicles because of the more complex configurations and different operation modes. Meanwhile it is commonly recognized that the energy management for HEVs has more influence than in conventional vehicles on vehicle performance improvements such as fuel consumption, emission and lifetime extension of power sources. [2], [3]

### **2.2 History of Hybrid Electric Vehicle**

The first hybrid vehicles reported were shown at the Paris Salon of 1899. These were built by the Pieper establishments of Liège, Belgium and by the Vendovelli and Priestly

Electric Carriage Company, France. The Pieper vehicle was a parallel hybrid with a small air-cooled gasoline engine assisted by an EM and lead-acid batteries. It is reported that the batteries were charged by the engine when the vehicle coasted or was at a standstill. When the driving power required was greater than the engine rating, the EM provided additional power. In addition to being one of the two first hybrid vehicles, and the first Parallel hybrid vehicle, the Pieper was undoubtedly the first vehicle with electric starter.

The other hybrid vehicle introduced at the Paris Salon of 1899 was the first series HEV and was derived from a pure Electric Vehicle (EV) commercially built by the French firm Vendovelli and Priestly. This vehicle was a tricycle, with the two rear wheels powered by independent motors. An additional  $\frac{3}{4}$  [hp] gasoline engine coupled to a 1.1 [kW] generator was mounted on a trailer and could be towed behind the vehicle to extend the range by recharging the batteries. In the French case, the hybrid design was used to extend the range of an EV by recharging the batteries and not to supply additional power to a weak ICE.

In 1900, while employed at Lohner Coach Factory, Ferdinand Porsche developed the Mixte; a 4WD series-hybrid version of "System Lohner-Porsche" electric carriage previously appeared in 1900 Paris World Fair, Figure 2 shows Ferdinand Porsche's First Hybrid Vehicle.



**Figure 2: Ferdinand Porsche's First Hybrid Vehicle (1900)**



The Mixte included a pair of generators driven by 2.5 [hp] Daimler ICE to extend operating range and it could travel nearly 65 [km] on battery alone. It was presented in the Paris Auto Show in 1901. The Mixte broke several Austrian speed records, and also won the Exelberg Rally in 1901. It used a gasoline engine powering a generator, which in turn powered electric hub motors, with a small battery pack for reliability. It had a top speed of 50 [km/h] and a power of 5.22 [kW] during 20 [min]. [4]

Frenchman Camille Jenatzy presented a parallel hybrid vehicle at the Paris Salon of 1903. This vehicle combined a 6 [hp] gasoline engine with a 14 [hp] EM that could either charge the batteries from the engine or assist them later. Another Frenchman, H. Krieger, built the second reported series hybrid vehicle in 1902. His design used two independent DC motors driving the front wheels. They drew their energy from 44 lead-acid cells that were recharged by a 4.5 [hp] alcohol spark-ignited engine coupled to a shunt DC generator.

Other hybrid vehicles, both of the parallel and series type, were built during a period ranging from 1899 until 1914. Although electric braking has been used in these early designs, there is no mention of regenerative braking. It is likely that most, possibly even all, designs used dynamic braking by short circuiting or by placing a resistance in the armature of the traction motors. The Lohner-Porsche vehicle of 1903 is an example of this approach.

Early hybrid vehicles were built in order to assist the weak ICE of that time or to improve the range of EVs. They made use of the basic electric technologies that were then available. In spite of the great creativity that featured in their design, these early hybrid vehicles could no longer compete with the greatly improved gasoline engines that came into use after World War I. The gasoline engine made tremendous improvements in terms of power density, the engines became smaller and more efficient, and there was no longer a need to assist them with electric motors. The supplementary cost of having an EM and the hazards associated with the lead-acid batteries were key factors in the disappearance of hybrid vehicles from the market after World War I.

However, the greatest problem that these early designs had to cope with was the difficulty of controlling the electric machine. Power electronics did not become available

until the mid-1960s and early electric motors were controlled by mechanical switches and resistors. They had a limited operating range incompatible with efficient operation. Only with great difficulty could they be made compatible with the operation of a HV.

In 1967 the series hybrid design was revived by Dr. Ernest H. Wakefield, where he coupled a small engine to an AC generator, with an output of 3 [kW], and used it to keep a battery pack charged. However, his experiments were quickly stopped because of technical problems. Other approaches studied during the 1970s and early 1980s used range extenders, similar in concept to the French Vendovelli and Priestly 1899 design. These range extenders were intended to improve the range of EVs that never reached the market. Other prototypes of hybrid vehicles were built by the Electric Auto Corporation in 1982 and by the Briggs & Stratton Corporation in 1980. These were both parallel hybrid vehicles.

Dr. Victor Wouk is recognized as the modern investigator of the HEVs movement. In 1975, along with his colleagues, he built a parallel hybrid version of a Buick Skylark. The engine was a Mazda rotary engine, coupled to a manual transmission. It was assisted by a 15 [hp] separately excited DC machine, located in front of the transmission. Eight 12 [V] automotive batteries were used for energy storage. A top speed of 130 [km/h], 80 [mph], was achieved with acceleration from 0 to 100 [km/h] in 16 [s].

Despite the oil crises of 1973 & 1977, and despite growing environmental concerns, no HEV made it to the market. The researchers' focus was drawn by the EV, where many prototypes were built during the 1980s. The lack of interest in HEVs during this period attributed to the lack of practical power electronics, modern electric motor, and battery technologies.

The 1980s witnessed a reduction in conventional ICE powered vehicle sizes, the introduction of catalytic converters, and the generalization of fuel injection. The HEV concept drew great interest during the 1990s when it became clear that EVs would never achieve the objective of saving energy. The Ford Motor Corporation initiated the Ford HEV Challenge, which drew efforts from universities to develop hybrid versions of automobiles.

Automobile manufacturers around the world built prototypes that achieved tremendous improvements in fuel economy over their ICE powered counterparts. In United States (US), Dodge built the Intrepid ESX 1, 2, and 3. The ESX-1 was a series hybrid vehicle, powered by a small turbocharged three cylinder diesel engine and a battery pack. Two 100 [hp] electric motors were located in the rear wheels. The U.S. government launched the Partnership for a New Generation of Vehicles (PNGV), which included the goal of a mid-size sedan that could achieve 130 [km/h], 80 [mph]. The Ford Prodigy and General Motors (GM) Precept resulted from this effort. The Prodigy and Precept vehicles were parallel HEVs powered by small turbocharged diesel engines coupled to dry clutch manual transmissions. Both of them achieved the objective but production did not follow.

Efforts in Europe are represented by the French Renault, a small parallel hybrid vehicle using a 750cc spark-ignited engine and two electric motors. This prototype achieved 70 [mpg] with maximum speed 113 [km/h] and acceleration performance comparable to conventional vehicles. Volkswagen also built a prototype, the Chico. The base was a small EV, with a nickel-metal hydride battery pack and a three-phase induction motor. A Small two-cylinder gasoline engine was used to recharge the batteries and provide additional power for high speed cruising.

The most significant effort in the development and commercialization of HEVs was made by Japanese manufacturers. In 1997, Toyota released the Prius sedan in Japan. Honda also released its Insight and Civic Hybrid. These vehicles are now available throughout the world. They achieve excellent figures of fuel consumption. Prius and Insight have historical value in that they are the first hybrid vehicles commercialized in the modern era to respond to the problem of personal vehicle fuel consumption. [3]

### **2.3 Hybrid Electric Vehicle Architectures**

One of the most common ways to classify HEVs is based on configuration of the vehicle drivetrain. HEV incorporate multiple energy storage and conversion units for propulsion. A hybrid powertrain is one where a conventional thermal engine fueled by

diesel, petrol, gas, is either supplemented by electric traction or alternatively generates on-board electrical energy which is then used to power electric traction.

As a result of the wide range of possibilities involved in integrating the elements of a hybrid propulsion system, different vehicle architectures evolved. The specific choice of a HEV configuration depends on several factors including type of the application, cost and weight considerations and expectations of the targeted customers. A HEV propulsion system typically consists of a fuel tank, an ICE, one or more electrical energy carriers (e.g. batteries, super-capacitors), electric machines, power converters, a transmission and various driveline linkages. These elements can be combined in various ways to accomplish different objectives.

The architecture of HEV is loosely defined as the connection between the components that define the energy flow routes and control ports. Traditionally, there are two mainstream concepts. The first is by using an electric traction motor to assist the conventional system. The effect of this is to have a smaller conventional thermal engine driveline than would otherwise be used for a given vehicle payload and performance. In this case the electric traction provides additional power. The second is by using an on-board thermal engine/generator set to generate electrical energy at peak efficiency and a mechanically separate electric drive line provides all the power necessary to give the vehicle the required performance.

As shown in Figure 3, HEVs are presently classified as being: series hybrid, parallel hybrid, series-parallel hybrid, or a complex hybrid. Scientifically, the classifications above are not very clear and may cause confusion. Actually, in a HEV, there are two kinds of energy flow in the drivetrain: one is mechanical energy and the other is electrical energy. Adding two power streams together or splitting one power into two at the power merging point always occurs with the same power type, that is, electrical or mechanical, not electrical and mechanical. [3], [5]

The key distinguishing feature of the series hybrid is to couple the engine with the generator to produce electricity for pure electric propulsion, whereas the distinguishing

feature of the parallel hybrid is to couple both the engine and the EM with the transmission via the same drive shaft to propel the wheels. The series-parallel hybrid is a direct combination of both the series and parallel hybrids.

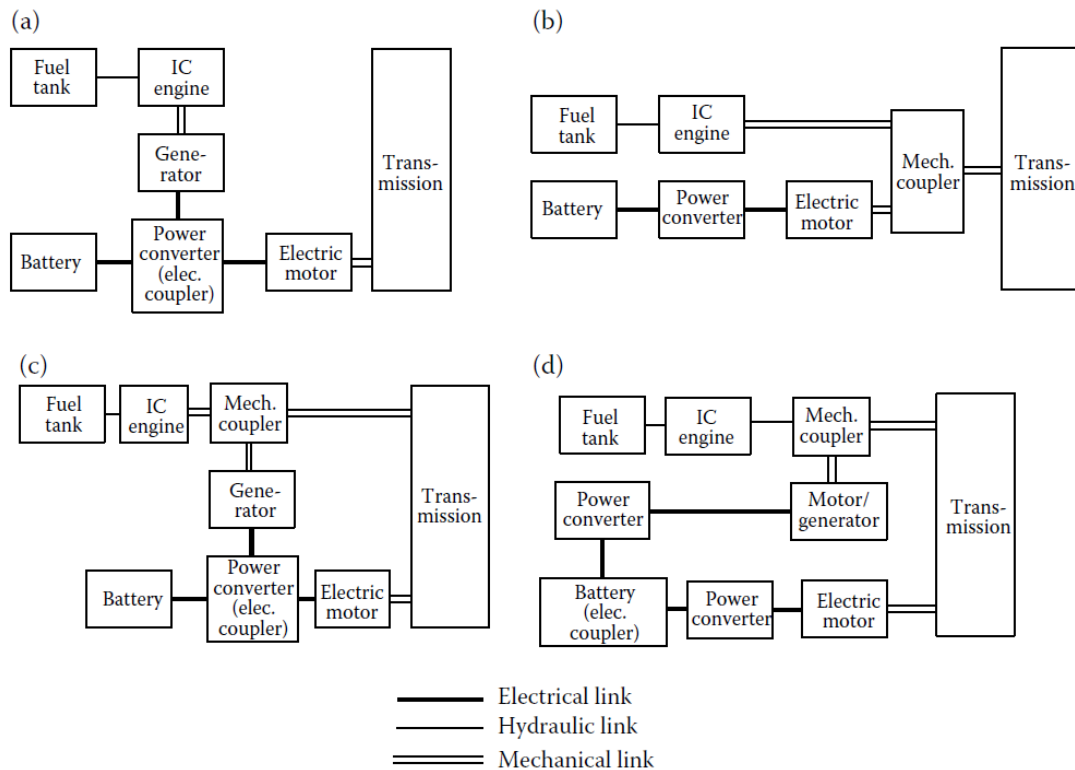


**Figure 3: Classifications of HEVs.**

**(a) Series, (b) Parallel, (c) Series-Parallel, (d) Complex Hybrid**

### 2.3.1 Series Hybrid Configuration

The tractive power is supplied directly by one or more electric machines in series HEV architectures. An ICE, operated at its efficient operating region, drives an electric generator to charge the Electrical Energy Storage System (EESS). Series hybrid vehicle architecture is typically used in heavy-duty vehicles such as trucks and locomotives. Also, a vehicle that uses wheel hub motors is most suited to operate with the series hybrid principle.

The key feature of this configuration is that two electrical power sources are added together in the power converter, which functions as an electric power coupler to control the power flows from the batteries and generator to the EM. The fuel tank, the ICE, and the

generator constitute the primary energy supply and the batteries function as the energy bumper.

The on-board thermal engine power plant provides a continuous power source. A mechanically isolated electric traction system provides, at all times, the tractive power required to achieve the vehicle performance. This arrangement is optimized so that the efficiency of generation is totally isolated from the optimized traction and auxiliary load so this architecture is probably the ideal choice where the vehicle is subject to a high start-stop duty cycle. Because the vehicle traction is pure electric it greatly benefits from the efficiency of the traction drive during acceleration, continuous operation and regenerative braking cycle. The on-board power plant ensures significant efficient operational range and is optimized for efficient generation by running both the matched engine and generator within a narrow band operational revolutions at or close to peak efficiency.

The drive train needs a controller to control the operation and power flows based on the driver's operating command through accelerator and brake pedals and other feedback information from the components. The vehicle controller will control the ICE through its throttle, electric coupler (controllable rectifier and DC/DC converter), and traction motor to produce the demanded propelling torque or regenerative braking torque during operation on different modes. Figure 4 shows a typical series hybrid configuration. [3]

The power flow control can be illustrated by four operating modes as shown in Figure 5. During startup, normal driving or acceleration modes, both the engine (via the generator) and the battery deliver electrical energy to the power converter, which then drives the EM and, hence, the wheels via the transmission. At light load, the engine output is greater than that required to drive the wheels, so the generated electrical energy is also used to charge the battery until the battery capacity reaches a proper level. During braking or deceleration, the EM acts as a generator which transforms the kinetic energy of the wheels into electricity, hence charging the battery via the power converter. Also, the battery can be charged by the engine via the generator and power converter, even when the vehicle comes to a complete stop. The Toyota Coaster HEV has adopted this series hybrid control. [5]

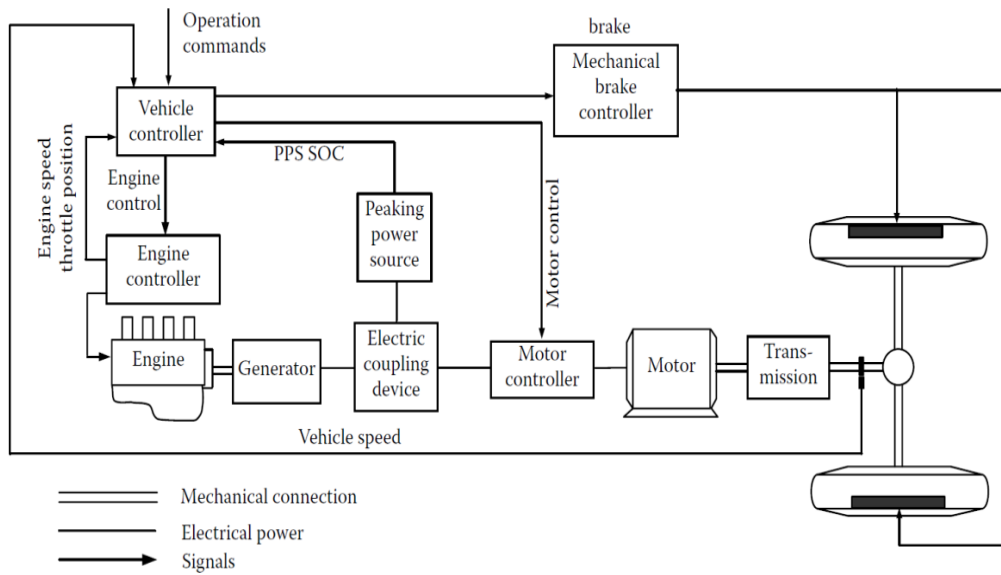


**Figure 4: Series Hybrid Configuration**

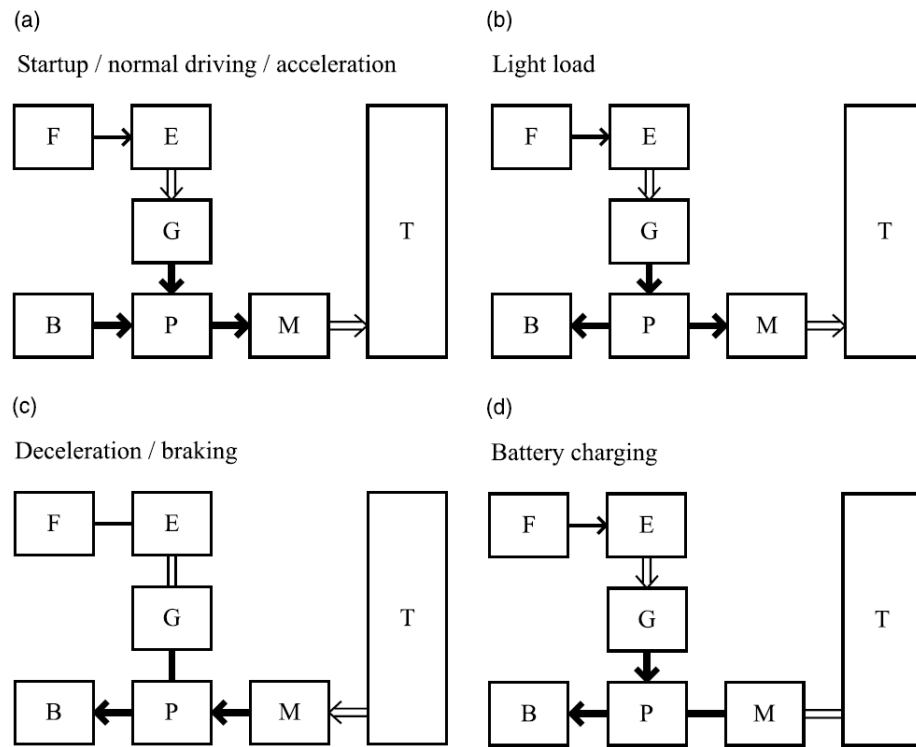


**Figure 5: Series Hybrid Operating Modes**

**B: Battery E: Engine F: Fuel Tank G: Generator M: Motor P: Power Converter T: Transmission**

### 2.3.2 Parallel Hybrid Configuration

In Parallel hybrid electric vehicles, the tractive power is supplied by a proper combination of the ICE and the EM. A dedicated generator or a motor/generator can be used to maintain the EESS in a desired SOC range. The distinguished feature of this architecture is that two mechanical powers from the ICE and EM are added together by a mechanical coupler. Figure 6 shows a typical parallel hybrid configuration.

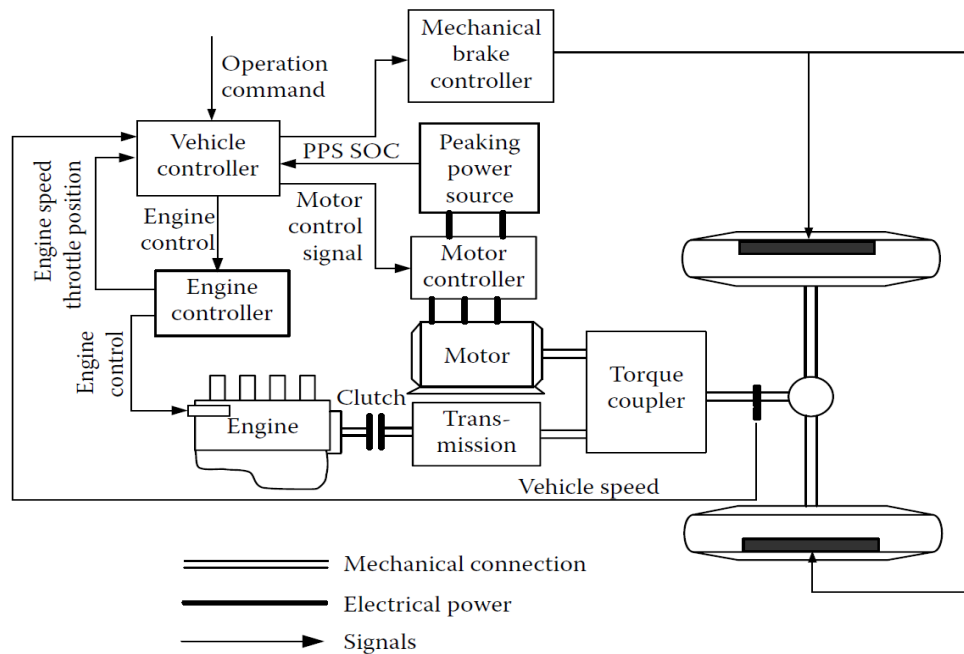


**Figure 6: Parallel Hybrid Configuration**

Generally, mechanical coupling consists of torque coupling and speed coupling or both. In torque coupling, the mechanical coupler adds the torques of the ICE and EM together and delivers the total torque to the driven wheels. The ICE and EM torques can be independently controlled. But the speeds of the ICE, EM, and vehicle are linked together with a fixed relationship and cannot be independently controlled because of the power conservation constraint. In a typical parallel design, consisting of an ICE and an EM in a torque-combining configuration, either the ICE or the EM can be considered the primary energy source depending on the vehicle design and the EMS.



Similarly in speed coupling, the speeds of the ICE and EM can be added together and all torques are linked together and cannot be independently controlled. Based on the type of coupler used, a two or one shaft configuration maybe constituted. In each, transmission maybe placed in different positions with different gears, resulting in various tractive characteristics, more information can be found in [3].

There are many possible of configurations in a parallel hybrid drivetrain. The design methodology for one configuration may not be applicable to others. Each particular configuration may be only applicable to the specified operation and mission requirement.

Torque coupling parallel HEV can be further divided into two categories according to the location of the EM. A pre-transmission parallel hybrid which has an EM connected to the ICE prior to the transmission. A post-transmission parallel hybrid which has a traction EM connected to either the driven axle, after the final drive, or the non-driven axle. The major advantages of a torque-coupling parallel configuration over a series configuration are: non-necessity of a generator, a smaller traction motor, and only part of the engine power going through multi-power conversion. Hence, the overall efficiency can be higher than in the series hybrid. However, control of the parallel hybrid drivetrain may be more complex than that of the series hybrid drivetrain, because of the simultaneous mechanical coupling between the engine and the driven wheels. [3]

Figure 7 illustrates the four operating modes of the parallel HEV. During startup or full-throttle acceleration, both the engine and EM proportionally share the required power to propel the vehicle. Typically, the relative distribution between the engine and the EM is 80% (engine) - 20% (EM). During normal driving, the engine solely supplies the necessary power to propel the vehicle, while the EM remains in the off mode. During braking or deceleration, the EM acts as a generator to charge the battery via the power converter. Also, since both the engine and EM are coupled to the same drive shaft, the battery can be charged by the engine via the EM when the vehicle is at light load. Recently, the Honda Insight HEV has adopted a similar power flow control. [5]

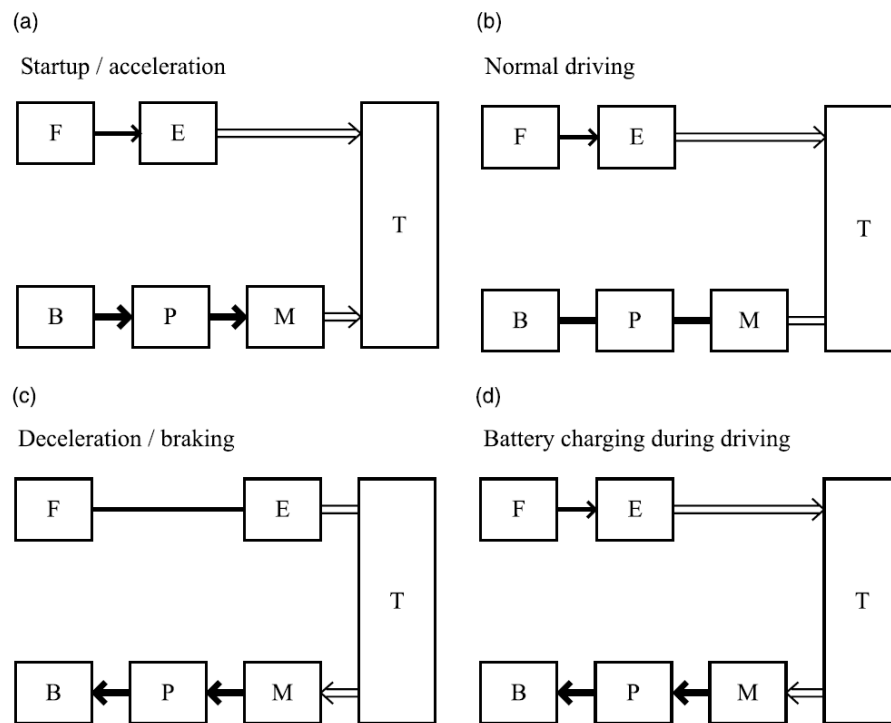


**Figure 7: Parallel Hybrid Operating Modes**

**B: Battery E: Engine F: Fuel Tank G: Generator M: Motor P: Power Converter T: Transmission**

### 2.3.3 Series-Parallel Hybrid Configuration

This hybrid topology as shown in Figure 8 offers both a series and parallel power train in one scheme. However, two traction motor/generator and more complex control power electronics are required. The choice of parallel or series operation is determined by a clutch position. In this configuration the thermal engine can provide the drive through the transmission to drive wheels or alternatively drive the generator to charge the battery but not both simultaneously. Clearly, the thermal engine can be isolated and the vehicle driven in battery only operation. Yet another possibility is electric assistance to the thermal engine powertrain, this however depends on the control electronics algorithms and permissible modes of operation.

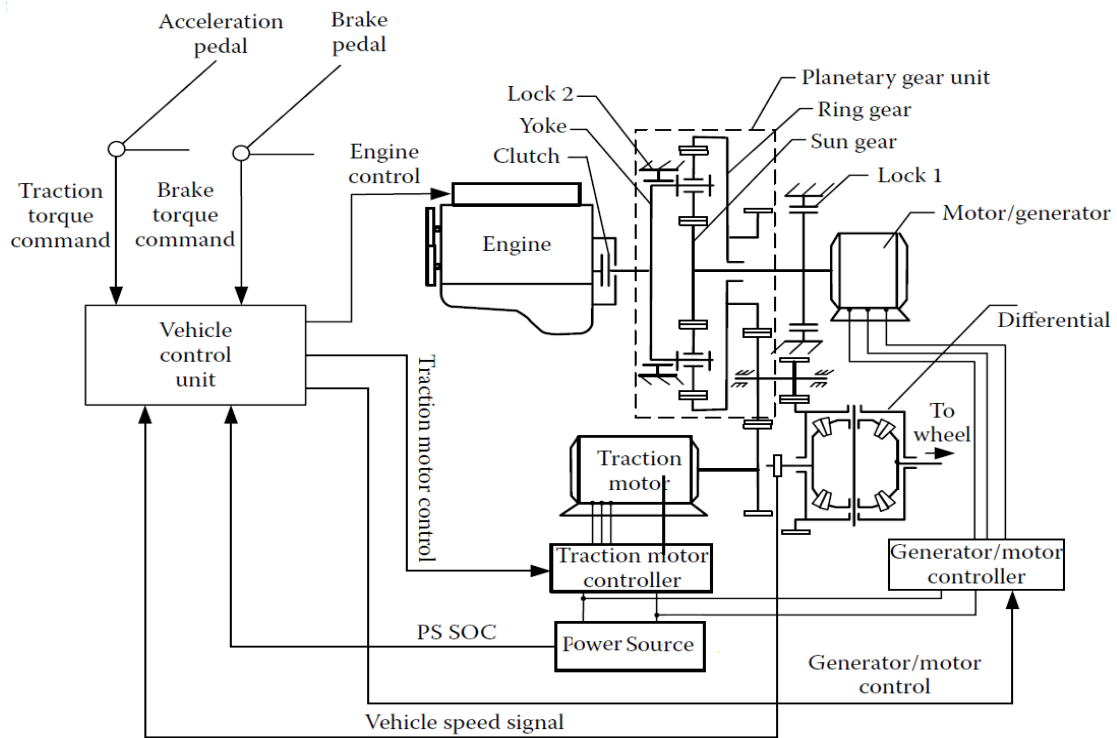


**Figure 8: Series-Parallel Hybrid Configuration**

The series-parallel hybrid system involves the features of series and/or parallel hybrids. Thus, there are many possible operating modes to perform its power flow control. Basically, we can identify them in two groups, namely engine-heavy and electric-heavy. The engine-heavy one denotes that the engine is more active than the EM for series-parallel hybrid propulsion, whereas the electric-heavy one indicates that the EM is more active. There are six operating modes in an engine-heavy series-parallel hybrid system, a startup, full throttle acceleration, normal driving, braking or deceleration, battery charging during driving, and battery charging. A similar power flow control system has been applied to the Nissan Tino HEV. The electric-heavy series-parallel hybrid system operates in six modes, startup and driving at light load, full throttle acceleration, normal driving, braking or deceleration, battery charging during driving, and battery charging. This power flow control system has been adopted in the Toyota Prius HEV. [5]

### 2.3.4 Complex Hybrid Configuration

The development of complex hybrid control has been focused on the dual axle propulsion system for HEVs. In this system, the front wheel axle and rear wheel axle are separately driven. There is no propeller shaft to connect the front and rear wheels, so it enables a more lightweight propulsion system and increases the vehicle packaging flexibility. Moreover, regenerative braking on all four wheels can significantly improve the vehicle fuel efficiency and, hence, the fuel economy.

The complex hybrid seems to be similar to the series-parallel hybrid, since the generator and EM are both electric machinery. However, the key difference is due to the bidirectional power flow of the EM in the complex hybrid and the unidirectional power flow of the generator in the series-parallel hybrid. This bidirectional power flow can allow for versatile operating modes, especially the three propulsion power (due to the engine and two electric motors) operating mode, which cannot be offered by the series-parallel hybrid. Similar to the series-parallel HEV, the complex hybrid suffers from higher complexity and costliness. Nevertheless, some newly introduced HEVs adopt this system for dual axle propulsion.

The dual axle complex hybrid system has six different operating modes depending on the hybrid drive location. The front wheel axle could be propelled by a hybrid drive train, and the rear wheel axle is driven by an EM. In this case, the six operating modes are startup, full throttle acceleration, normal driving and/or battery charging, driving at light load, deceleration/braking, and axle balancing in case of wheel slip. However, if the front wheel axle is driven by an EM and the rear wheel axle is propelled by a hybrid drive train. The six operating modes are startup, starting the engine, full throttle acceleration, normal driving, braking or deceleration, and battery charging during driving. [5]

Other HV concepts incorporating mechanical or hydraulic storage devices have been also developed. However, the four categories listed above cover majority of the hybrid vehicle architectures available today.

## 2.4 Control Levels in HEVs

Hybrid vehicle powertrains have been widely studied recently because of their potential to significantly improve fuel economy and reduce emissions of ground vehicles. Due to the multiple-power-source nature and the complex configuration, the control strategy of a hybrid vehicle is more complicated than that of an ordinary vehicle. First, one needs to determine the optimal operating mode among five possible modes (electric only, engine only, power assist, recharge, and regenerative). Furthermore, when the power assist mode or the recharge mode is selected, the engine power, motor power and transmission gear ratio need to be selected to achieve optimal fuel economy, emissions reduction, charge balance, and drivability. The main function of the control strategy is power management, i.e., the design of the high-level control algorithm that determines the proper power split between the motor and the engine to minimize fuel consumption and emissions, while satisfying constraints such as drivability, charge sustenance and component reliability.

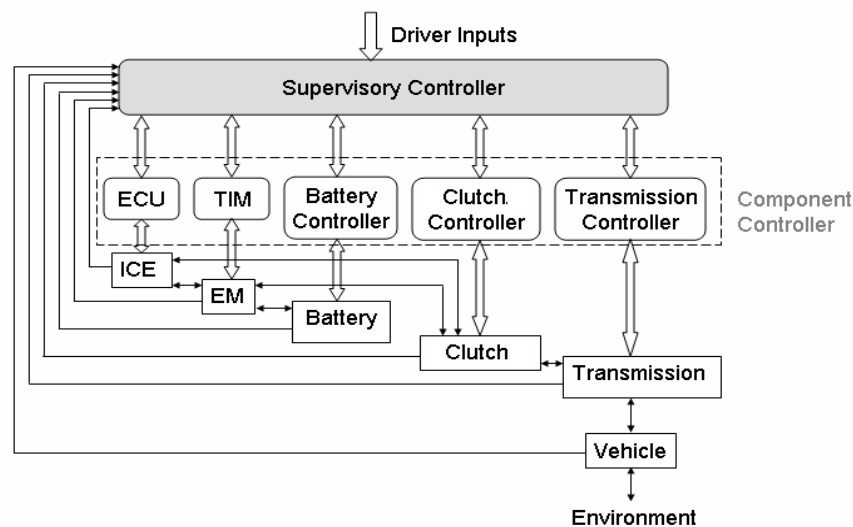


**Figure 9: Control Levels in a HEV**

Control in HEVs is recognized as two levels of controllers, supervisory controller and component controller, as shown in Figure 9. The supervisory controller functions primarily as an energy management unit, or generally it is an algorithm to realize energy management and drivetrain control, splitting power request between chemical (fuel) and

electrical (batteries or ultra-capacitors) energy sources. It translates driver's intentions into power requirements and coordinates powertrain components to achieve certain objectives. Common objectives include minimizing fuel consumption and emissions while maintaining or improving performance and drivability. On the other hand, the component controller receives commands from the supervisory controller and generates detailed control instructions for its actuators.

#### **2.4.1 Supervisory Control Level**

The supervisory powertrain controller is regarded as a high-level vehicle control system that coordinates the overall powertrain to satisfy certain performance target, it serves as an energy management unit which splits power requirements between the ICE and the EM. Improving fuel consumption and reducing emissions are the two primary objectives for supervisory control level design. The supervisory controller sits at the top to manage the operation of the hybrid powertrain system. It is designed to include the following functions: energy management strategy, regenerative braking control, transmission shift logic and shifting control, vehicle launch control, I/O communication, and system fault detection. [6]

Minimizing power losses implies higher efficiency and less fuel consumption. This is accomplished through optimizing powertrain design and control. Powertrain optimal design is composed of configuration design and component design. Not only the drivetrain architecture and each component need to be power efficient, but these components need to be matching in type and size to obtain high overall efficiency.

For a given driver demand and vehicle operation conditions, the supervisory controller maintains the vehicle at its most efficient operating point by managing the power among the various components of the vehicle and coordinating the operating state of the engine, generator, motor, and battery. In addition, it ensures the required vehicle's performance and drivability.

Vehicle fuel economy is mainly determined by the supervisory control strategy which could be globally optimized, for example, using Dynamic Programming (DP). Alternatively, the global optimum can be approximated by a local optimum, as done in the Equivalent Consumption Minimization Strategy (ECMS). Besides the more analytically based optimizations methods, control strategies can also be heuristically based, as with rule-based controllers' [7], fuzzy logic [8], and artificial neural networks.

#### **2.4.2 Component Control Level**

HEV is an integrated system that consists of many subsystems/components including engine, transmission, EM, battery, clutch, brakes, etc. Each subsystem is also a complex system that has its own functionality and desired performance. In this case, almost every subsystem is equipped with sensors, actuators, and a control system to regulate its behavior. Moreover, all subsystems need to be coordinated in an optimal manner to achieve the required objectives, e.g. fuel economy, emissions reduction, and drivability. So, the control system of the drivetrain consists of a controller to control the ICE power, a transmission controller, an EM controller, a brake controller and a clutch controller.

The supervisory controller is the highest level controller. It receives the operation command from the driver through the accelerator and brake pedals, and other operating variables of the vehicle and its components, which includes vehicle speed, engine speed and throttle position, battery SOC, and so on. By processing all the received signals and based on the drivetrain control algorithm, the supervisory controller generates control commands and sends them to the corresponding component controllers. The component controllers control the corresponding components to carry out the commands coming from the vehicle supervisory controller to meet the requirements of the drivetrain. The supervisory controller plays a central role in the operation of the drivetrain. It should fulfill various operation modes, according to the data collected from components and the driver's command, and should give the correct control command to each component controller. Hence, the control strategy in the supervisory controller is the key in the success of the drive train operation. [3]

## 2.5 Vehicle Energy Management

Because of the variations in HEV configurations, different power control strategies are necessary to regulate the power flow to and from different components. The energy management problem of automotive vehicles deals with controlling the amount of power exchange such that the desired objectives and behavior of the vehicle is obtained. Desired behavior can be expressed by demands on fuel consumption, exhaust emissions, component wear, comfort, and prolonging lifetime of power sources as the battery, while satisfying restrictions on operating points of components and energy storage levels, and enhancing vehicle drivability and reliability. These control strategies aim to maximize fuel economy, minimize emissions, and ensure good driving performance.

The term “energy management” refers to the design of the higher-level control algorithm that determines the proper power (torque) level to be generated, and its split between the EM and the ICE while satisfying the power demand from the driver and maintaining adequate energy in the energy storage device. When accomplishing these objectives, items noted below have to be considered while developing the proper EMS. [5]

- The engine needs to be regulated at proper speed avoiding fast fluctuations and thus minimizing engine dynamics.
- The engine has to be turned off when the speed is below a threshold level because the fuel economy is low at such a speed.
- The frequent turning on and off leading to additional fuel consumption and emissions which should be avoided.
- The engine has a preferred operating region on the torque-speed plane where the fuel economy is high.
- The battery should be kept at a proper SOC level for both supplying sufficient power for acceleration and absorbing regenerative braking power.
- The battery voltage may dramatically change during the processes of discharging, generator charging, or regenerative charging.



### **2.5.1 Energy Management in Hybrid Electric Vehicles**

In recent years, a lot of research has been carried out in the field of HEV, especially the research activity on EMS for HEVs, and because of the relevance to the work presented in this dissertation; a detailed literature overview will be given on the EMS for HEVs.

EMS is a critical aspect of hybrid vehicle development. It determines at what time, under what load, and how long the ICE as well as EM are used. The primary information necessary for energy management is the total power demand from the vehicle, the actual SOC of the traction battery, and the performance characteristics of the ICE and EM.

The primary objective of the EMS is to coordinate the power flow between the energy carriers (electrical or thermal), the actuators and the environment in response to the driver's power demand, while improving fuel economy, reducing exhaust emissions and maintaining various subsystems in their desired states without compromising vehicle performance constraints, such as acceleration, gradeability, and regulation of energy storage system SOC, ensuring seamless operation of the drivetrain. EMS involves optimization of powertrain component selection and sizing, determining anticipated driving cycles, performance feedback from various sensors, and selection of control algorithms.

Effective operations of HEVs depend largely upon the sophisticated design of vehicle controller with optimal EMS that commands each subsystem to its best for the global system efficiency. Many researchers [9]–[13] have devoted their attention to the design of EMS because of its importance to the HEVs. Due to the complexity of HEVs, the design of the EMS poses a considerable challenge to engineers.

In fact, EMS for HEVs, which is the philosophy behind the supervisory controller, can be categorized focusing on some of their characteristics into two categories: rule-based and optimization-based strategies as shown in Figure 10. [14]– [16]

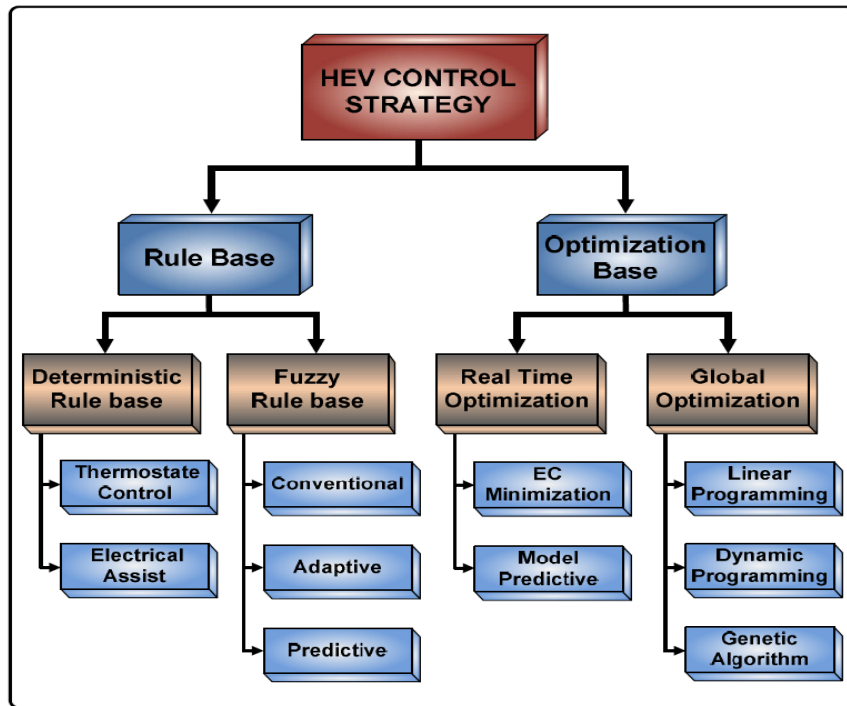


Figure 10: HEV Energy Management Control Strategies

### 2.5.2 Rule-Based Energy Management Strategies

These are fundamental control schemes that depend on mode of operation and are mainly based on engineering intuition and do not involve explicit minimization or optimization. However, due to the multi-variable nature of HEV control problems; these rules usually fail to capture the entire important phenomenon. The main aspect involved in these strategies is their effectiveness while implementation in real-time supervisory control, to manage power flow in a hybrid powertrain. The rules are designed based on heuristics, human expertise, and even mathematical models, and generally, without a priori knowledge of a predefined driving cycle. Strategies that are based on heuristics can easily be implemented in a real vehicle by using a rule-based strategy [7], [17], [18] or fuzzy logic [19]–[24]. Although these strategies can offer a significant improvement in energy efficiency, fuel consumption and emissions of a HEV, they cannot guarantee an optimal system performance result in all situations. However, these strategies are robust and computationally efficient, requiring lower computational load than minimization-based methods.

The knowledge-based strategies use rules or fuzzy logic for energy management implementation in a real HEV. The categories of this knowledge are stated as:

- Heuristic knowledge that is dependent on the efficiency map of an engine.
- Knowledge about the proper power split between the power sources for the minimization of the equivalent consumption cost, generated by optimal methods.
- Prediction of driving environment using neural networks and fuzzy logic.

Most of the rule-based control strategies are based on 'if-then' type of control rules and perform load balancing within the vehicle. The main goal is to move ICE operation closer to the optimal region of fuel economy, efficiency, and emissions. However, for this type of systems, fairly good fuel economy can be found at lower engine torques and speeds. Thus, small acceleration can result in higher fuel economy. This strategy is further subcategorized into deterministic rule-based and fuzzy logic rule-based.

Deterministic rule-based control strategies are designed with the aid of fuel economy or emission data, ICE operating maps, power flows within the powertrain, and driving experience. Implementation of the rules is performed via lookup tables, to share the power demand between the ICE and the EM. Thermostat and Electric assist control strategies are examples of the deterministic rule-based control strategy.

Fuzzy logic rule-based control strategies are knowledge-based systems. The knowledge of an expert can be used to form a rule-base, and by utilizing decision making quality of fuzzy logic, a real-time control can be realized [22]. Fuzzy logic control strategies portray a nonlinear structure that can deal with the nonlinear structure of the power split problem. Moreover, they are robust and can also be tuned and adapted easily. Due to the highly nonlinear and time-varying nature of the HEV powertrain, control strategy implementation using fuzzy logic is one of the most reasonable methods to handle HEV energy management problems [23]. The problem with fuzzy logic is the optimization and mathematical manipulation of defuzzification system. The defuzzification process consumes memory and time in the controller. [16]

### 2.5.3 Optimization-Based Energy Management Strategies

These usually rely on a model to compute the best control strategy. These strategies are subcategorized into Global Optimization and Real-time Optimization. The model can be either analytical or numerical; if the optimization is performed over a fixed driving cycle, a global optimal solution could be found. Obviously, this approach cannot be used directly for real-time energy management. On the other hand, by definition of an instantaneous cost function, a real-time optimization control strategy can be adopted. Such a function has to depend only upon the system variables at the current time. Of course, the solution of this method is not globally optimal, but it can be used for real-time implementation.

The Global optimization technique requires the knowledge of the entire driving pattern. It includes driving conditions, driver response, and route prediction. This method could be a good analysis, design, and assessment tool for other control strategies. However, due to computational complexity, they are not easily implementable for practical applications. To find the optimal solution, techniques as linear programming [25], optimal control [26], [27], genetic algorithms, and DP [9], [10], [28], [29] are used to resolve vehicle energy management issues. In general, these techniques do not offer an online solution, because they assume that the future driving cycle is entirely known. These methods give the optimal solution over the prescribed driving cycle but are not implementable due to the necessity of knowing a priori the driving cycle. Nevertheless, their result can be used as a bench-mark for the performance of other strategies, or to derive rules for a rule-based strategy. If only the present state of the vehicle is considered, optimization at each instant can be beneficial, but profits will be limited [30]. Another possibility is to perform an instantaneous optimization over the current time step, using a cost function that makes a tradeoff between fuel consumption, battery use and optionally a penalty on undesired behavior as done in [31], [32].

In [10], C. C. Lin et al, proposed a design procedure that uses Deterministic Dynamic Programming (DDP) to find the optimal solution and then extracts implementable rules to form the control strategy. Even though the control laws they obtained have performed well

in a real HEV, there were two drawbacks in this approach. First, this approach performs optimization with respect to a specific driving cycle and might be neither optimal nor charge-sustaining under other cycles; secondly, the feedback solution to the DDP is not directly implementable and the rule extraction process can be time-consuming. A different approach was taken in [33]–[35]. Instead of focusing on one particular driving cycle, a certain set of driving cycles was considered, resulting in a stochastic optimization approach. This technique is implementable online but tends to require high computational capabilities in which statistical methods are used to predict the most likely future driving cycle.

The main aim of Real-time Optimization is to reduce global criterion to an instantaneous optimization, by introducing a cost function that depends only on the present state of the system parameters, due to the causal nature of global optimization techniques, they are not suitable for real-time analysis. Moreover, global optimization techniques do not consider variations of battery SOC in the problem. Hence, in order to derive cost functions for instantaneous optimization of power split, while maintaining battery charge, real-time optimization is performed. The Equivalent Consumption Minimization Strategy (ECMS) [36], [37] introduces the real-time energy management of HEVs. Where equivalent fuel consumption is the extra fuel required to charge the battery. On this basis, an instantaneous cost function can be calculated and minimized at each time step of the optimization horizon, by selecting a proper value for torque split control variable. The total equivalent fuel consumption is the sum of the real fuel consumption of ICE and the equivalent fuel consumption of the EM.

#### **2.5.4 Energy Management as an Optimization Problem**

The HEV energy management is typically a multi-objective nonlinear optimization problem with multiple input variables and multiple constraints. It is not easy to decide the rules to meet all important trade-offs among multiple variables in the control system of a HEV. The study of optimal strategy such as DP is beneficial to comprehend the drawbacks of the rules, and achieve construction of better rules.

For the design of a near-optimal EMS, a cost function needed to be defined for minimizing the combination of fuel consumption and emissions, then using DP to find the optimal control. Hence the correct gear shifting and power split between ICE and EM can be defined while maintaining the battery SOC in a certain preset thresholds. [10]

The DP solutions result in the rules for the gear shift logic and power split strategy which leads to the applicable rules. In addition, the power demand, engine speed and transmission input speed, can be selected as inputs to the control strategy to predict the optimal motor power in a split mode. The following three benefits result from the application of DP approach to establish rules in a parallel HEV: [38], [39]

- Optimal performance is known from the DP solutions.
- The rule-based algorithm is tuned to obtain near-optimal solution, under the predetermined rule structure and number of free parameters.
- The design procedure is re-useable for other types of HEVs or other objectives.

Many EMSs based on predefined driving cycles cannot be implemented online due to the fact that they optimize fuel economy for known driving cycles. Driving situation, road condition, and driver driving style are not part of the optimization process. An intelligent controller can predict the future condition; hence it can further optimize the vehicle performance in real world driving.

The energy management problem can be formulated as an optimization problem, where a cost function is minimized subject to constraints. The state variables are vehicle speed, engine speed, and energy storage levels. The control variables can be continuous, for instance, the power flow, or discrete, such as engine on/off, or complementary, meaning that only one of a set of variables can be nonzero at a time, like the gear position.

This optimization problem can be carried out off-line for a specific driving cycle. This gives a lower bound for what can be achieved in practice. For online application of an EMS, computation time is limited and a prediction of the future driving cycle is usually unavailable, which requires modifications to the optimization problem. [28]

## 2.6 HEV Powertrain Modeling and Simulation

Computer modeling and simulation can be used to reduce the expense and length of the design cycle of hybrid vehicles by testing configurations and EMS before prototype construction begins. Many designers use models in product development process, especially in automotive industries where shortening development cycle and reducing cost is critical under high competition pressure. Validated models which represent system characteristics accurately allow designers to explore options using virtual instead of physical systems and hence reduce resource investments significantly. Simulations accelerate powertrain design and control development in the early stage of the vehicle design process and certainly require mathematical models. Considering model inaccuracy, simulation error and environmental disturbances, designs need to pass experimental tests before they are finalized. Experimentations also play a role in tuning and calibrating simulation-based designs, especially for vehicle controllers.

Generally, sophisticated models increase modeling difficulty and time. Furthermore, simulations based on complex models may lengthen the execution time and make real-time processing impractical. Oversimplified models, on the other hand, may lead to improper results of the EMS if it is not able to correctly distinguish between operating points with different efficiency characteristics. Reasonable assumptions and simplifications can reduce model complexity, but at the price of modeling accuracy. Therefore, modelers need to make a compromise between these two factors to select models which are best suitable for their applications. The best model is the one that represents all the phenomena that are relevant to the intended purpose with the lowest complexity. Due to the existence of model uncertainty and disturbance, no model is perfect. However, if a model captures the main behaviors of a physical system with satisfactory accuracy, we consider that it is acceptable and valid.

Interest in hybrid vehicle simulation grew in the 1970's with the development of several prototypes that were used to collect a considerable amount of test data on the performance of hybrid drivetrains [40]. Activities under this area have resulted in the

development of a unique set of software tools to support vehicle technologies research. It is always interesting to evaluate what other researchers have already done. In this section other simulation programs will be briefly described. The last ten years simulation programs dedicated for the evaluation of vehicles have known an important progress. Most simulation tools were originally designed to evaluate specific drivetrains and each model has been implemented for its own particular scenario. They were mostly written in text-based languages, with data structures that were difficult to access. Admission for many of these programs is limited by commercial considerations. Multimedia technology allows now relatively rapid development of highly graphical and interactive user interfaces.

Most of the EMS based on global optimization (either numerical or analytical), and rely on mathematical models of the vehicle in order to calculate the fuel consumption starting from the driving cycle. For an accurate estimate of the fuel consumption, it is not necessary to capture all the details in the dynamic behavior of the powertrain, but it is important to take into account all losses and all the interactions between components. A low-level dynamic model of the powertrain including only vehicle and engine inertia, accounting for losses in all the major powertrain components, is sufficient to capture almost all the energy flows in the vehicle. Energy management approaches in vehicles can be realized through considering a number of factors including: environmental conditions, driver behavior, and vehicle specifications. In order to develop an EMS, a number of models need to be implemented and used.[1]

### **2.6.1 General Concepts**

A model is a mathematical representation of the behavior of a process, a logic concept, or the operation of a system. Mathematical models of dynamical systems, such as the system studied in this dissertation, are mostly executed in numerical simulation environments. The purpose of a numerical simulation is to mimic the actual behavior of a system under controlled operating conditions. Analyzing the model predictions allows one to improve the targeted aspects of the system in consideration. In automotive control applications, component and system models are used to achieve several objectives:



- Design Verification prior to implementation.
- Reduction in development time & calibration process.
- Reducing the need to perform costly and cumbersome experiments using a prototype of the physical system, so improving reliability.

Generally, two main approaches are usually used in vehicle simulation. These approaches are usually categorized according to the propagation of power flow inside the simulators. So, Forward-facing modeling simulates the physical behavior of each component with control instruction, handles state changes, and generates vehicle performance as output. While Backward-facing modeling takes the assumption that the vehicle meets the target performance, and calculates the component states. Backward-facing approach is beneficial in simplicity and computation cost, though they are usually used to define trends, while forward-facing approach is advantageous in utilizing performance details, though allow selection of powertrain configurations as well as development of controls that will later be implemented in the vehicles.

### **2.6.2 Forward facing models**

Forward-facing models follow a more realistic chain of computations from the standpoint of the causality of events that take place in an actual vehicle. In a forward-facing model, a driver model compares the simulated vehicle speed with the speed profile and generates accelerator and brake commands to the different powertrain and component controllers in order to follow the desired vehicle speed as shown in . These commands along with other feedback variables are then received by the HEV controller and are then translated into a torque provided by the ICE and/or EM and an energy use rate where a power split is computed. Using this power split, the energy consumption is calculated using look-up tables. The power provided by the actuators is then propagated downstream, in the direction of the physical power flow in the vehicle through the driveline by taking into account the component energy losses until it results in a tractive force at the tire/road interface. The resulting tractive power and the predicted road loads are used to compute

the vehicle speed which can be different from the original speed trace. The resultant acceleration is computed from  $a = F/m_{eff}$ , where  $m_{eff}$  includes the effect of rotational inertias in the drivetrain. The driver model will then modify its command depending upon how close the trace is followed. As components react as in reality to the commands, we can implement advanced component models, take into account transient effects (such as engine starting, clutch engagement/disengagement, or shifting), or develop realistic control strategies that would be later implemented in real-time applications. So, a forward-facing model requires smaller time steps, more component feedback, and more advanced simulation control for accurate vehicle modeling. This approach better represents how a vehicle is operated. Simulating a vehicle using a forward-facing model gives greater insight into the supervisory control strategy, which is a critical component for alternative fuel vehicles due to their more complicated operational modes. These types of simulators are well-suited for the implementation and comparison of control strategies and they enable prediction of maximum effort events and validation of actual vehicle behavior.

The forward-facing approach is particularly desirable for hardware development and detailed control simulation. Since forward-facing models deal in quantities measurable in an actual drivetrain such as control signals and true torques, vehicle controllers can be developed and tested effectively in simulations. Also, dynamic models can be included naturally in a forward vehicle model. Finally, this approach is well-suited to the calculation of maximum accelerations, as they are essentially Wide Open Throttle (WOT) events.

The main drawback in the forward-facing approach is the relatively poor simulation speed, where drivetrain power calculations rely on the vehicle states, including drivetrain component speeds that are computed by integration. Therefore, higher-order integrations using relatively small time steps are necessary to provide stable and accurate results. So, in these models, the driver commands are taken to calculate vehicle response, hence the flow of information is exactly the same as in the physical system. As a result, forward-facing simulation can be time-consuming for use in preliminary design studies.[41]

### 2.6.3 Backward facing models

In contrast, models that simulate vehicle operation based upon a velocity request at the wheels are defined as backward-facing models. In this type of models, the desired vehicle speed is transferred from the vehicle model back to the engine to finally find out how each component should be used to follow the speed cycle. The term backward-facing defines the direction that the power flows in order to meet the performance demands of the requested speed. Because of this model organization, quasi-steady models can only be used and realistic control cannot be developed. Consequently, transient effects cannot be taken into account. However, backward models are fast, reliable and require a straightforward solution strategy.

These models operate based on the assumption that a predefined vehicle speed trace is met by the vehicle. Therefore, the driver behavior is not modeled in the simulator. Based on the predicted road loads, the force required to accelerate the vehicle through the time step is calculated directly from the required speed trace. The required force is then translated into a torque that must be provided by the component directly upstream, and the vehicle's linear speed is likewise translated into a required rotational speed. Component by component, this calculation approach is carried backward through the drivetrain, against the tractive power flow direction, until the fuel use or electrical energy use that would be necessary to meet the trace is computed.

This modeling approach is convenient because automotive drivetrain components tend to be tested in a laboratory environment such that a table of efficiency or loss versus output torque and speed (or power) is developed. This means that a straightforward calculation can determine a component's efficiency and allow the calculation to progress. The explicit nature of the efficiency/loss calculation also allows very simple integration routines (e.g. Euler) to be used with relatively large time steps on the order of 1 [s]. Thus, simulations using the backward-facing approach tend to execute faster than forward-facing models; however, they pose major weaknesses as a result of the assumption that the vehicle speed trace is already met. Therefore, it is not possible to simulate events such as

full throttle acceleration in which the vehicle speed trace is not defined a priori and the maximum effort of the vehicle is to be determined.

Weaknesses of this approach come from the assumption that the trace is met and from the use of efficiency or loss maps. Since the backward-facing approach assumes that the trace is met, this approach is not well suited to compute best-effort performance, such as case occurs when the accelerations of the speed trace exceed the capabilities of the drivetrain. Also, because the efficiency maps are generally produced by steady-state testing, dynamic effects are not included in the maps or in the backward-facing model's estimate of energy use. A related limitation of the backward-facing model is that it does not deal in the quantities directly measurable in a vehicle. For example, control signals such as throttle and brake position are absent from the model, further hindering dynamic system simulation and detailed control system development.

When using backward-facing models, the control logic does not have to consider complicated system constraints because the models calculate the exact torque or speed that a system requires and allow the controller to have only feasible control options. In contrast, in forward-facing models, the controller considers constraints and component losses and instantaneously makes decisions for the entire system. Therefore, the controller needs to collect the information it requires from the components and produce a control signal according to time, and in a manner similar to that used by real vehicles. For these reasons, forward-facing models are considered to be more realistic than those that are backward-facing. The models developed in this work are also of forward-facing type.

#### **2.6.4 Modeling Tools**

Simulation tools are critical for implementation and verification of EMSs. So there are several effective vehicle simulators used in the initial phase for strategy development of vehicles. Effective and reliable software tools play a critical role in the optimization of vehicle structure, and verification of control strategies, especially energy management approaches, in the initial phase for vehicle design and development. Numerical modeling

and analysis for vehicle components are accomplished in these software tools where interconnection of vehicle powertrain components operating in different energy domains is permitted.[2]

Several computer programs have been developed to model the operation of hybrid electric powertrains, including: Simple Electric Vehicle Simulation (SIMPLEV) from the Department of Energy (DOE) Idaho National Laboratory, CarSim from AeroVironment Inc., JANUS from Durham University [42], Advanced Vehicle Simulator (ADVISOR) [41], [43], [44], Powertrain System Analysis Toolkit (PSAT), and Autonomie [45] from the DOE's National Renewable Energy Laboratory, GT-Suite [46], Matlab/ Simulink [47], [48].

The Automotive Research Center of the University of Michigan had developed a Hybrid Electric Vehicle Simulation (HE-VESIM) to study the potential fuel economy and emission benefits of a parallel hybrid propulsion system [49]. A previous simulation model (ELPH), and other work conducted by the hybrid vehicle design team at Texas A&M University is reported in [50], [51]. All of these software packages were designed to study issues related to EV and HEV design such as energy efficiency, fuel economy, vehicle emissions, power plant configurations, component sizing, EMS, and the optimization of important component parameters for several types of hybrid or electric configuration.

Simulation tools, more specifically forward-facing approaches which target specific vehicles, are widely used in the industry to properly address the component interactions that affect fuel consumption and performance. The backward-facing modeling system employed in ADVISOR determines the acceleration required throughout a driving cycle and calculates the powertrain torque required at each instant. In contrast, a forward-facing model such as PSAT employs a virtual driver that compares the trace speed with the actual vehicle speed and compensates with an adjusted torque command. This latter method of modeling is a more realistic simulation of vehicle performance. Consequently, control strategies are more accurately modeled in PSAT.[52]

## 2.7 Driving Cycles

The advantages of hybrid vehicles depend on how the vehicle is used. In particular, the hybridization advantages consist essentially in recovering potential and kinetic energy that would otherwise be dissipated in the brakes, and in operating the engine in its highest efficiency region. If the engine had a constant efficiency and the vehicle drove at constant speed on a flat road, there would be no advantage in a hybrid electric configuration. For that reason characteristics of the driving cycle will be considered in this section.

A driving cycle represents the way the vehicle is driven during a trip, and the road characteristics. The driving cycles generally, give appropriate weightage to the city and highway type of driving patterns. In the simplest case, it is defined as a sequence of vehicle speed and road grade. Together with some vehicle characteristics, this completely defines the road load, i.e., the force that the vehicle needs to exchange with the road during the driving cycle, which is the sum of inertia, grade, rolling, and aerodynamic drag resistances. It is important to point out that each term is a function of both the driving cycle (speed, acceleration, and grade) and the vehicle (mass, frontal area, coefficients of aerodynamic and rolling resistance). For this reason, the fuel consumption of a vehicle must always be specified in reference to a specific driving cycle. On the other hand, given a driving cycle, the absolute value of the road load and also the relative magnitude of its components depend on the vehicle characteristics.

Fuel economy is measured on a driving cycle for testing compliance of the vehicles with regulations. US, Europe and Japan have developed their own test procedures to measure vehicle emissions and fuel economy. Other countries have adopted these procedures, sometimes with modifications to suit their driving conditions. The driving cycle used is designed to represent the actual driving pattern on road. The US and European cycles are composed of a driving schedule that represents city driving pattern and another representing the highway driving. Europe uses the same cycle as the one used for emission measurement. This cycle is called New European Driving Cycle (NEDC). In Japan the (10-15) mode test cycle is used. By 2015 when new regulations would come in force a new cycle,

JC08 would be employed. South Korea has adopted only the city driving cycle of the US test procedure for their regulations.

### 2.7.1 United States (US) light-duty vehicle driving cycles

The necessity for a standard method to evaluate fuel consumption of all vehicles on the market, and to provide a reliable basis for their comparison, led to the introduction of a small number of regulatory driving cycles: any vehicle sold in a country has to be tested, according to detailed procedures, using one or more of these standard cycles. Several US driving cycles are defined, among them:

- The U.S. Federal Test Procedure (FTP) cycle, is based on the Urban Dynamometer Driving Schedule (UDDS), which simulates an urban route of 12.07 [km], 7.5 [miles] with frequent stops. The maximum speed is 91.2 [km/h], 56.7 [mph] and the average speed is 31.5 [km/h], 19.6 [mph]. Figure 11 is an updated version of the FTP driving cycle, in which the first 505 [sec] is repeated as a worm start phase.

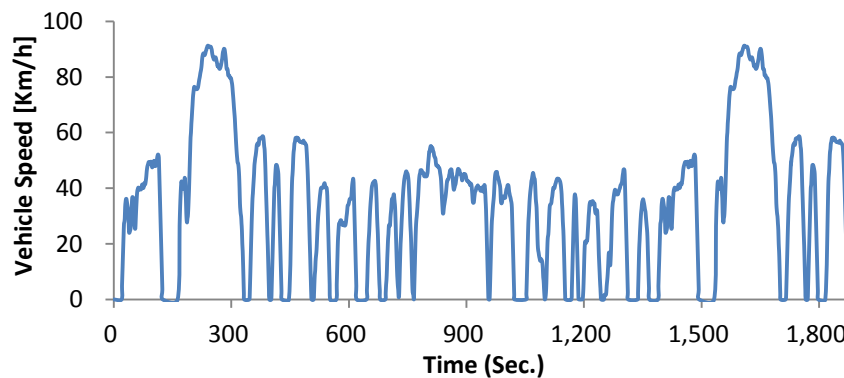


**Figure 11: The FTP-75 Driving Cycle**

- The Highway Fuel Economy Driving Schedule (HWY), Figure 12, is a chassis dynamometer driving schedule, developed by the US Environmental Protection Agency (EPA) for the determination of fuel economy of light duty vehicles representing highway driving conditions under top speed of 97 [km/h], 60 [mph]. The total duration of the cycle is 765 [sec], total distance of 16.45 [km], 10.26 [miles] and average Speed of 77.7 [km/h], 48.3 [mph].

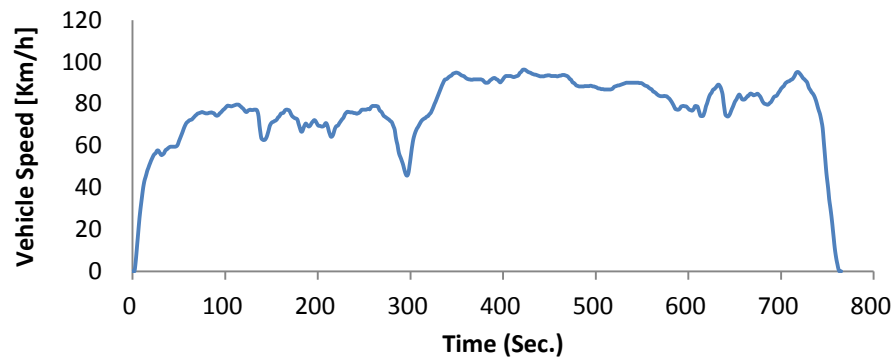


**Figure 12: The Highway Fuel Economy (HWY) Driving Cycle**

These driving cycles are designed to be representative of urban and extra-urban driving conditions, and reproduce measures of vehicle speed in real roads. Some of them and their test procedures have been recently updated to better suit modern vehicles.

### 2.7.2 European Union light-duty vehicle driving cycle

The New European Driving Cycle (NEDC), Figure 13, is performed on a chassis dynamometer for emission testing and fuel consumption. It is supposed to represent the typical usage of a car in Europe. It consists of four repeated Urban Driving Cycles (UDC), simulating city driving, and an Extra-Urban driving cycle (EUDC), simulating highway driving conditions.

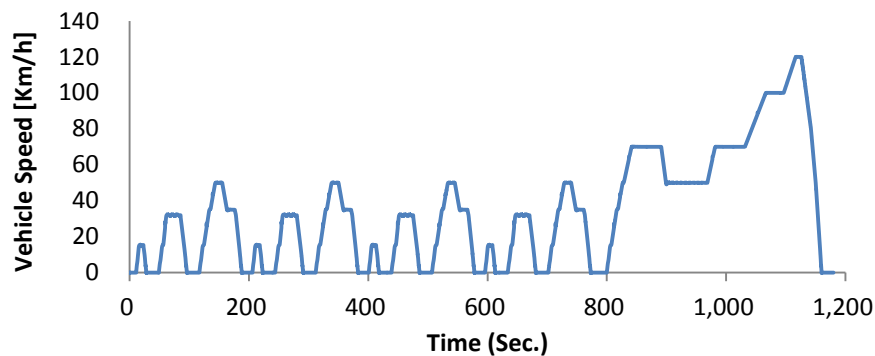


**Figure 13: The New European Driving Cycle (NEDC)**

It is noticed that the driving cycles used in different countries vary in average and maximum vehicle speeds, rate of accelerations and decelerations, frequencies of stop and start, idling time and total duration apart from actual driving pattern. All these factors affect



fuel economy ratings significantly. Some key parameters for these test cycles are compared in Table 1.

**Table 1: Comparison of Different Driving Test Cycles**

Test Cycle	Duration [sec]	Length [km]	Average Speed [km/h]	Maximum Speed [km/h]	Maximum Acceleration [m/s <sup>2</sup> ]	% Idle time
FTP	1874	17.77	34.1	91.2	0.65	18%
HWY	765	16.45	77,4	96.4	1.475	0%
NEDC	1180	11.01	33.6	120	0.833	23.4%

Even with the current improvements, these cycles should be considered a comparison tool rather than a prediction tool. In fact, it is not possible to predict how a vehicle will be driven, since each vehicle has a different usage pattern and each driver has his/her driving style. In order to obtain more realistic estimations of real-world fuel consumption for a specific vehicle, vehicle manufacturers may develop their own testing cycles. In the case of hybrid vehicles, estimating the actual driving cycles becomes an even more important task, because the actual fuel consumption is affected by the supervisory control strategy implemented, which is tuned using simulations based on the estimated driving cycles.

## 2.8 Summary

A brief overview was given in this chapter, focusing on the history of HEVs, different powertrain architectures, HEV control levels, energy management, control strategies, HEV powertrain modeling, and the role of vehicle driving cycles. A more complete introduction to HEV can be found in textbooks [2], [3], [53]–[57]. Several other theses and dissertations [58]–[60] also deal with the problem and provide details about some of the aspects that are not studied in detail in this work.

## Chapter 3. HEV Powertrain Modeling

### 3.1 Overview

Modeling approach has become an essential tool for mechanical engineers and automotive researches in improving efficiency and timing of vehicle design and development, resulting in the delivery of significant cost saving as well as environmental benefits. Modeling and simulation is generally defined as mathematical realization and computerized analysis of abstract representation of systems. Modeling and simulation help achieve insight into the functionality of the modeled systems, and investigate the systems behavior and performance. It is used in a variety of practical contexts relating to the design, development, and use of conventional as well as advanced vehicles including: design and evaluation of vehicle fuel consumption, emission, energy storage devices, ICE, hybrid powertrains, accessories, composite materials, determination of drag using wind tunnel, training drivers through virtual vehicle, collecting and analyzing sensory information, identifying critical test conditions, investigating crash factors, characterizing road topology, testing and analyzing EMS, and so on. [16]

Computer modeling and simulation can be used to reduce the expense and length of the design cycle of hybrid vehicles by testing configurations and EMS before prototype construction begins. Interest in HV simulation grew in the 1970's with the development of several prototypes that were used to collect a considerable amount of test data on the performance of hybrid drive trains. [47]

Since there exist modeling inaccuracy and hardware uncertainty, simulation is mainly used in the early stage of the design process to extract the designs that are inferior even in simulations. Obviously, any design needs to be tested in real systems before it is finalized for mass production. In addition to evaluating designs, simulation is also useful in guiding designs, e.g. system analysis, parametric study and sensitivity study. Moreover, real-time simulation finds applications in model validation and design calibration by using the Hardware in the Loop (HIL) and the Software in the Loop (SIL) methodologies.

Hybrid vehicles offer the promise of higher energy efficiency and reduced emissions when compared with conventional vehicles, but they can also overcome the range limitations inherent in a purely EV by utilizing two distinct energy sources for propulsion. In a hybrid powertrain, energy is stored as a petroleum fuel and in an electrical storage device, such as a battery pack, and is converted to mechanical energy by an ICE and EM, respectively. The EM is used to improve energy efficiency and vehicle emissions while the ICE provides extended range capability.[61]

The improvement in FE of HEV is achieved by the proper power split between the EM and the ICE, where the performance of the EMS is closely related to the power demand throughout the driving cycle. The power demand depends on the road, and the velocity profile. The performance of energy management can be improved if it is optimized for the driving conditions. Therefore, information about the driving route, a weather forecast, and traffic conditions, are very important in guaranteeing optimal performance of the EMS.

The opportunity to build models to evaluate conventional and hybrids allows the study of various designs to compare advantages and disadvantages of each configuration under the aspects of consumption, emissions and performance. The goal of the simulation program is to study power flows in drivetrains and corresponding component losses, as well as to compare different drivetrain topologies. This comparison can be realized at the level of consumption (fuel, electricity) and emissions ( $\text{CO}_2$ , HC,  $\text{NO}_x$ , CO) as well as at the level of performances (acceleration, range, gradeability). The general aim of the simulation program is to know the energy consumption of a vehicle while driving a certain reference cycle.

This chapter demonstrates modeling and simulation of a traditional ICE operated vehicle and a developed hybrid versions of the same vehicle using GT-Suite software. GT-Suite is a product of Gamma Technologies Inc. (GTI), a specialist software company which is solely focused on engines and vehicle industry, practically all leading engine makers and suppliers have chosen GT- Suite because it is supplied as an all-inclusive package with many valuable productivity tools that are included. These tools increase user efficiency, where it offers a versatile set of tools for simulation of vehicles with conventional, HEV or EV

drivelines, as well as the control systems and strategies that are keys to the operation of these vehicles. GT-Suite handles, in a single software tool, a wide variety of vehicle and engine technical applications. It is a versatile multi-physics platform for constructing a wide range of engineering models through a combination of different libraries. It is a unique tool, which provides the ability to execute integrated simulations of the entire vehicle and engine system. Such simulations are an industry trend that is gaining in importance and they constitute the next frontier in Computer Aided Engineering (CAE) applications. GT-Suite has long been recognized for its high degree of accuracy in predicting the behavior of complex engine related phenomena. At its core, the solver is based on the 1D solution of the fully unsteady, nonlinear equations. Beyond this core lie state of the art thermodynamic and phenomenological model solvers to capture the effects of combustion, heat transfer, evaporation, in-cylinder motion and turbulence, engine and tailpipe emissions.

In this study, the GT-Suite software is used for comparison between an ICE only vehicle and different hybrid architectures with the same engine. Separate models are investigated with rule-based EMS performing the same driving cycles. This includes a conventional vehicle, Series, Parallel and Series-Parallel hybrid configurations. Typical values of road resistances are used while running the models. The presented simulation models are dynamic, modular, forward-type simulation and consist of a driver sub-model trying to follow a predetermined speed profile. A demonstration of GT-Suite interface and a simple example assembly in order to give an introduction to the software could be found in [62].

### **3.2 Conventional ICE Vehicle Model**

A conventional ICE-driven drive train powered with a 2.0 [L] gasoline engine is modeled as a map-based engine representing engine performance, power output, fuel consumption, and other characteristics. The engine maps for these quantities are specified as a function of engine speed and load. Figure 14 shows the engine performance map used with the minimum Brake Specific Fuel Consumption (BSFC) line in red. An ICE controller is used to simulate engine control functions such as idling and fuel cut off, this object is recommended for applications where maximizing fuel economy is important.

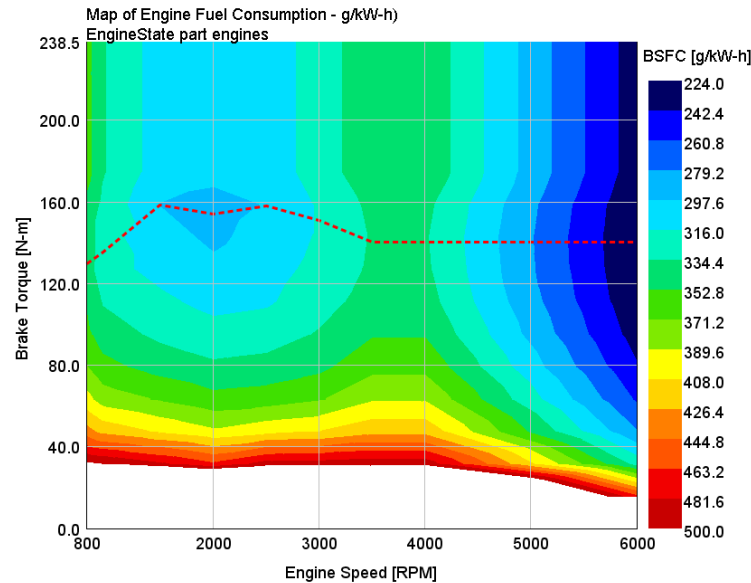


**Figure 14: ICE Performance Map**

The engine torque which is applied at the crankshaft is modeled by a look-up map and varies with accelerator pedal positions and engine speeds. A driver module is incorporated to represent the driver actions that control the accelerator pedal, brake pedal, and transmission gear number during driveway and shifting. The 'Driver Controller' is a model based controller that is typically used when performing dynamic driving cycle analysis. The model consists of a feed forward component which calculates the engine load torque required to correlate the desired vehicle speed or acceleration. For this calculation, the driver controller extracts key information from the vehicle drivetrain. Once the reference load torque is calculated a standard PI controller is used to correct the demanded load from the engine or brakes to minimize the remaining error between target and instantaneous values. A Transmission Controller is used to represent automatic transmission control logic for gear selection. This component is used to recall specified transmission shift logic to determine the desired transmission gear number. A Lockup clutch connection is used to model the action of a friction clutch between the engine and transmission. An Environment module is used to specify the ambient air conditions that affect the aerodynamic force on the vehicle. Several attributes are used to determine the air density including relative humidity, ambient air temperature and pressure. The wind velocity and direction are used

to determine the effective vehicle-air velocity. The density and effective air velocity are used in drag and lift force calculations. A Road module is used to model the road properties that affect vehicle dynamics including road grad, elevation, curvature radius, and rolling resistance. The conventional power plant model is shown in Figure 15, and Table 2 shows the engine and vehicle specifications used in the model.

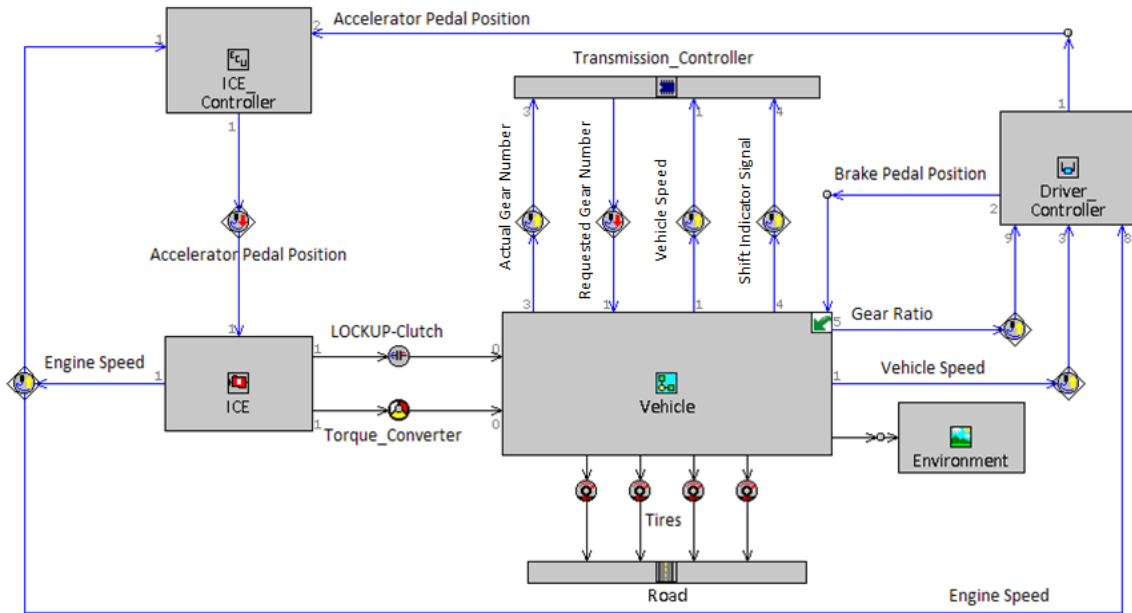


Figure 15: Conventional Power Plant Model

Table 2: Conventional ICE and Vehicle Specifications

Engine Specifications				
Total Displacement	2.0 L	Min Operating Speed	500 rpm	
Max Torque	225 Nm @ 3000 rpm	Engine Idle Speed	800 rpm	
Max Power	127 HP @ 4500 rpm	Max Engine Fueling Speed	6000 rpm	
Engine Inertia	0.6 kgm <sup>2</sup>			
Vehicle Specifications				
Vehicle weight	2000 kg	Vehicle Drag Coefficient	0.31	
vehicle rolling resistance coefficient	0.01	Vehicle Frontal Area	2.5 m <sup>2</sup>	
		Wheel Base	2 m	
Transmission Gear Ratios				
Gear #1	Gear #2	Gear #3	Gear #4	Gear #5
3.5	2.1	1.4	1	0.72

### 3.3 Hybrid Vehicle Model

Traditionally, HEVs were classified into two basic layouts, series and parallel. With the introduction of some HEVs offering the features of both the series and parallel hybrids, the classification has been extended to three kinds, series, parallel and series–parallel. Figure 3 shows the corresponding functional block diagrams, in which the electrical and mechanical links are bidirectional while the hydraulic link is unidirectional. [5]

In addition to the same 2.0 [L] gasoline ICE, typical components which are commonly found in HEV configurations are developed and modeled. These include map-based modules for traction motor and generator. The model considers the specification of electrical power request or mechanical brake power or torque, plus an electrical-to-mechanical (or vice versa) power conversion efficiency and mechanical friction characteristic. The traction motor and generator are controlled via two electro-mechanical controllers which are programmed to follow the control strategy rules. The brake power necessary to follow a certain driving cycle is calculated by a power demand template, which is also a model based controller. It calculates the necessary tractive power or axle torque required for a targeted vehicle speed or acceleration including tire rolling resistance, aerodynamic drag, road curvature and road grade effects.

A model for the battery pack of a capacity of 23 [Ah] is developed and represented by charge and discharge lookup maps for internal resistance and open-circuit voltage that are already given in the GT-Suite library. The battery model calculates the State of Charge (SOC) which is defined as the level of electric capacity remaining in the battery. The SOC is calculated based on the power being drawn from or supplied to the electric circuit, depending on the direction of the current. An inverter is used in conjunction with the battery pack template to ensure the maximum discharge and charge power limits of the battery are not exceeded when it is connected to the electrical or electromagnetic components. The inverter is a control-based compound that outputs the electrical power limits based upon the maximum available discharge and charge power as given in Table 3.

**Table 3: HEV Model Specifications**

Battery / Inverter Specifications			
Batt. max. charge current	50 A	Batt. capacity	23 Ah
Batt. max. discharge current	100 A	SOC max. limit	0.7
Batt. max. voltage	400 V	SOC min. limit	0.5
Batt. min. voltage	200 V		

A Braking Module is introduced to calculate the brake pedal position based upon the desired braking power, and maximum torque capability of the brakes. This module is equipped with a braking control strategy that allow for energy regeneration according to the vehicle operating mode and under the supervision of the main control strategy.

The supervisory controller acts as a high-level vehicle control system that coordinates the overall powertrain to satisfy certain performance target, and serves as an energy management unit. The EMS refers to a control algorithm that determines the proper power/torque level to be generated, and its split between the EM and the ICE while satisfying the power demand from the driver and maintaining sufficient energy in the energy storage device. The primary objective of the EMS is to coordinate the power flow between the energy carriers and the environment in response to the driver's power demand, while improving fuel economy, reducing exhaust emissions and maintaining various subsystems in their desired states without affecting vehicle performance constraints, such as acceleration and gradeability, ensuring seamless operation of the drivetrain.

The supervisory controller in the represented HEV models is based on a rule-based EMS which is a heuristic approach that is often applied in real-time implementations, where the power source is assigned to the ICE, the battery pack, or to a combination of both, based not only on the battery SOC status, but also on the power demand from the driver. The design process starts from interpreting the driver pedal signal as a power request, and according to this power request the EMS should determine the power flow in the hybrid



powertrain, how much power is needed to drive the wheels based on the acceleration command, and how much is needed to charge the battery based on the SOC. Then it should split the requested power between the ICE and the EM. If the battery needs to be recharged, the ICE should provide the power for both driving the wheels and charging the battery.

The Rule-based control strategies are composed of “if-then” type rules in accordance with the ICE operating conditions: it shuts down or it can provide a fraction of the total power request. This strategy uses the ICE as a primary power source, while utilizes the EM for supplemental power. The main aspect involved in these strategies is their effectiveness while implementation in real-time supervisory control to manage power flow in a hybrid powertrain. [7], [18]

### **3.3.1 Series HEV Model**

A Series HEV configuration dynamically runs different driving cycles is modeled, where the brake power necessary to follow a driving cycle is calculated by the power demand template and the request is actuated on the traction motor, which is also used for regenerative braking. The battery discharge limiter ensures that the connected battery with the traction motor and generator is not overdrawn. The generator acts as an integrated starter/generator so the ICE can be shutoff and turned back on.

The control strategy is a "thermostat on-off" strategy. The ICE/generator set is shutoff when the battery SOC is between certain limits during battery discharge. When the battery SOC decreases below 0.5, the starter/generator turns the engine on and the generator charges the battery. The ICE is run at its lowest BSFC speed for maximum efficiency. When the battery SOC is charged above 0.7, the ICE/generator set is shut back off. The Series HEV plant modeled is shown in Figure 16.

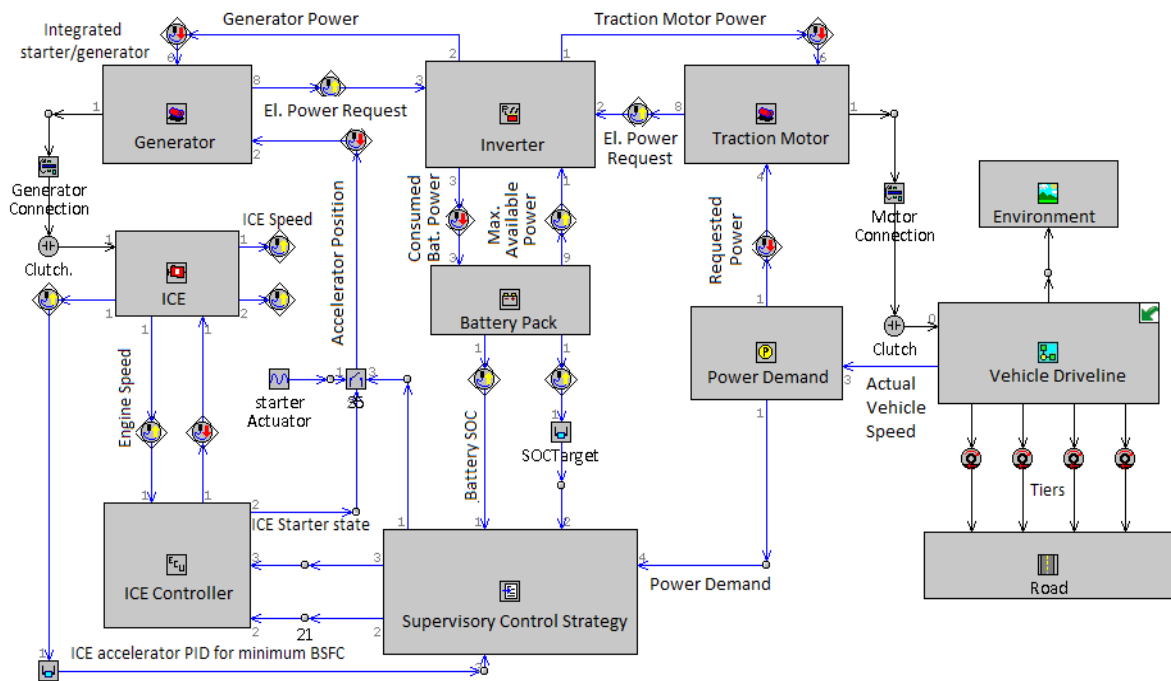


**Figure 16: Series HEV Power Plant Model**

### 3.3.2 Parallel HEV Model

A torque coupling-type parallel HEV was modeled as a basic model which could be further modified into two configurations according to the location of the traction motor. A pre-transmission parallel hybrid, in which the traction motor is connected to the ICE prior to the transmission, and a post-transmission parallel hybrid, in which the traction motor is connected to either the driven axle, after the final drive, or the non-driven axle.

In the presented parallel pre-transmission hybrid configuration there is only one traction motor that acts as propulsion motor or generator for charging the batteries as shown in Figure 17. The vehicle has the features of motor drive away, idle stop and regenerative braking. The control system is setup in such a way that, anytime the vehicle stops for over a second, the engine is switched off. When the vehicle begins to move again, the motor powers the driveline and also cranks up the engine. Once the engine reaches a preset speed, the motor actuator position is set to zero. Until the engine reaches the preset speed, it is merely motored and not fueled hence increasing fuel economy.

The regenerative braking works by setting a negative actuator position when the brake pedal position is positive. Since the regenerative brakes may not be able to provide enough braking torque for every braking event, friction brakes are also provided. There is a charging circuit that sets a negative actuator position for the EM depending on the battery SOC.

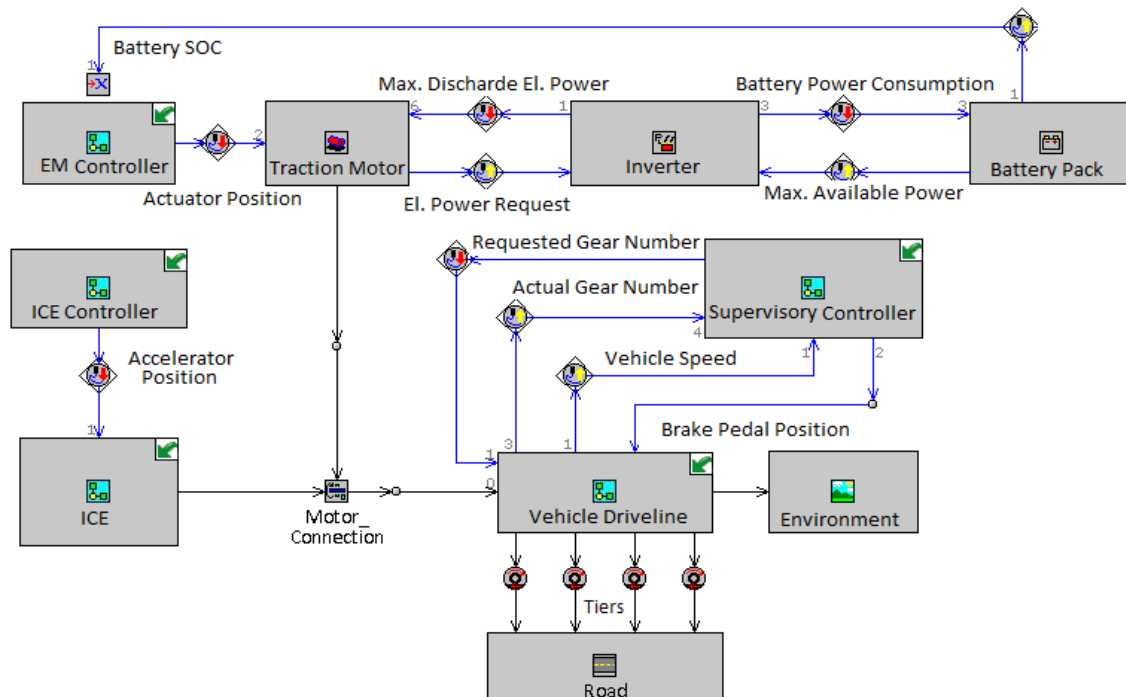
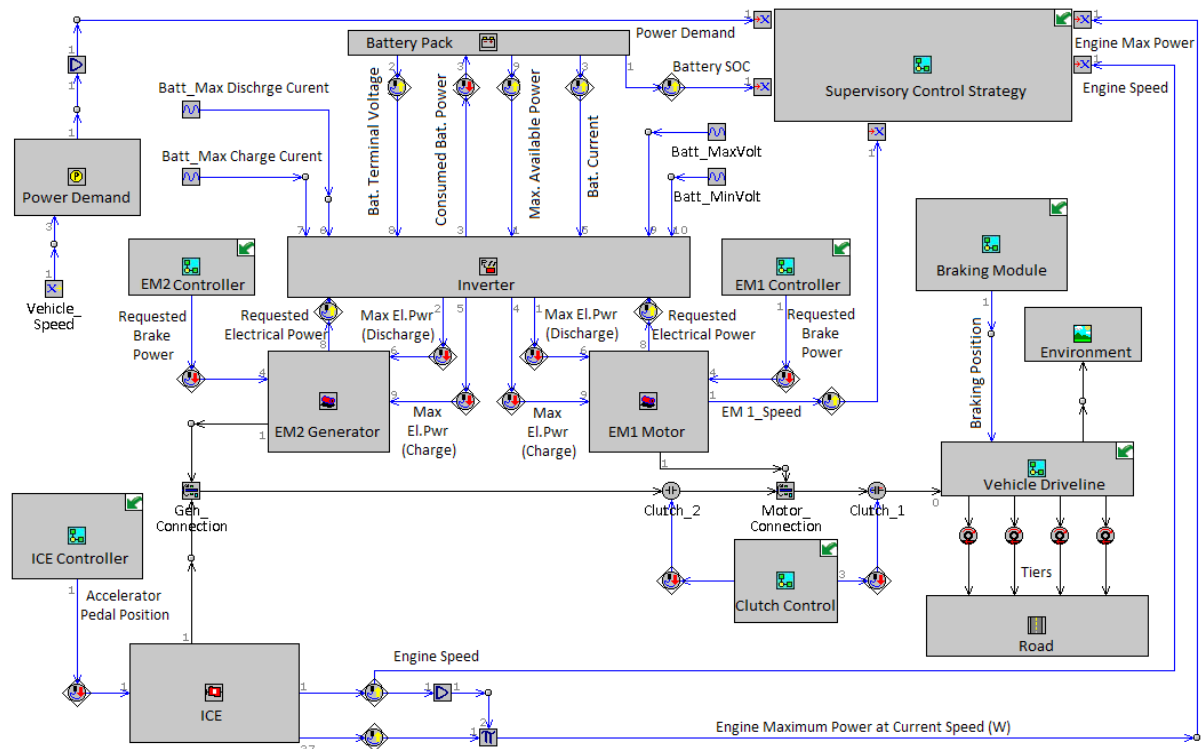


Figure 17: Parallel HEV Power Plant Model

### 3.3.3 Series-Parallel HEV Model

The model of the Series-Parallel HEV configuration consists of a combination of ICE and generator subsystem using a planetary gear set to connect each other and an electric drive subsystem, constructing two driving power sources, each has its own controller. In order to ensure the proper functionality of all controllers together to meet the required driver's power demand and provide an efficient onboard energy usage, a supervisory controller is required to maintain the vehicle at its most efficient operating conditions by managing the power among the two driving power source subsystems.

The series-parallel HEV architecture combines the advantages of both series and parallel powertrains. The model utilizes the same map-based 2.0 [L] gasoline ICE with some modifications made to its controller to allow the execution of the main control strategy rules. The necessary tractive power to follow a certain driving cycle is calculated by the power demand template. The torque request includes the necessary torque to accelerate the vehicle and its cargo mass as well as the vehicle system inertias. Two map-based modules, EM1\_Motor and EM2\_Generator, are used to model the electro-mechanical motor and generator, which are controlled via two programmed controllers to follow the control strategy rules. The traction motor and the generator are configured such that by closing a single clutch the architecture can be changed from series to parallel. Clutch\_1 is used to model the action of a dry clutch between two 1-D rotational mechanical assemblies, naming traction motor shaft and driveline input shaft. Clutch\_2 is used to model a simple clutch which is either engaged or disengaged by applying a constraint to set the two angular velocities on either side of the clutch equal to each other. Figure 18 shows the configuration of the developed series-parallel HEV power plant model.



**Figure 18: Series-Parallel HEV Power Plant Model**

There are six independent input parameters that affect the control strategy as follow:

1. The necessary tractive power demand to follow a given driving cycle.
2. Battery status which is determined via the battery SOC and helps to switch between charging and discharging modes according to the prescribed limits.
3. Vehicle and engine speeds which are used to select of the best operating mode.
4. Engine max power at current speed which helps in combination with the power demand in determination of the amount of power required from the EM.
5. Traction motor speed aids in determination of the maximum available motor braking power during regenerative braking and provides information of the required additional braking by the mechanical friction brakes.

The control strategy of the series-parallel HEV evolves two main operational modes; the series mode which is shown in Figure 19, in which the traction motor draws power from the battery and provides propulsion to the vehicle as long as the traction power demand is positive while the ICE is turned off. The vehicle is operated in series (electric only) mode until the vehicle speed reaches a switching speed limit, and then the parallel (ICE only) mode is triggered and the ICE is turned on and provides traction. Additionally, in series mode, the engine will also be turned on if battery SOC falls below the minimum limit, battery charging is triggered to allow for recharging the battery through the generator and lasts until it reaches the maximum battery SOC charging limit. Figure 20 shows the parallel mode operation strategy. In this mode, the ICE provides traction power as long as the vehicle speed is higher than the switching speed. During driving on this mode, if the required traction power exceeds the engine's power, the EM is launched and the hybrid mode is triggered to deliver power, if not and the SOC is lower than the maximum battery charging limit, the battery charging mode starts.

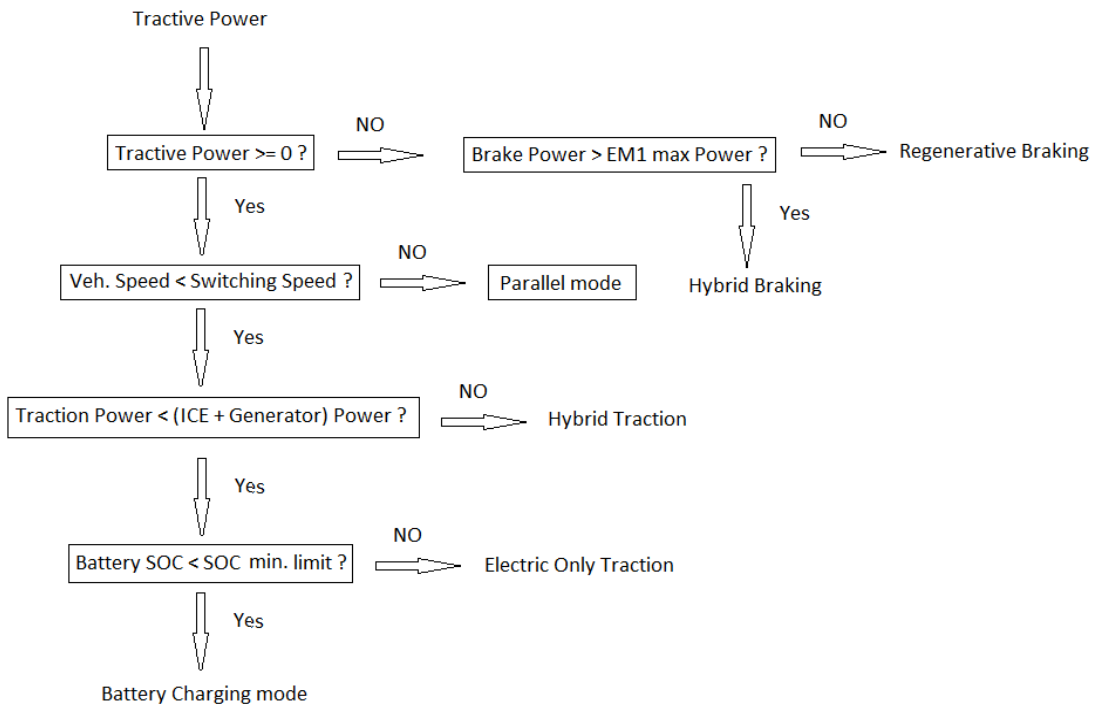


**Figure 19: Series Mode Strategy**

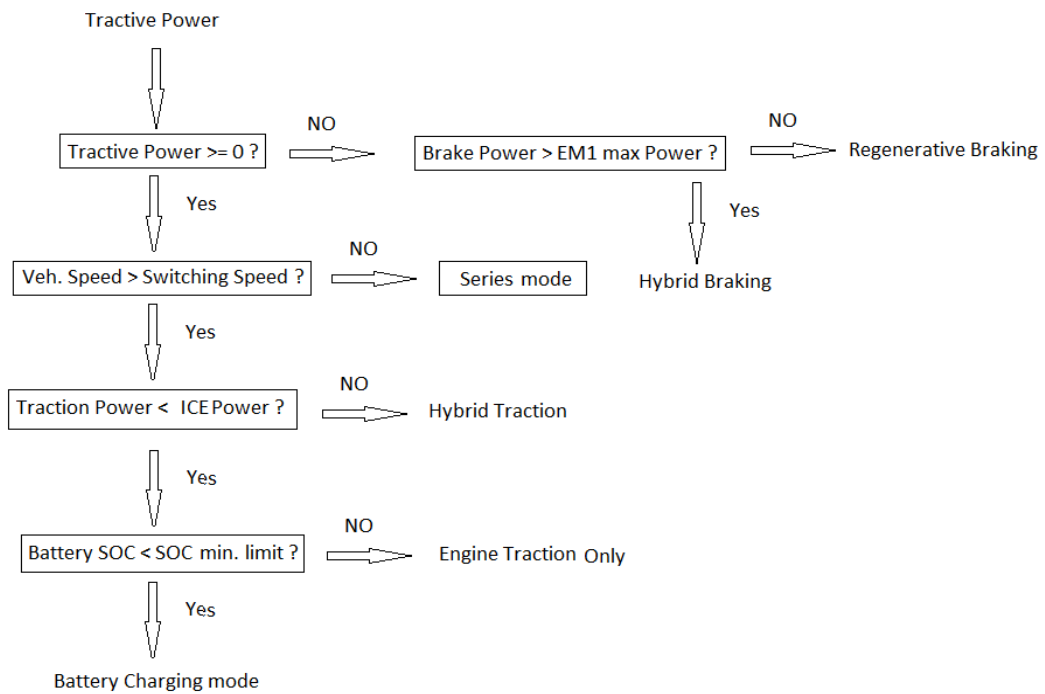


**Figure 20: Parallel Mode Strategy**

### 3.3.4 Selection of Driving Cycles

For the purpose of quantitative validation of the developed plant models, the FTP city drive cycle is used. This driving cycle is mainly selected for the fuel-economy related validation. The HWY fuel economy driving cycle, which represents a mixture of rural and interstate highway driving, is used to simulate typical longer trips in free-flowing traffic with no stops. Also, the US06 is used. Finally the NEDC, which is performed on a chassis dynamometer for emission testing and fuel consumption, to represent the typical usage of a car in Europe is used.

### 3.4 Model Governing Equations

The GT-Suite uses velocity and time data from the driving cycle to compute the vehicle energy use and to do this, as any other modeling program, the forces acting on the vehicle must be calculated prior to determining energy use. The forces acting on the vehicle are calculated from the road load equation as follows:

$$F = \frac{1}{2} \cdot \rho \cdot C_D \cdot A_f \cdot V^2 + C_R \cdot M_v \cdot \cos(\theta) + M_v \cdot g \cdot \sin(\theta) \quad (3.1)$$

The power demand calculated by the models includes the external forces contained in the road load equation: aerodynamic drag, tire rolling resistance, and road grade and road curvature. The torque request also includes the torque necessary to accelerate the vehicle and cargo mass as well as major vehicle system inertias, such as the axle/wheel inertias and the effect of overall driveline efficiency. By multiplying the road load by the velocity, the road power is calculated as a function of time as follows:

$$P(t) = \left[ \frac{1}{2} \cdot \rho \cdot C_D \cdot A_f \cdot v(t)^2 + C_R \cdot M_v \cdot \cos(\theta) + M_v \cdot g \cdot \sin(\theta) \right] \cdot v(t) \quad (3.2)$$

The power is then converted to energy by multiplying the road power by the time step giving the road load energy as follows:

$$E_{RL}(t) = P(t) \cdot \Delta t \quad (3.3)$$

In order to take into account the energy associated with acceleration or deceleration as velocity changes over each time step. The kinetic energy required to accelerate or decelerate the vehicle over each time interval is computed as:

$$\Delta KE = E_{KE}(t) = \frac{1}{2} \cdot M_v \cdot (v(t + \Delta t)^2 - v(t)^2) \quad (3.4)$$

The energy losses comprised from the powertrain losses, and the rotational inertial losses. The powertrain energy losses ( $E_{PTL}$ ) depend on the powertrain component efficiency. This quantity is the combined energy losses between the energy sources and the road. The inertial energy losses associated with acceleration or deceleration of the vehicle is computed as follows:

$$E_{Inertia}(t) = I \cdot \alpha(t) \quad (3.5)$$

Then the overall energy requirement is found by the summation of the road load energy, kinetic energy required for acceleration or deceleration, powertrain energy losses, and inertial energy losses as follows:

$$E_{Overall} = \sum E_{RL}(t) + \sum E_{KE}(t) + E_{PTL}(t) + \sum E_{Inertia}(t) \quad (3.6)$$

Using the fuel lower heating value and the ICE BSFC, the fuel conversion efficiency, which is the ratio of work produced to the amount of fuel energy supplied, is calculated as follows:

$$\eta_{fuel} = \frac{1}{BSFC \cdot Q_{HV}} \quad (3.7)$$

In order to measure the fuel economy, which is the distance traveled using a specific volume. The BSFC is obtained from the map-based engine at certain engine speed and load. Then the equivalent fuel mass is computed using the fuel conversion efficiency along with the fuel lower heating value as follows:

$$m_f = \frac{E_{Overall}}{\eta_{fuel} \cdot Q_{HV}} \quad (3.8)$$

Then the equivalent volume is computed, and the distance traveled is divided by the equivalent volume.



### 3.5 Simulation Results

First, the conventional ICE vehicle model is run with the aforementioned ICE and vehicle specifications using the selected driving cycles and the most interested outputs were plotted to be used in a comparative analysis with the three different HEV powertrain models results. The results of this section were presented in [61].

#### 3.5.1 FTP Driving Cycle Outputs

The FTP driving cycle results are categorized and represented in two groups:

- The first group is illustrated in Figure 21 to Figure 24, and demonstrates the fuel consumption rate and the battery SOC for different layouts during the driving cycle.
- The second group is illustrated in Figure 25 to Figure 28, and demonstrates the corresponding vehicle power demand, engine power and the traction motor power produced to follow the driving cycle.

For the simulated series HEV powertrain, the ICE/generator set provides more power to run the motor and charge the battery pack whenever the battery SOC hits its lower limit, and stops whenever it hits its upper limit. Because of the increased utilization of all electric driving, a higher percentage of fuel usage is eliminated, and under certain driving conditions it is not necessary to use on-board fuel at all as shown in Figure 22, and Figure 26.

For the parallel HEV powertrain, it is clear that the vehicle behavior follows the control strategy during the FTP driving cycle, where the EM acts as propulsion motor during starting and as a generator for charging the batteries during regenerative braking mode, and assists the ICE during high power demand periods as shown in Figure 23, and Figure 27.

For the simulated series-parallel HEV powertrain, the developed model follows the previously explained EMS, where the ICE provides power under certain conditions, either the required speed exceeds the switching speed or the battery SOC drops under its minimum limit, otherwise the EM provides the demanded power to follow the prescribed driving cycle speed as shown in Figure 24, and Figure 28.

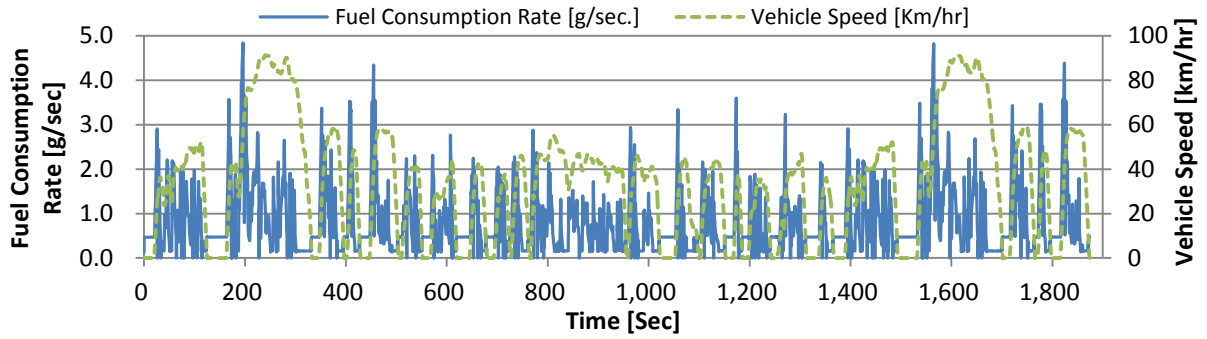


Figure 21: Conventional Vehicle Undergoing FTP Driving Cycle

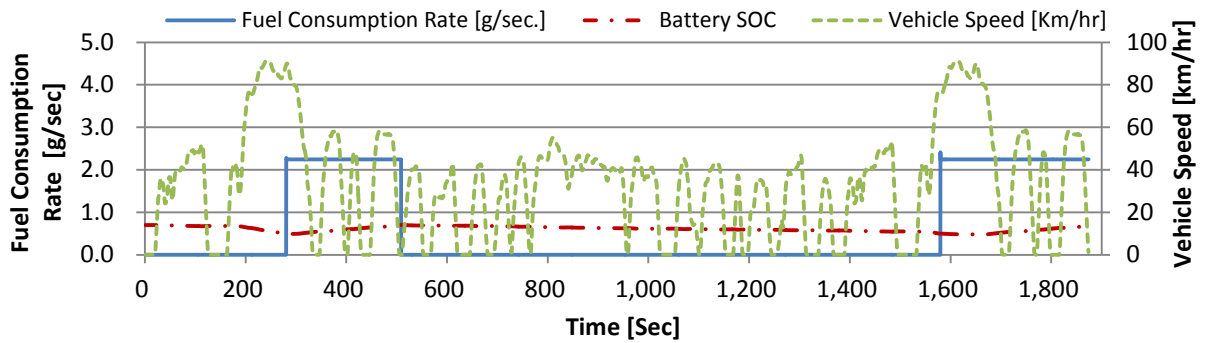


Figure 22: Series HEV Undergoing FTP Driving Cycle

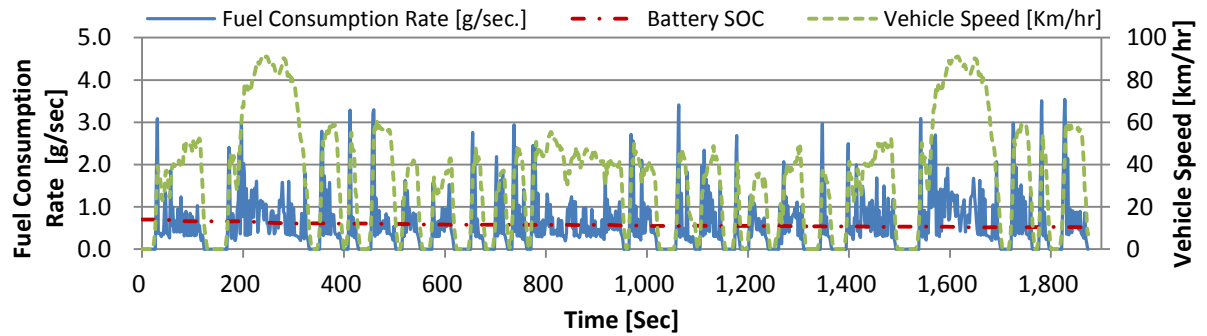


Figure 23: Parallel HEV Undergoing FTP Driving Cycle

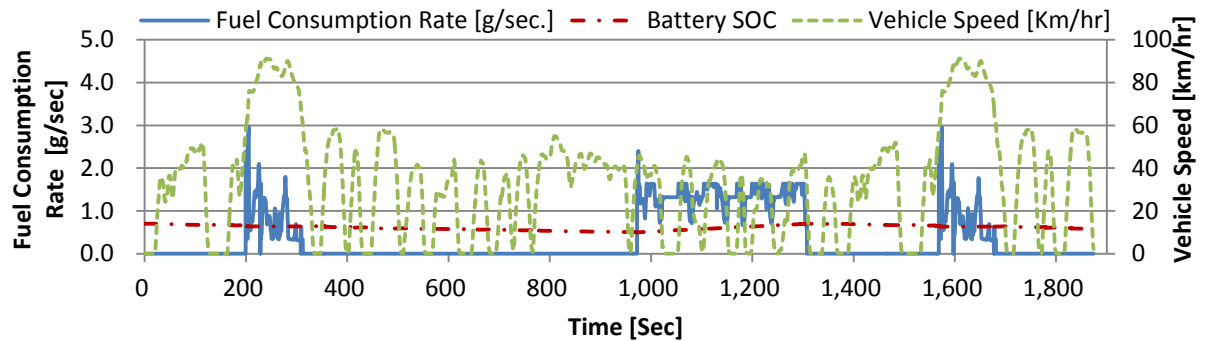
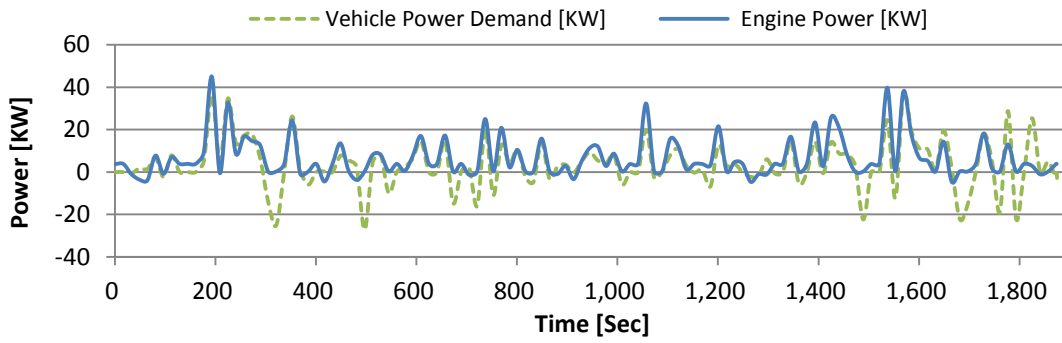
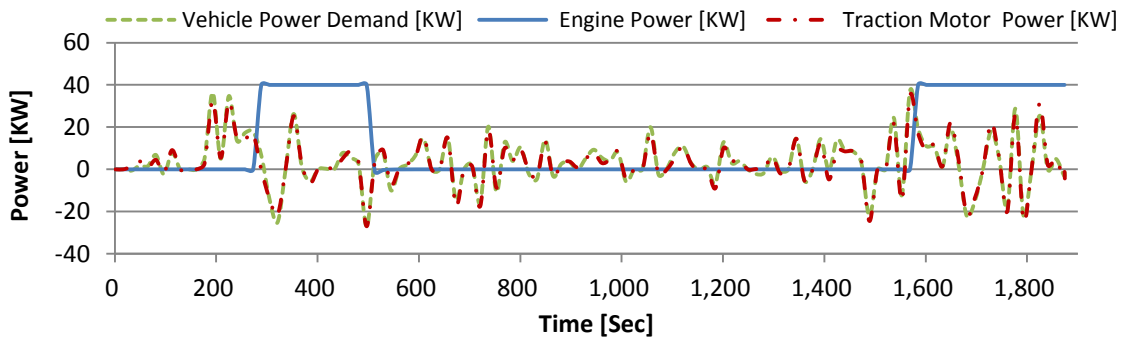


Figure 24: Series-Parallel HEV Undergoing FTP Driving Cycle



**Figure 25: FTP: Power Demand and Power Production in Conventional Vehicle**



**Figure 26: FTP: Power Demand and Power Production in Series HEV**

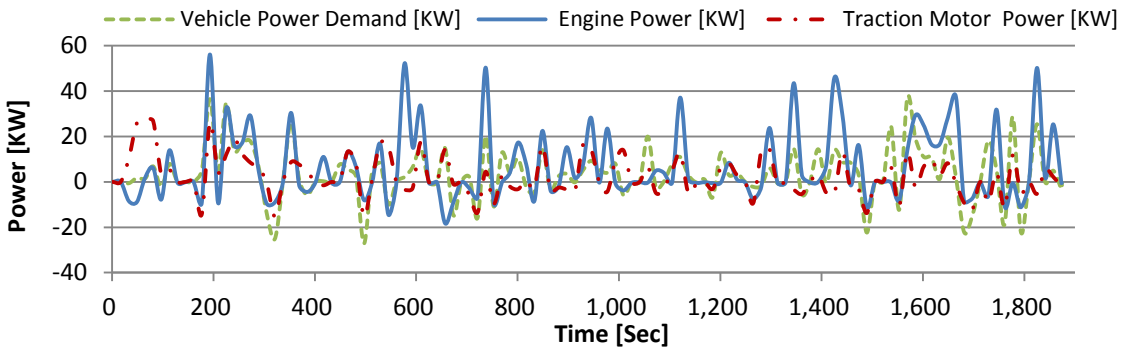


**Figure 27: FTP: Power Demand and Power Production in Parallel HEV**

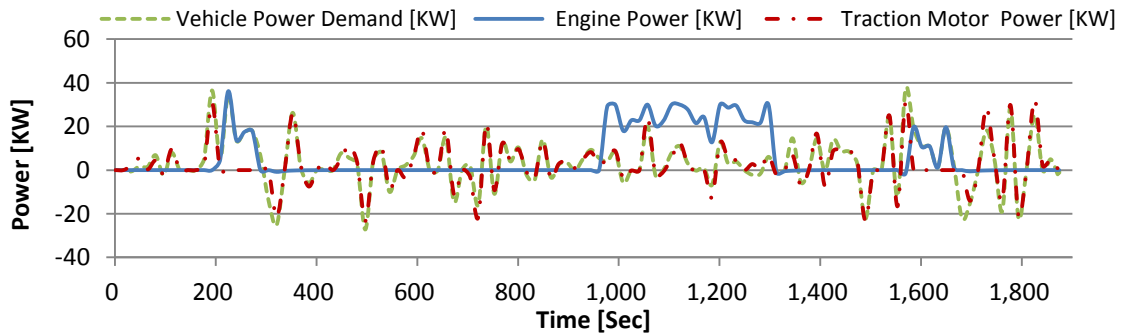


**Figure 28: FTP: Power Demand and Power Production in Series-Parallel HEV**

### 3.5.2 HWY Driving Cycle Outputs

The HWY driving cycle results are categorized and presented in the same two groups:

- The first group is illustrated in Figure 29 to Figure 32, and demonstrates the fuel consumption rate and the battery SOC for different layouts during the driving cycle.
- The second group is illustrated in Figure 33 to Figure 36, and demonstrates the corresponding vehicle power demand, engine power and the traction motor power produced to follow the driving cycle.

For the simulated series HEV powertrain, it is clear that the vehicle's behavior obeys the control strategy, where the ICE/generator set provides more power to run the motor and charge the battery pack whenever the battery SOC hits its lower limit, and stops whenever it hits its upper limit. But during the HWY driving cycle and due to the high power demand arises from the high vehicle speed requirements, the ICE is running much longer periods as shown in Figure 30, and Figure 34. The tradeoff of the series powertrain is that there are always two energy conversions, mechanical to electrical, and electrical to mechanical, resulting in greater energy losses. For this reason, the series hybrid vehicle consumes more fuel than a conventional ICE during highway driving.

For the parallel HEV powertrain, it is clear that the vehicle behavior follows the control strategy during the HWY driving cycle, where the EM acts as propulsion motor during starting and as a generator for charging the batteries during regenerative braking mode as in Figure 31, and assists the ICE during high power demand periods. It is also computed that the ICE doesn't switched off because the vehicle doesn't stop as shown in Figure 35.

For the simulated series-parallel HEV powertrain, the developed model follows the previously explained EMS, where the ICE provides power under certain conditions, either the required speed exceeds the switching speed or the battery SOC drops under its minimum limit, otherwise the EM provides the demanded power to follow the prescribed driving cycle speed as shown in Figure 32, and Figure 36.

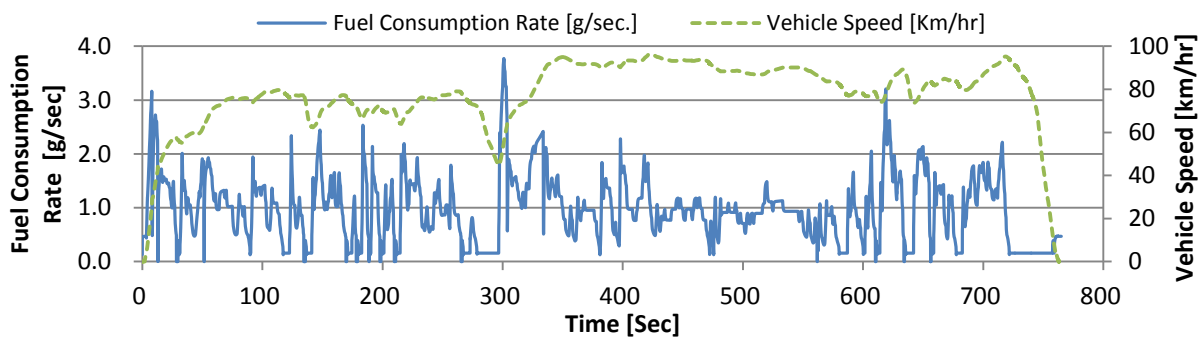


Figure 29: Conventional Vehicle Undergoing HWY Driving Cycle

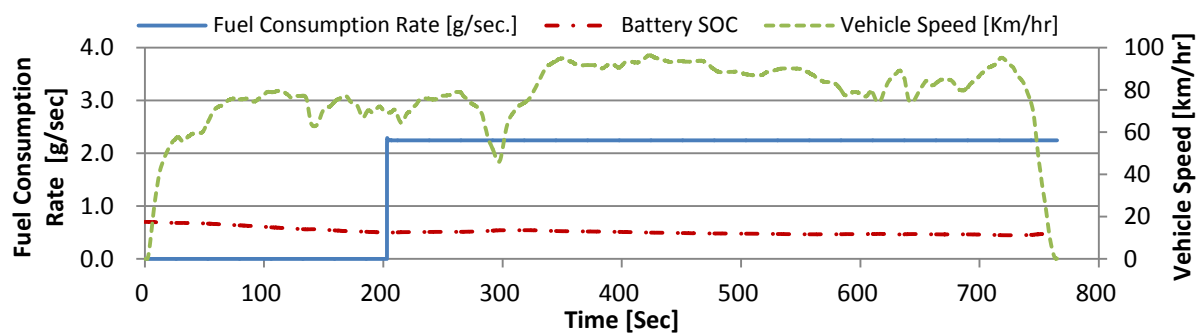


Figure 30: Series HEV Undergoing HWY Driving Cycle

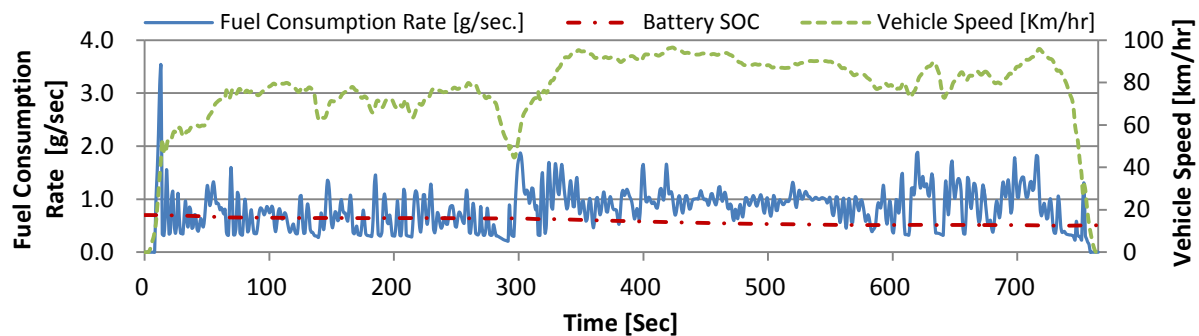


Figure 31: Parallel HEV Undergoing HWY Driving Cycle

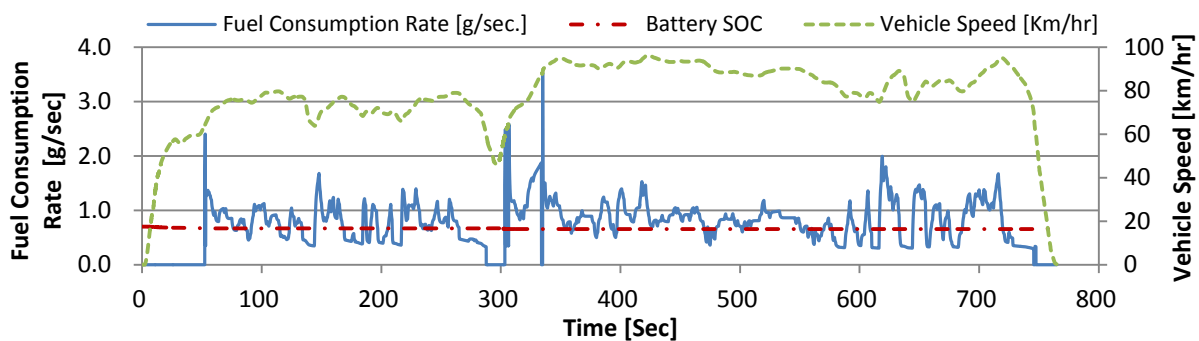
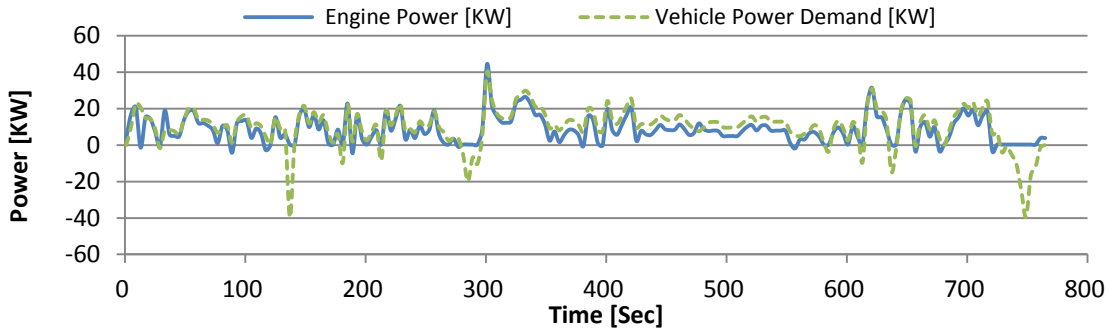
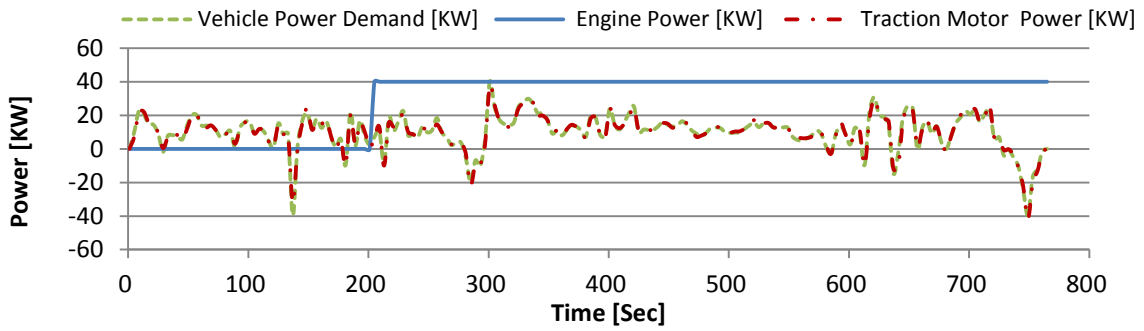


Figure 32: Series-Parallel HEV Undergoing HWY Driving Cycle



**Figure 33: HWY: Power Demand and Power Production in Conventional Vehicle**



**Figure 34: HWY: Power Demand and Power Production in Series HEV**

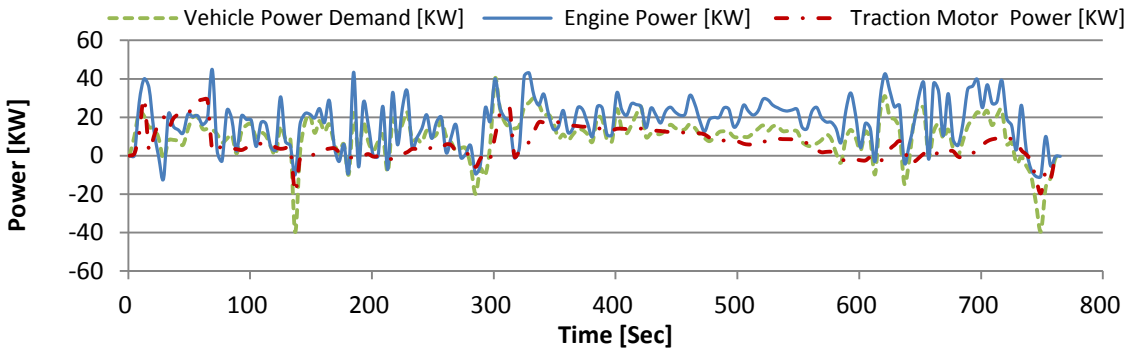


**Figure 35: HWY: Power Demand and Power Production in Parallel HEV**

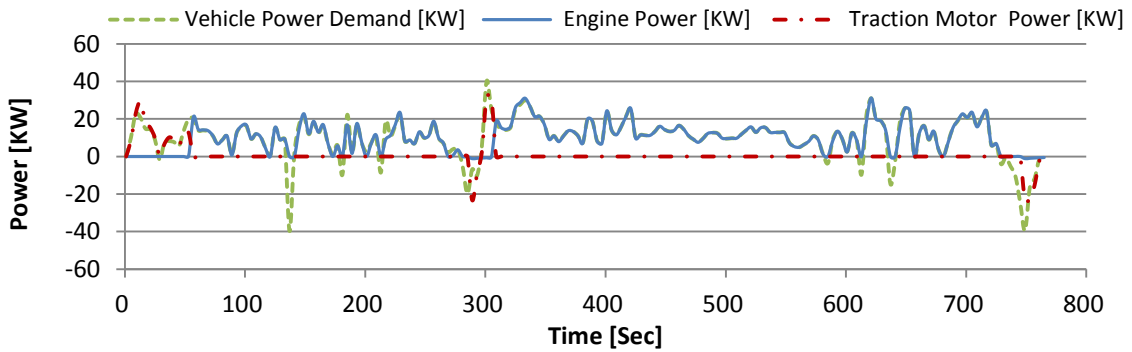


**Figure 36: HWY: Power Demand and Power Production in Series-Parallel HEV**

### 3.5.3 US06 Driving Cycle Outputs

The same results for the US06 driving cycle simulation are grouped in two groups, categorized and presented as follows:

- The first group is illustrated in Figure 37 to Figure 40, and demonstrates the fuel consumption rate and the battery SOC for different layouts during the driving cycle.
- The second group is illustrated in Figure 41 to Figure 44, and demonstrates the corresponding vehicle power demand, engine power and the traction motor power produced to follow the driving cycle.

For the simulated series HEV powertrain, it is clear that the vehicle's behavior obeys the control strategy, where the ICE/generator set provides more power to run the motor and charge the battery pack whenever the battery SOC hits its lower limit, and stops whenever it hits its upper limit. But due to the aggressive features of the US06 driving cycle and due to the high power demand arises from the high acceleration requirements, the ICE is running much longer periods as shown in Figure 38, and Figure 42.

For the parallel HEV powertrain, it is clear that the vehicle behavior follows the control strategy during the US06 driving cycle, where the EM acts as propulsion motor during starting and as a generator for charging the batteries during regenerative braking mode as in Figure 39, and assists the ICE during high power demand periods. It is also computed that the ICE is switched off when the vehicle stops as shown in Figure 43.

For the simulated series-parallel HEV powertrain, the developed model follows the previously explained EMS, where the ICE provides power under certain conditions, either the required speed exceeds the switching speed or the battery SOC drops under its minimum limit, otherwise the EM provides the demanded power to follow the prescribed driving cycle speed as shown in Figure 40, and Figure 44.

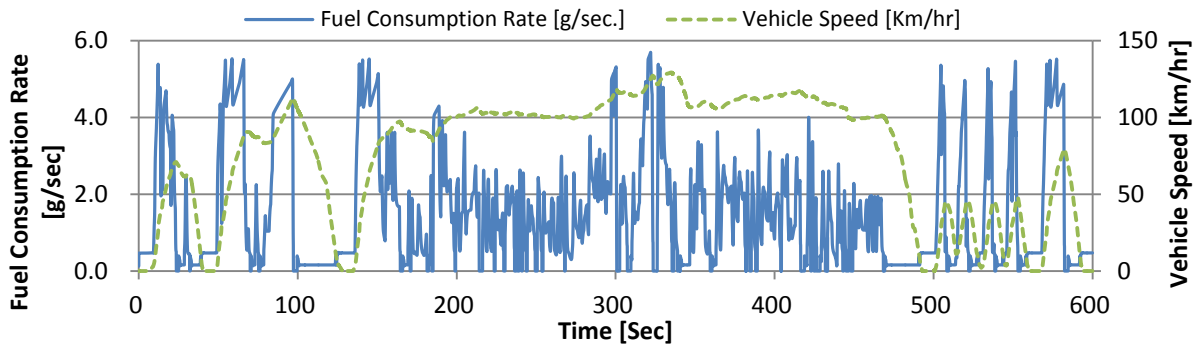


Figure 37: Conventional Vehicle Undergoing US06 Driving Cycle

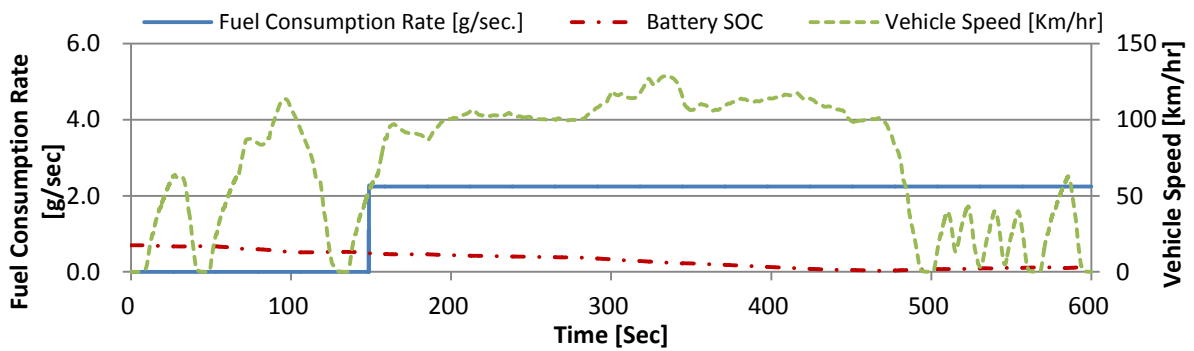


Figure 38: Series HEV Undergoing US06 Driving Cycle

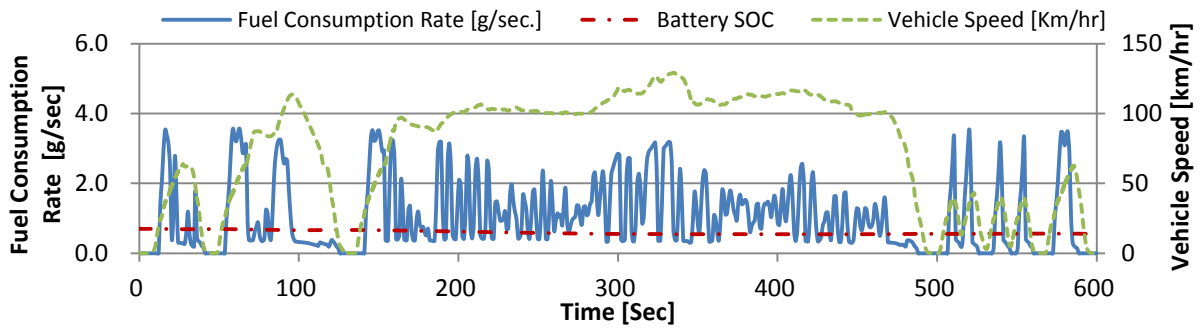


Figure 39: Parallel HEV Undergoing US06 Driving Cycle

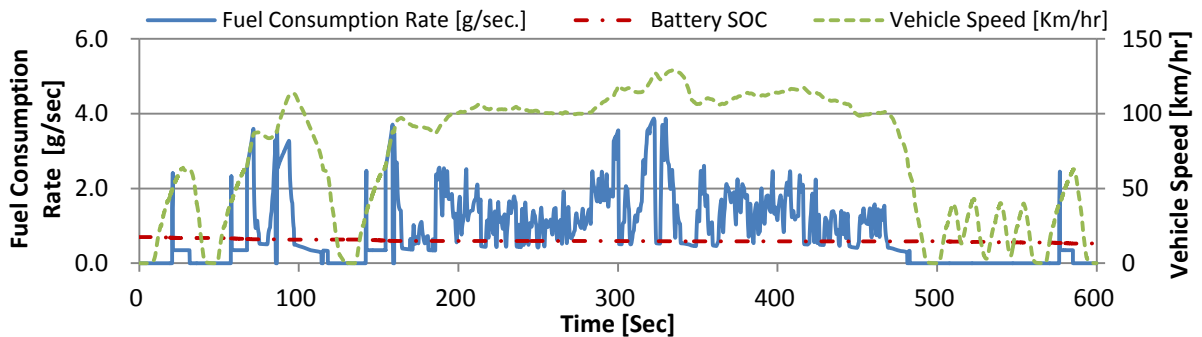


Figure 40: Series-Parallel HEV Undergoing US06 Driving Cycle.



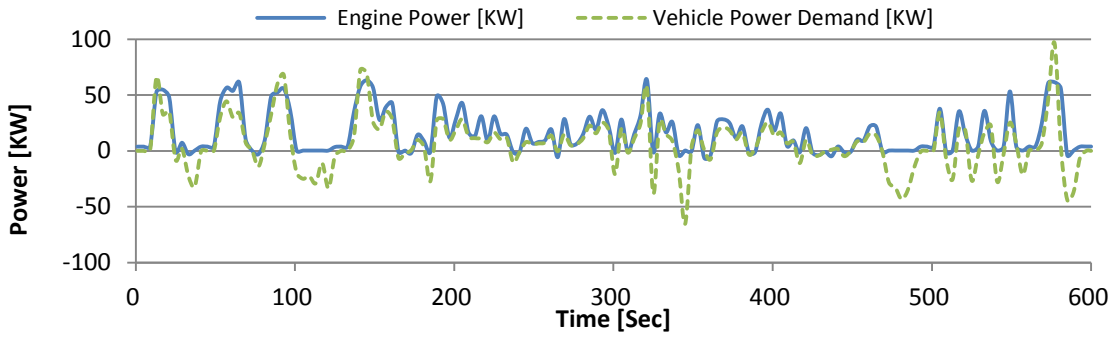


Figure 41: US06: Power Demand and Power Production in Conventional Vehicle

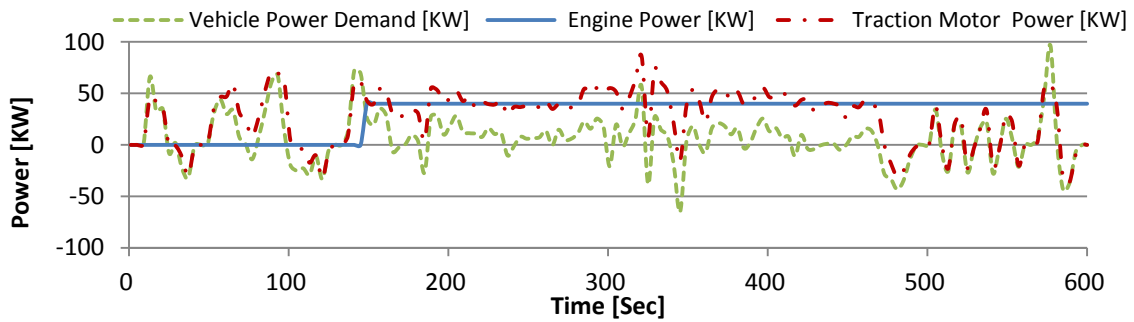


Figure 42: US06: Power Demand and Power Production in Series HEV

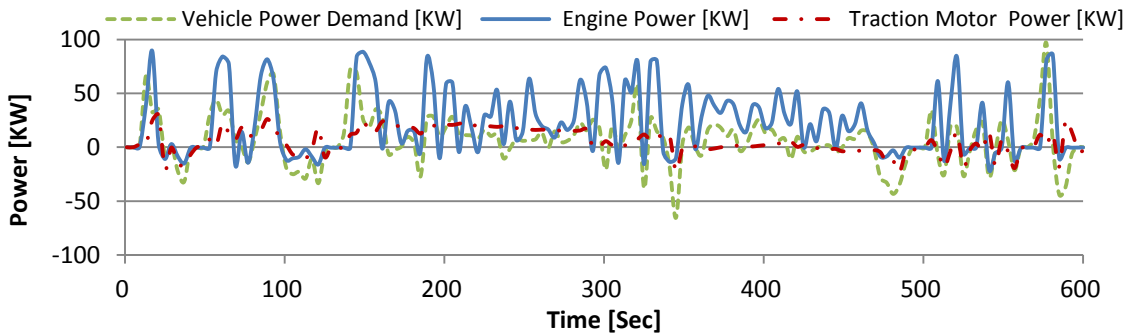


Figure 43: US06: Power Demand and Power Production in Parallel HEV

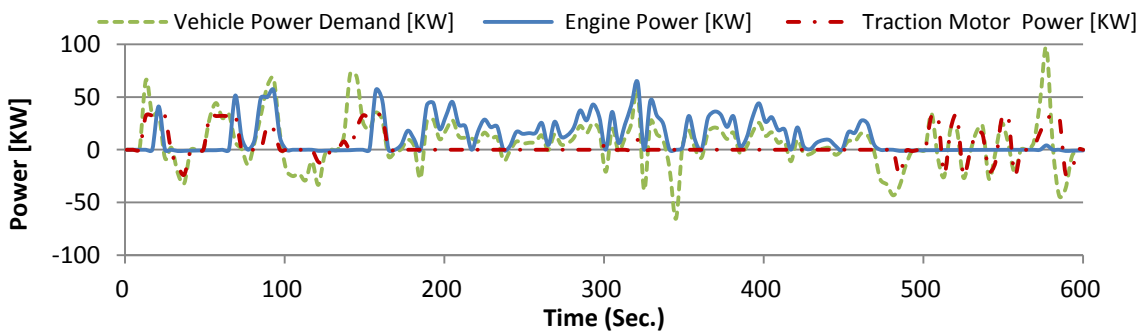


Figure 44: US06: Power Demand and Power Production in Series-Parallel HEV

### 3.5.4 NEDC Driving Cycle Outputs

The same two results groups for the NEDC driving cycle simulation are categorized and presented as follows:

- The first group is illustrated in Figure 45 to Figure 48, and demonstrates the fuel consumption rate and the battery SOC for different layouts during the driving cycle.
- The second group is illustrated in Figure 49 to Figure 52, and demonstrates the corresponding vehicle power demand, engine power and the traction motor power produced to follow the driving cycle.

For the simulated series HEV powertrain, it is clear that the vehicle's behavior obeys the control strategy, where the ICE/generator set provides more power to run the motor and charge the battery pack whenever the battery SOC hits its lower limit, and stops whenever it hits its upper limit as shown in Figure 46, and Figure 50.

For the parallel HEV powertrain, it is clear that the vehicle behavior follows the control strategy during the NEDC driving cycle, where the EM acts as propulsion motor during starting and as a generator for charging the batteries during regenerative braking mode as in Figure 47, and assists the ICE during high power demand periods. Also it is computed that the ICE is switched off when the vehicle stops and switched on again when the vehicle starts moving after hitting its preset starting speed and provides power to propel the vehicle in hybrid mode as shown in Figure 51.

For the simulated series-parallel HEV powertrain, the developed model follows the previously explained EMS, where the ICE provides power under certain conditions, either the required speed exceeds the switching speed or the battery SOC drops under its minimum limit, otherwise the EM provides the demanded power to follow the prescribed driving cycle speed as shown in Figure 48, and Figure 52.

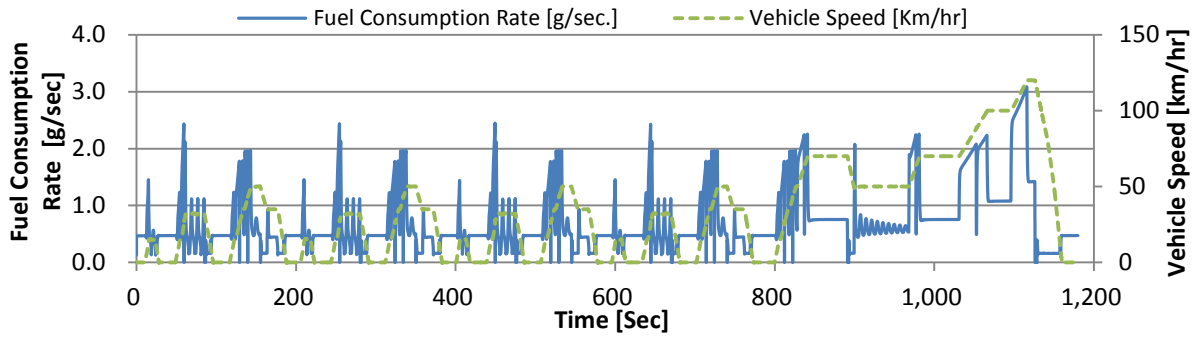


Figure 45: Conventional Vehicle Undergoing NEDC Driving Cycle

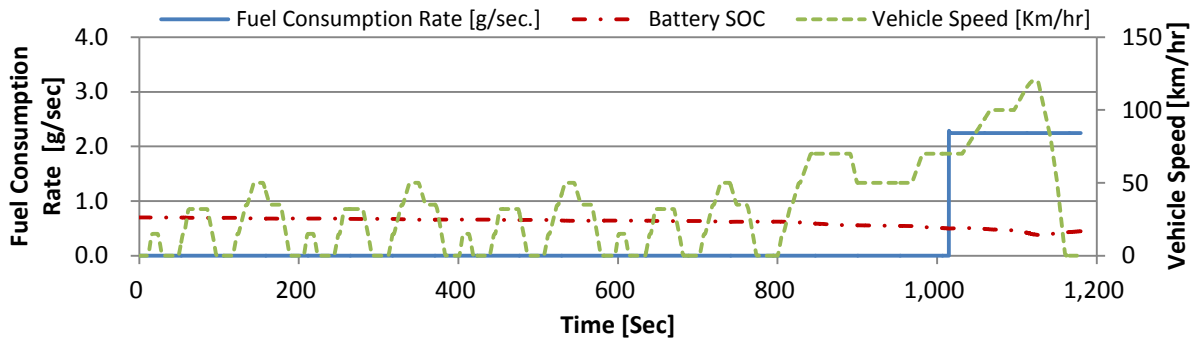


Figure 46: Series HEV Undergoing NEDC Driving Cycle

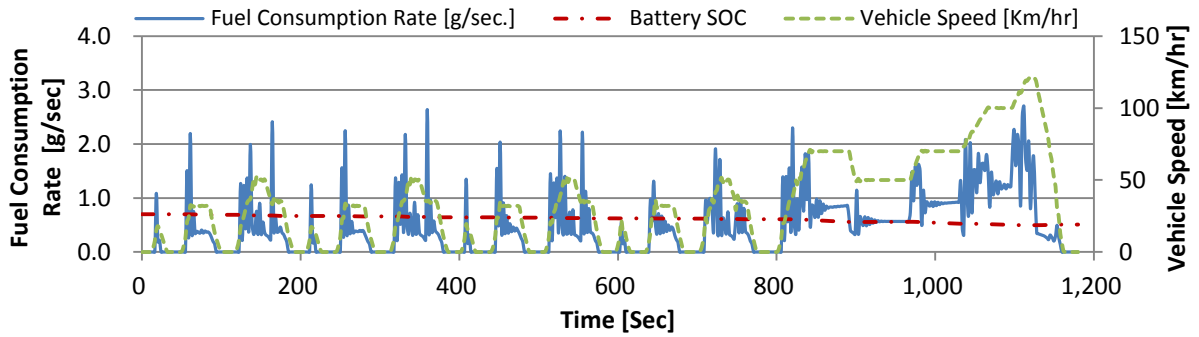


Figure 47: Parallel HEV Undergoing NEDC Driving Cycle

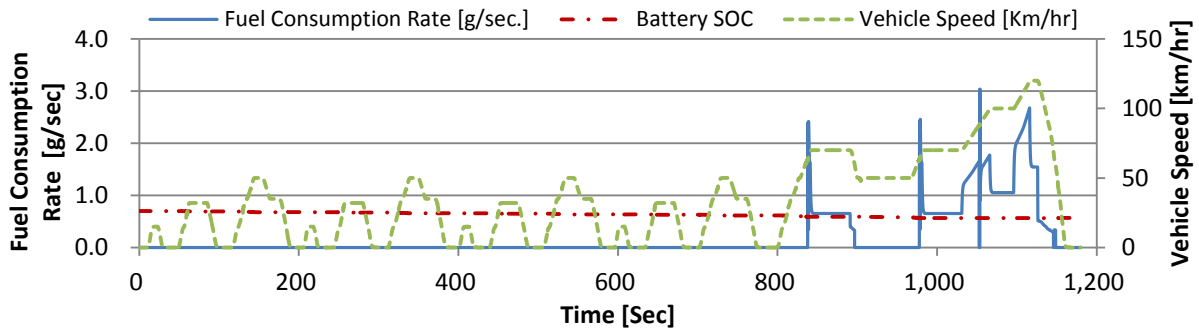
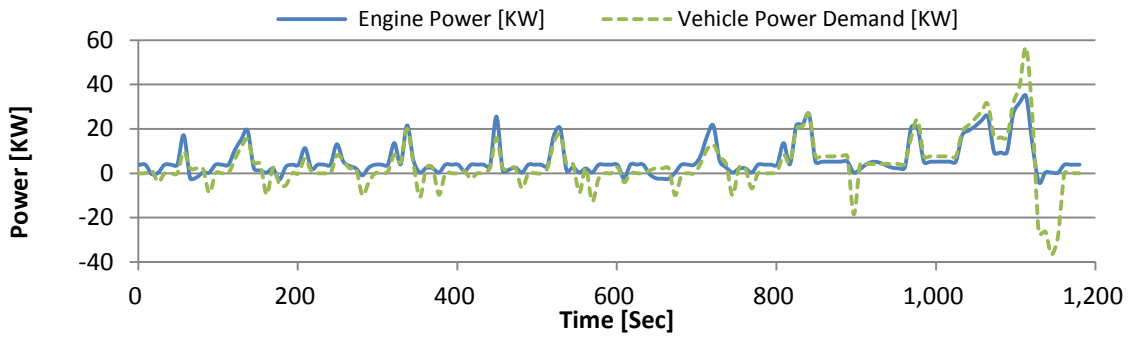
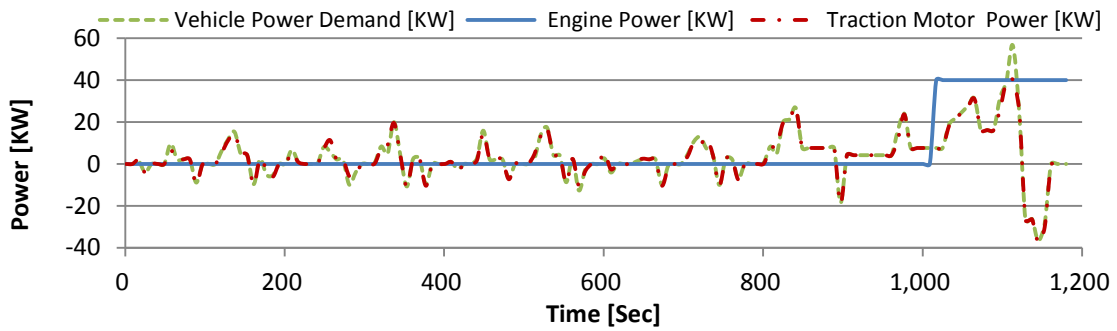


Figure 48: Series-Parallel HEV Undergoing NEDC Driving Cycle



**Figure 49: NEDC: Power Demand and Power Production in Conventional Vehicle**



**Figure 50: NEDC: Power Demand and Power Production in Series HEV**

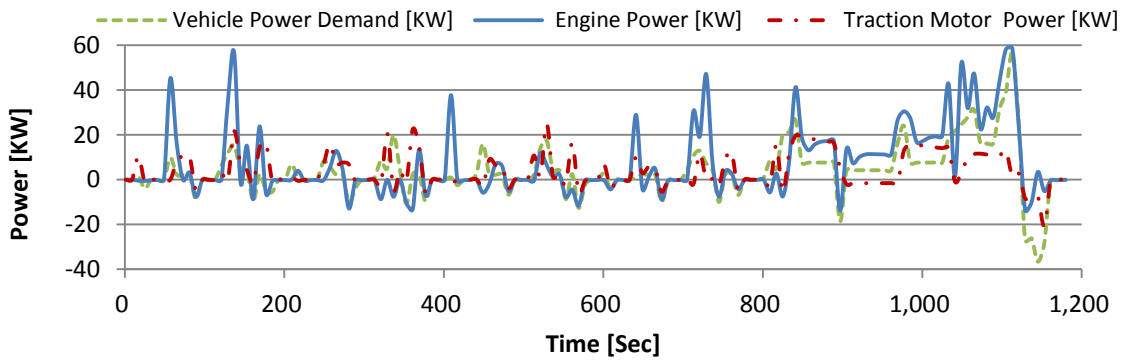


**Figure 51: NEDC: Power Demand and Power Production in Parallel HEV**

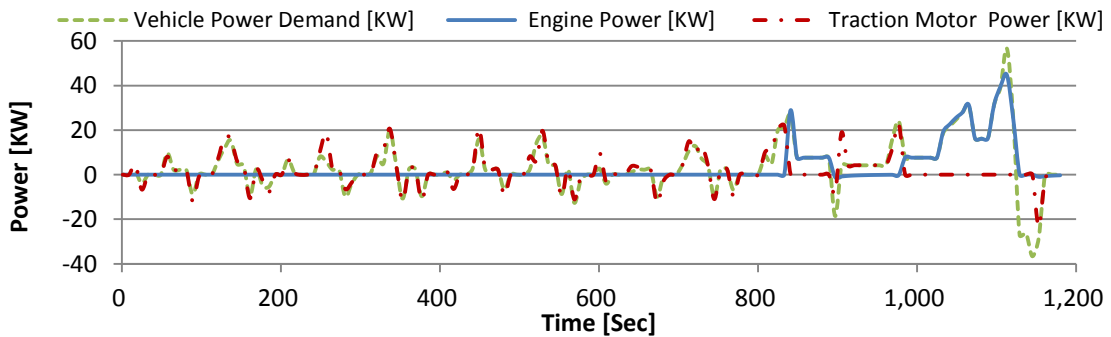


**Figure 52: NEDC: Power Demand and Power Production in Series-Parallel HEV**

## Chapter 4. Model Results & Validation

### 4.1 Overview

A sensitivity study of HEV fuel economy and HEV energy analysis will be conducted in this chapter to validate the GT-Suite models outcomes in the previous chapter. Fuel economy is calculated by employing a similar powertrain control strategy for each model. Fuel economy calculations are obtained for different driving cycles. Next, a comprehensive energy analysis is conducted for each model to explain the reasons for the fuel economy differences among the different architectures. The energy analysis considers the energy loss breakdown of the entire vehicle powertrain and driveline system, thus allowing for a global view of the energy management problem and the potential improvements for each design.

For the purpose of performance comparisons, several numerical simulations are carried out considering different powertrain configurations namely; conventional, series, parallel, and series-parallel HEVs. While the drivetrain architecture is different for each case, the ICE and EM components have the same technical specifications. For each drivetrain configuration, the numerical simulation is carried out in the GT-Suite environment considering the aforementioned four standard driving cycles namely; the FTP, the HWY, the US06, and the NEDC driving cycles.

### 4.2 Fuel Economy

For different HEV configurations and considering different driving cycles, the conventional ICE vehicle model shows a lower fuel economy for all driving situations, both city and highway driving. Additionally, the series HEV shows a lower fuel economy during HWY driving cycle which may be due to the excess fuel energy used to power the traction motor and charge the battery for a long period of the driving cycle. On the contrary, the series-parallel HEV model shows the best significant fuel economy for all driving scenarios.

The BSFC of the ICE, expressed in [g/kw.hr], applies to the distance of the entire driving cycle leading to fuel consumption in [g/km]. According to the model outputs shown in Table 4, the series-parallel and the parallel powertrain have better fuel economy for both

city and highway driving cycles, while the series powertrain is superior only in frequent stop and go driving. Figure 53 compares powertrain fuel economy for the different driving cycles.

**Table 4: Different Models Fuel Economy Outputs**

Model	Avg. /Max Vehicle Speed [km/hr.]	Avg. /Max Vehicle Speed [km/hr.]	Average BSFC [g/kW-h]	Avg. Fuel Consumption [g/km]	Avg. Gas Mileage [mpg]
<b>FTP City driving cycle</b>					
Conventional	34/91	21.1/56.5	396.2	84.6	21
Series HEV			202	66.1	26.9
Parallel HEV			169.5	59.5	29.9
Combined HEV			219.2	36.4	48.9
<b>HWY Driving cycle</b>					
Conventional	77 /96	47.8/60	395.1	59.3	29.5
Series HEV			202	76.4	23.3
Parallel HEV			160.6	37.7	47.1
Combined HEV			261.1	33.9	52.5
<b>US06 Driving cycle</b>					
Conventional	76/130	47.2/80.8	336	73.5	24.2
Series HEV			202	80.5	22.1
Parallel HEV			150	50	35.6
Combined HEV			242.2	40.4	44
<b>NEDC Driving Cycle</b>					
Conventional	33/120	20.5/74.6	420	78.2	22.7
Series HEV			202	33.7	52.8
Parallel HEV			174	51.9	34.2
Combined HEV			246.2	23.9	58.2

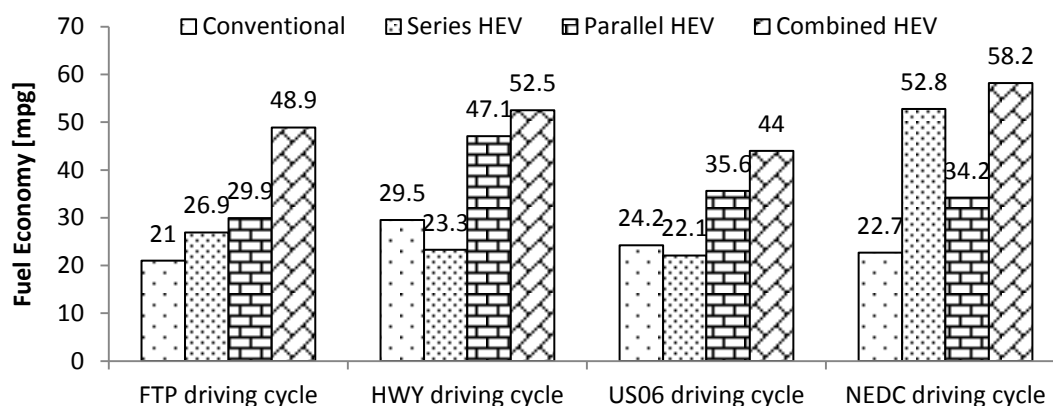


**Figure 53: Fuel Economy of Different Powertrain models**

### 4.3 Energy Analysis

Energy analysis considers the energy usage and losses breakdown of the entire vehicle powertrain and driveline system, thus allowing for a global view of the energy management problem and the potential improvements for each HEV design.

The overall energy analysis for different drivetrain layouts and different driving cycles is summarized in Table 5. The total chemical energy depleted during each driving cycle in [KJ] is a combination of the chemical (fuel) energy expend and the amount of added penalty. The added penalty arises from the conversion of chemical energy required to regain the battery SOC at the end of the driving cycle. The total energy used during a specific driving cycle for the different powertrains is the summation of the total chemical and regenerated energies.

**Table 5: Different Models Energy Analysis Outputs**

Model	Chemical Energy Depleted [KJ]	Penalty added [KJ]	Total Chemical Energy Depleted [KJ]	Regenerated Energy [kJ]	Total Energy Used [kJ]	Energy Saving %
<b>FTP City Driving Cycle</b>						
Conventional	65,902	0	65,902	0	65,902	0%
Series HEV	51,790	-3,407	48,383	3,823	52,206	20.8%
Parallel HEV	45,588	3,868	49,456	2,762	52,218	21.8%
Combined HEV	28,335	444	28,779	2,912	31,691	51.9%
<b>HWY Driving Cycle</b>						
Conventional	32,737	0	32,737	0	32,737	0%
Series HEV	55,694	4,235	59,929	236	60,165	-83.8%
Parallel HEV	27,456	4,672	31,128	311	32,439	1%
Combined HEV	24,686	866	25,552	149	25,701	21.5%
<b>US06 Driving Cycle</b>						
Conventional	41,424	0	41,424	0	41,424	0%
Series HEV	44,737	9,670	54,407	789	55,196	-33.2%
Parallel HEV	27,920	3,222	31,142	429	31,571	23.8%
Combined HEV	22,270	3,301	25,571	592	26,163	36.8%
<b>NEDC Driving Cycle</b>						
Conventional	37,907	0	37,907	0	37,907	0%
Series HEV	16,378	4,738	21,116	1,750	22,866	39.7%
Parallel HEV	25,150	4,568	29,718	1,430	31,148	17.8%
Combined HEV	10,142	3,107	13,249	1,311	14,560	61.6%

### 4.3.1 Energy Depleted and Stored

The purpose of hybridization is to eliminate some of the used onboard chemical energy and replacing it with stored and regenerated energy to maximize the vehicle's fuel economy. In this section an analysis of the depleted chemical, electrical, and regenerated energies in the different powertrain models presented before, undergoing different standard driving cycles will be discussed. The amount of chemical energy depleted is a summation of the fuel energy used by the ICE to finish the driving course and the excess amount needed to regain the initial battery charge by the end of the driving cycle.

For the FTP city driving cycle, it is clear that using different hybrid drivetrains layouts is significantly saving some energy percentages even after adding the penalty amount to recover the battery charge as mentioned in Table 5. This improvement is resulting from using the stored electrical energy and the capturing of energy via the regenerative braking during the frequent stops of the city driving profile. The Series powertrain model results shown in Figure 55 shows a 20.8% decrease in chemical energy used by the conventional powertrain shown in Figure 54, while the Parallel powertrain model results shown in Figure 56 shows a 21.8% decrease and the results of the Series-Parallel model shown in Figure 57 shows a higher chemical energy saving amount of 51.9%.

For the HWY driving cycle, it should be noted that, according to the simulated results, the series HEV powertrain expends much more chemical energy than the conventional powertrain, 83.8% more as shown in Figure 59. This can be referred to the lack of energy regeneration on highway driving, and using the ICE/Gen set to provide power to the traction motor and recharge the battery pack for long periods. Therefore the Series hybrid powertrain might be inefficient during highway scenarios, unless using a higher capacity battery pack. On the other side, the Parallel powertrain model expends almost the same amount of chemical energy as the Conventional powertrain after adding the penalty amount as shown in Figure 60 and that is for the lack of regeneration during such highway driving cycles, while the Series-Parallel powertrain model shows a 21.5% decrease in the chemical energy used without any significant regenerated energy as shown in Figure 61.



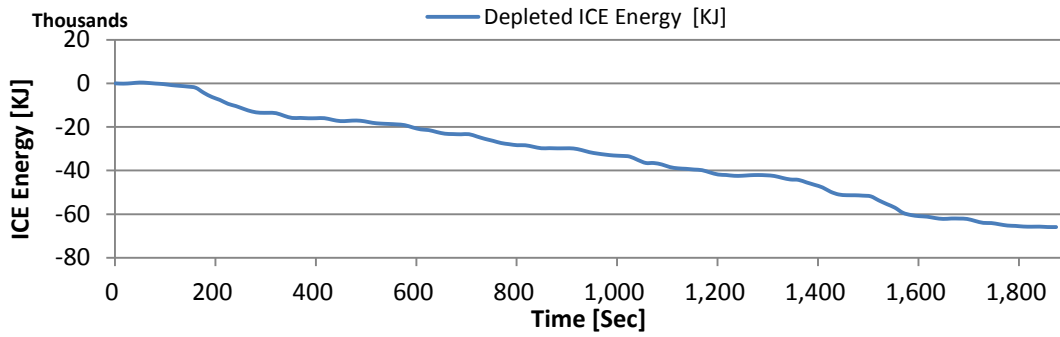


Figure 54: FTP: Depleted ICE Energy in Conventional Vehicle

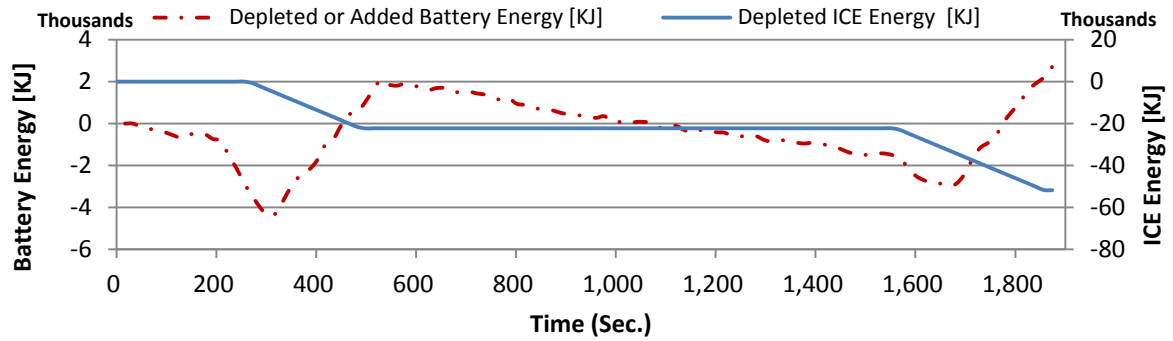


Figure 55: FTP: Depleted and Stored Energy in Series HEV

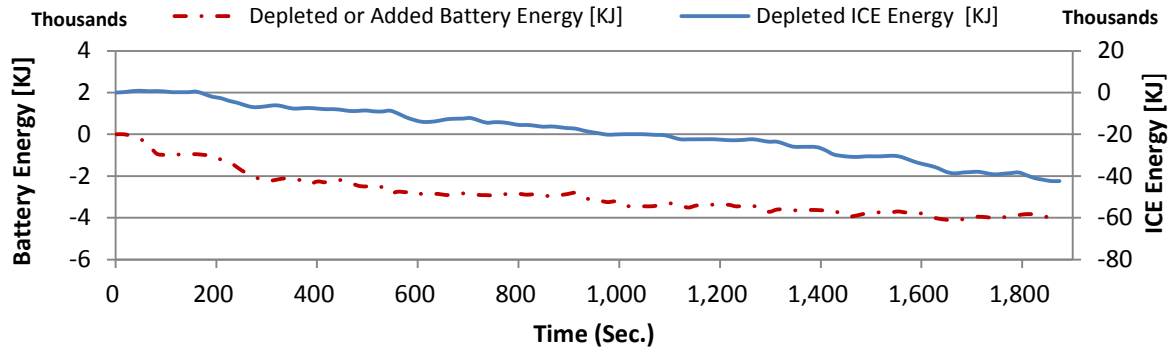


Figure 56: FTP: Depleted and Stored Energy in Parallel HEV

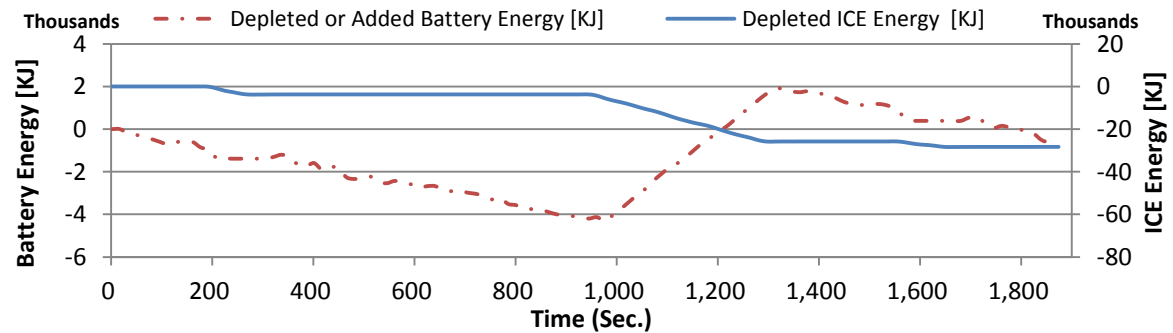


Figure 57: FTP: Depleted and Stored Energy in Series-Parallel HEV

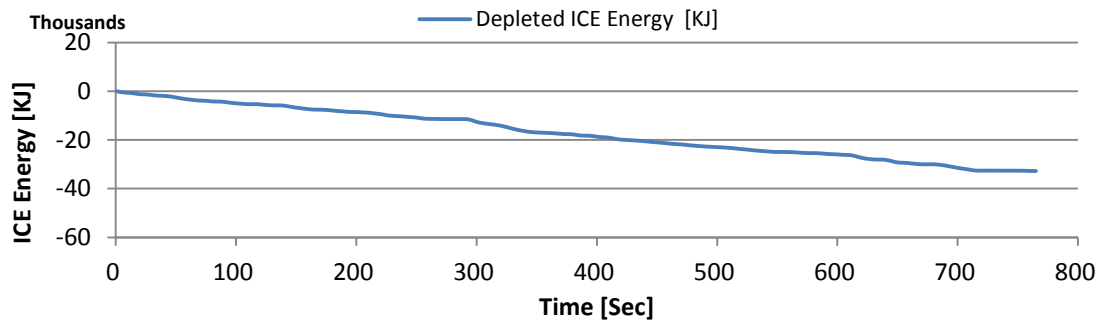


Figure 58: HWY: Depleted ICE Energy in Conventional Vehicle

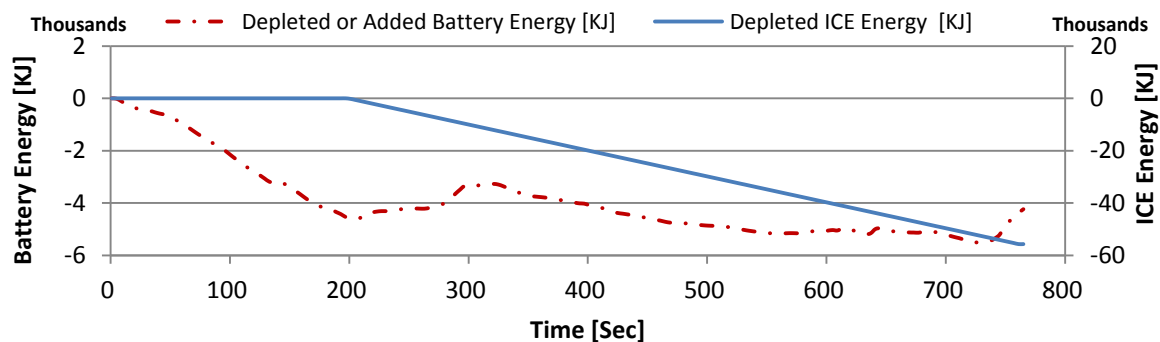


Figure 59: HWY: Depleted and Stored Energy in Series HEV

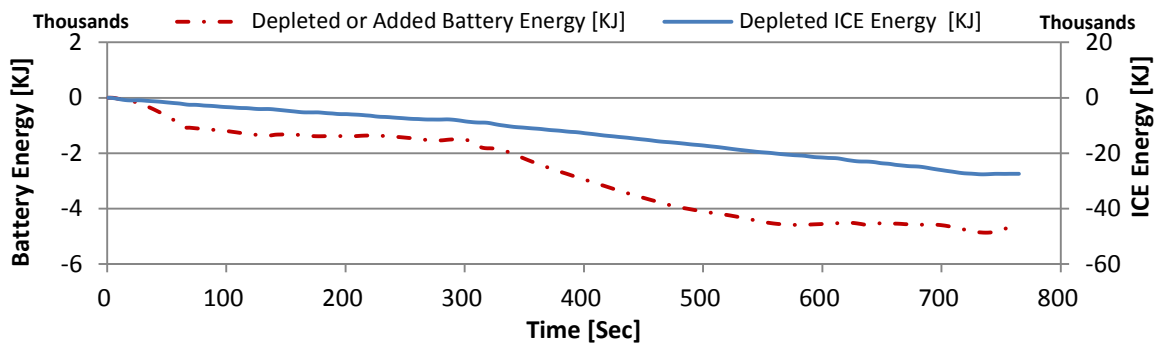


Figure 60: HWY: Depleted and Stored Energy in Parallel HEV

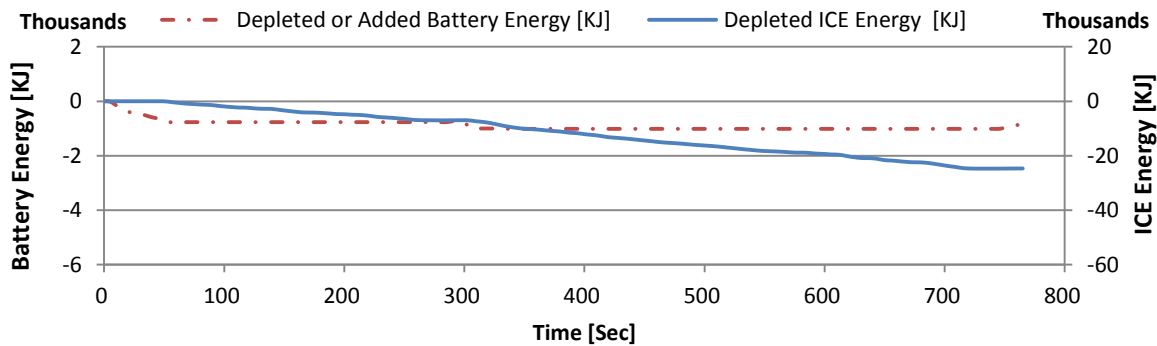


Figure 61: HWY: Depleted and Stored Energy in Series-Parallel

The results of the US06 city driving cycle seem to be close to the HWY driving cycle results. The series HEV powertrain expends 33.2% more chemical energy than the conventional powertrain, as shown in Figure 63. This can be referred to the high power demand due to the required high velocity, regeneration of small amount of energy on such driving situation, and using the ICE/Gen set to provide power to the traction motor and recharge the battery pack for a long period, which emphasis that the Series hybrid powertrain is inefficient during high velocity scenarios. On the other side, the Parallel powertrain model expends 23.8% chemical energy less than the Conventional powertrain after adding the penalty amount as shown in Figure 64, while the Series-Parallel powertrain model shows a significant decrease in the chemical energy used, 36.8%, as shown in Figure 65.

NEDC, the last standard driving cycle used to evaluate the different powertrain energy consumption, possess the characteristics of both city and highway driving conditions. According to the model results it is clear that using different hybrid drivetrains is significantly lowering the chemical energy usage by different respectable percentages even after adding the penalty amount to recover the battery charge. This improvement adheres to the capturing of energy via the regenerative braking during the driving scenario and the high electrical to mechanical energy conversion efficiency. The Series powertrain model results shown in Figure 67 shows a 39.7% decrease in chemical energy used by the conventional powertrain shown in Figure 66, while the Parallel powertrain model results shown in Figure 68 shows a 17.8% decrease and the results of the Series-Parallel model shown in Figure 69 shows a higher chemical energy saving amount of 61.6%.

For this specific driving cycle, the Series hybrid powertrain shows 26.6% decrease in energy consumption more than the Parallel hybrid powertrain. The reason for this phenomenon is that the ICE in the Parallel hybrid powertrain doesn't turned off during the entire driving cycle, while in the Series hybrid the ICE is turned off until the battery SOC drops below its lower value then it starts to generate energy to recharge the batteries and provide the traction motor with the required power to propel the vehicle.

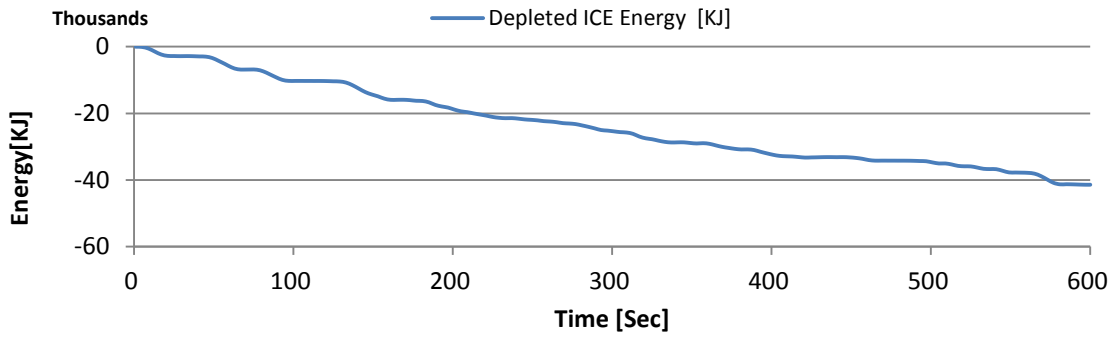


Figure 62: US06: Depleted ICE Energy in Conventional Vehicle

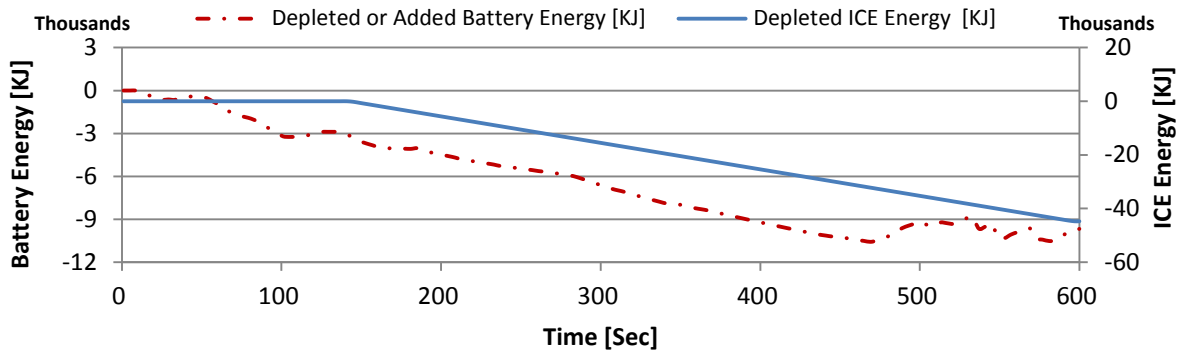


Figure 63: US06: Depleted and Stored Energy in Series HEV

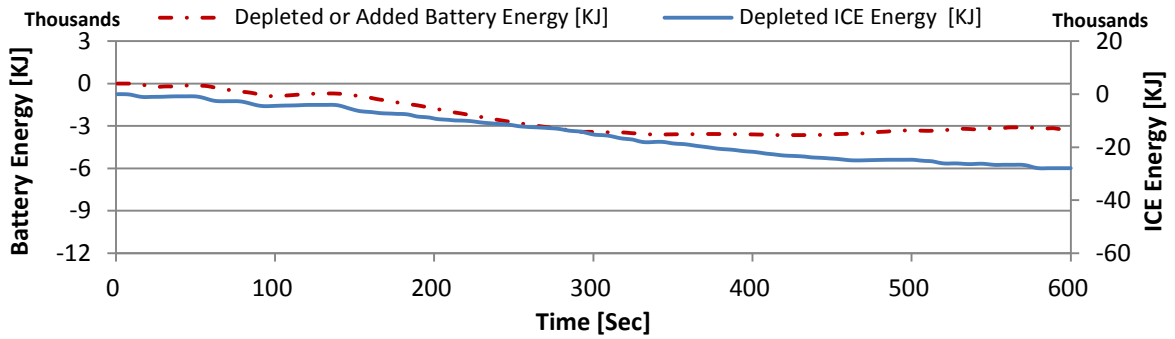


Figure 64: US06: Depleted and Stored Energy in Parallel HEV

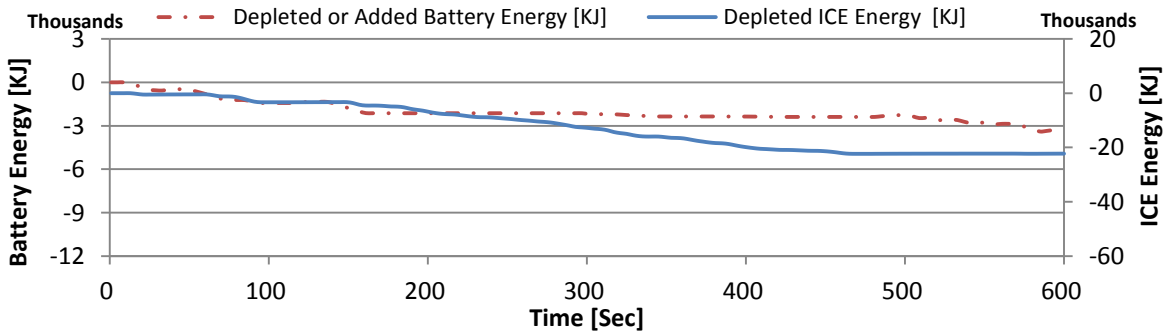


Figure 65: US06: Depleted and Stored Energy in Series-Parallel HEV

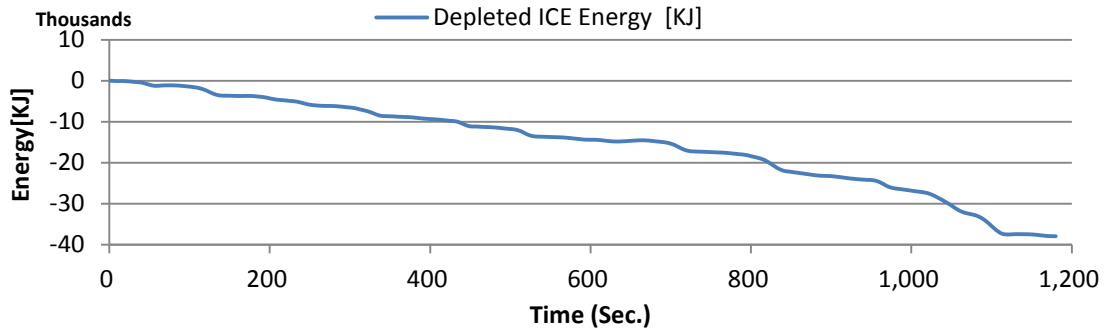


Figure 66: NEDC: Depleted ICE Energy in Conventional Vehicle

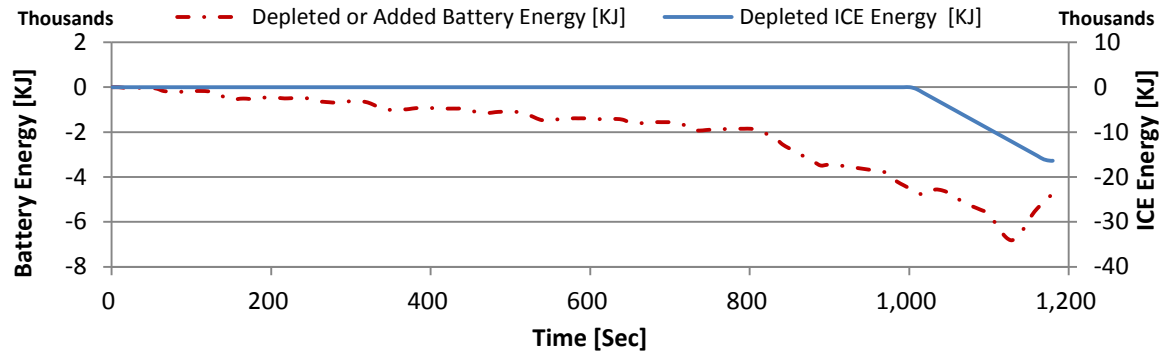


Figure 67: NEDC: Depleted and Stored Energy in Series HEV

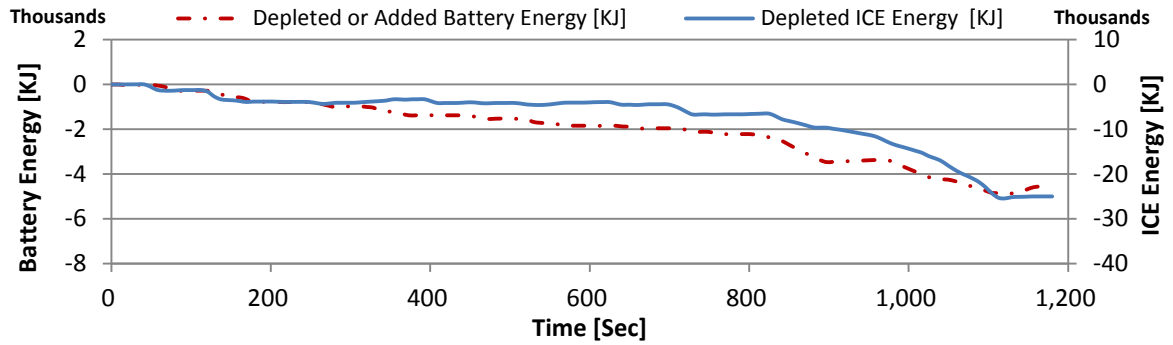


Figure 68: NEDC: Depleted and Stored Energy in Parallel HEV

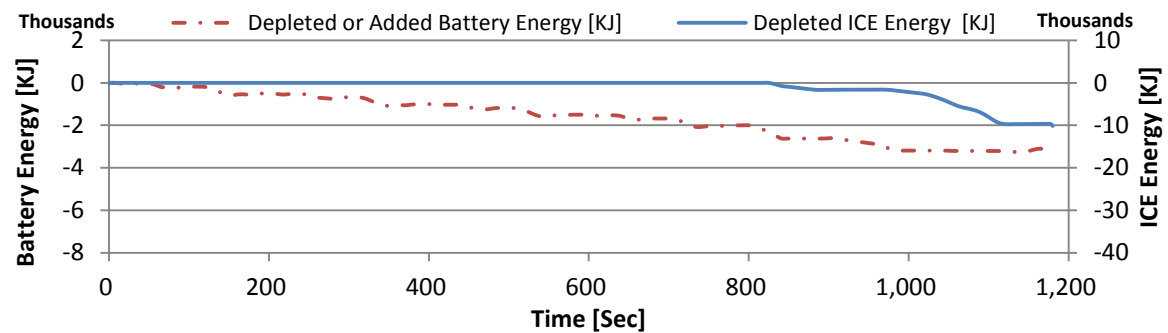


Figure 69: NEDC: Depleted and Stored Energy in Series-Parallel HEV

### 4.3.2 Energy Losses

To identify the possible reasons for the fuel economy benefits of particular architectures, energy balance charts were constructed. These charts represent the irreversible system losses, such as friction, efficiency losses, and auxiliary loads. Engine losses represent the largest system loss and are calculated as the difference in consumed fuel energy and output shaft brake work. Vehicle losses represent the second largest system losses and are calculated based upon the vehicle retarding loads, namely drag and rolling resistance losses and internal losses in transmission, differential and brakes. An overall numerical comparison of the four powertrain models is given in Table 6.

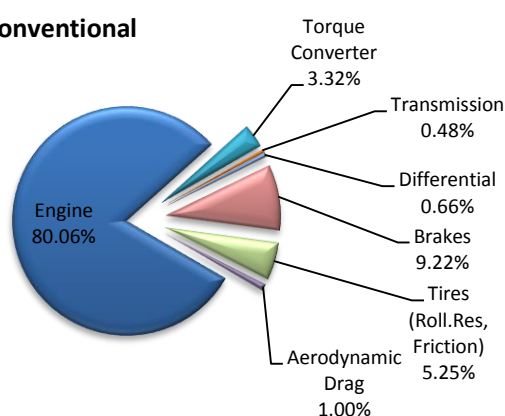
**Table 6: Different Powertrain Energy Losses in [KJ] during Different Driving Cycles**

Powertrain	Engine	Mot/Gen	Battery	Clutches	Torque Converter	Transmission	Differential	Brakes	Tires (Rolling Resistance, Friction)	Aerodynamic Drag	Total
<b>FTP City driving cycle</b>											
Conventional	52,762	0	0	0	2,190	315	436	6,076	3,463	660	65,902
Series HEV	30,912	11,017	3,837	0	0	297	591	1,410	3,482	660	52,206
Parallel HEV	29,424	13,689	715	642	0	594	572	1,805	4,151	626	52,218
Combined HEV	18,891	3,715	2,458	528	0	399	554	1,034	3,460	652	31,691
<b>HWY driving cycle</b>											
Conventional	26,097	0	0	0	361	134	247	1,417	3,235	1,246	32,737
Series HEV	33,219	18,000	1,252	0	0	189	373	2,000	3,238	1,894	60,165
Parallel HEV	14,040	9,351	312	532	0	326	315	1,720	3,945	1,898	32,439
Combined HEV	12,412	4,232	1,159	617	0	185	344	1,608	3,242	1,902	25,701
<b>US06 driving cycle</b>											
Conventional	33,044	0	0	0	1,019	203	352	2,872	2,504	1,430	41,424
Series HEV	27,185	13,073	7,985	0	0	259	511	2,286	2,468	1,429	55,196
Parallel HEV	15,471	7,329	459	780	0	399	443	2,701	2,529	1,460	31,571
Combined HEV	13,367	3,008	1,121	558	0	250	435	2,584	2,450	1,390	25,163
<b>NEDC driving cycle</b>											
Conventional	30,707	0	0	0	1,454	151	227	2,634	2,153	580	37,907
Series HEV	9,770	6,868	1,766	0	0	162	322	1,237	2,161	580	22,866
Parallel HEV	16,173	8,973	396	359	0	220	290	1,528	2,625	584	31,148
Combined HEV	7,834	1,012	309	498	0	191	296	1,681	2,160	579	14,560

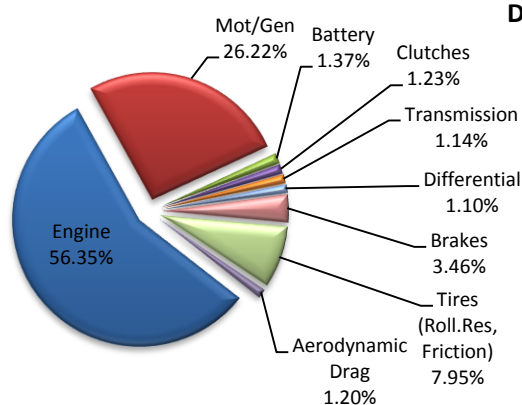
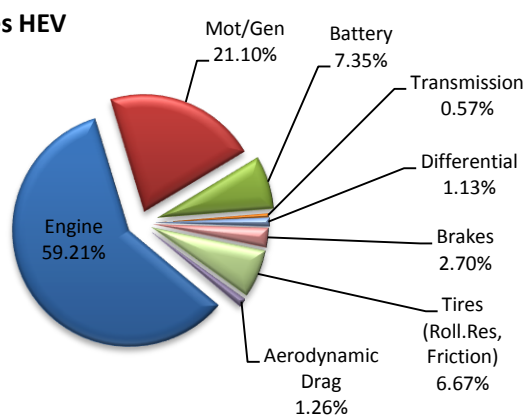
Figure 70 shows the percentages of energy losses during FTP city driving cycle. For the Conventional powertrain, it is clear that the ICE is inefficient for an energy loss of more than 80% of the total energy losses, but on the other side the hybrid powertrains show a significant decrease in engine losses which reduce the amount of fuel consumed and raise the vehicle fuel economy. By comparing the four powertrains, it is clear that a significantly large portion of the total losses come from the engine. This indicates that load points are far from the most efficient load curve, resulting from driving on low speed and power demand.

Energy regeneration in hybrid powertrain plays an important role in decreasing the amount of energy losses in the form of irreversible heat energy during coasting. The models predicted that there is a potential decrease in the wasted energy using hybrid powertrains.

**A: Conventional**



**B: Series HEV**



**D: Combined HEV**

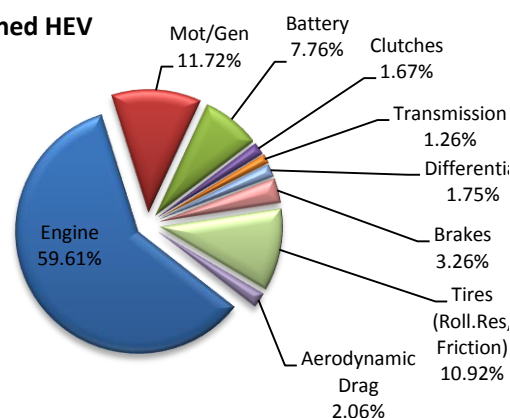


**Figure 70: Energy Losses during FTP Driving Cycle**

The Series HEV model shows a depletion of almost double the amount of energy used by the Conventional model to drive the HWY cycle as mentioned in Table 5. This is because during periods of high tractive power demand, the resulting necessary engine power can be significantly higher than the tractive power requirements due to the compounded electro-mechanical conversion efficiencies of the motor and generator which leads to poorer fuel economy during aggressive or higher speed driving conditions, and explains the higher amount of energy lost in the Series powertrain engine, 21% higher than the Conventional one as mentioned in Table 6. Figure 71 shows the percentages of energy losses during HWY driving cycle in each powertrain. The Mot/Gen energy losses in the Series hybrid powertrain model are the highest among all hybrid architectures, because it is the main driving source.

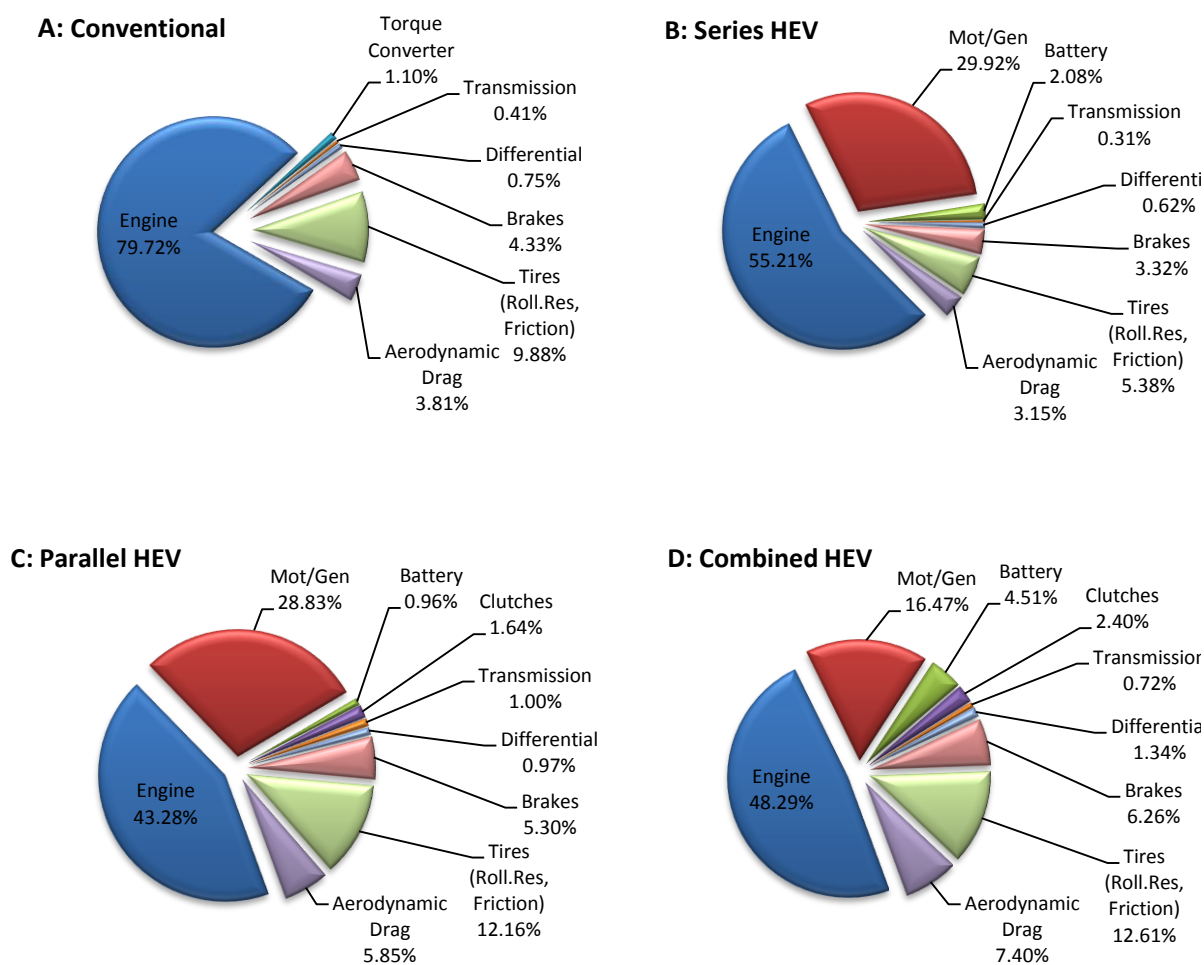
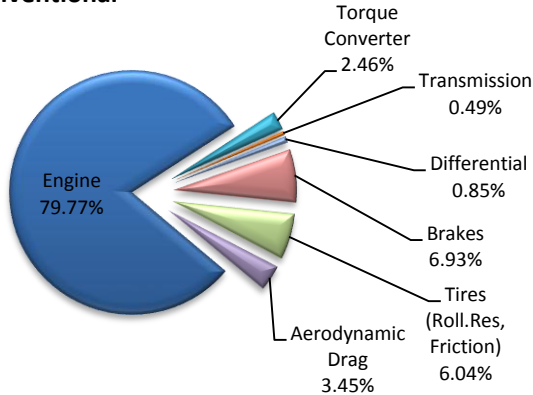


Figure 71: Energy Losses during HWY Driving Cycle

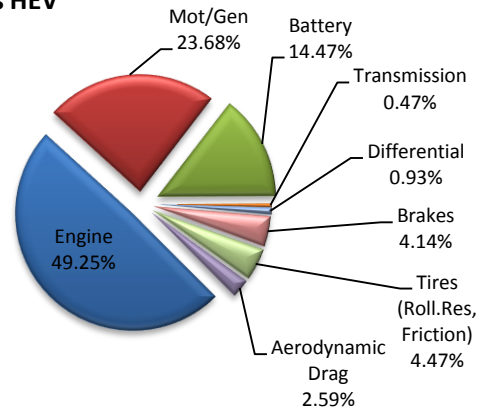


The main problem in HWY and US06 driving cycles is the lack of energy regeneration due to the high power and velocity requirements during the entire cycle as mentioned in the models numerical outputs in Table 5. The Combined HEV powertrain appears to be the best choice among all modeled hybrid architectures. The total amount of depleted/lost energy in the Combined HEV is the lowest, although the engine losses is about 50% of the total, it is still much lower than the other powertrain architectures as mentioned in Table 6. Percentages of energy losses during US06 driving cycle in each powertrain are shown in Figure 72.

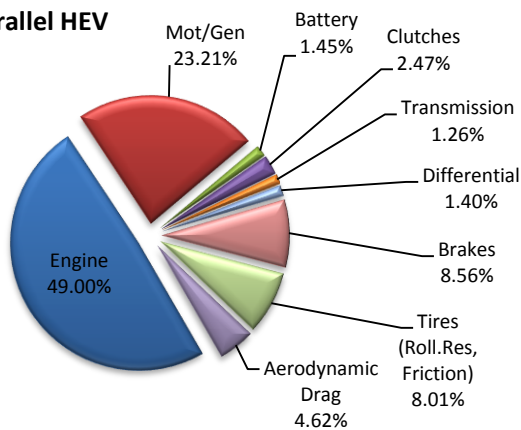
**A: Conventional**



**B: Series HEV**



**C: Parallel HEV**



**D: Combined HEV**

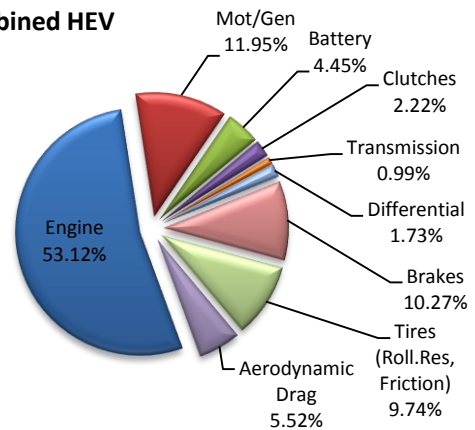


**Figure 72: Energy Losses during US06 Driving Cycle**

The NEDC is supposed to represent the typical usage of a car in Europe, and it consists of four repeated UDC, simulating city driving, and a EUDC, simulating highway driving conditions. The city driving cycles help in energy regeneration, but the highway driving conditions don't. From the numerical outputs in Table 6, it is clear that the Series HEV performed better than the Conventional and Parallel hybrid powertrains. The engine losses in the Series hybrid powertrain is 42% of the total losses, which is less than one third of the engine losses in the Conventional powertrain and is less than two third of the Parallel one. The loss breakdown for the different powertrain architectures during NEDC driving cycle is shown in Figure 73.

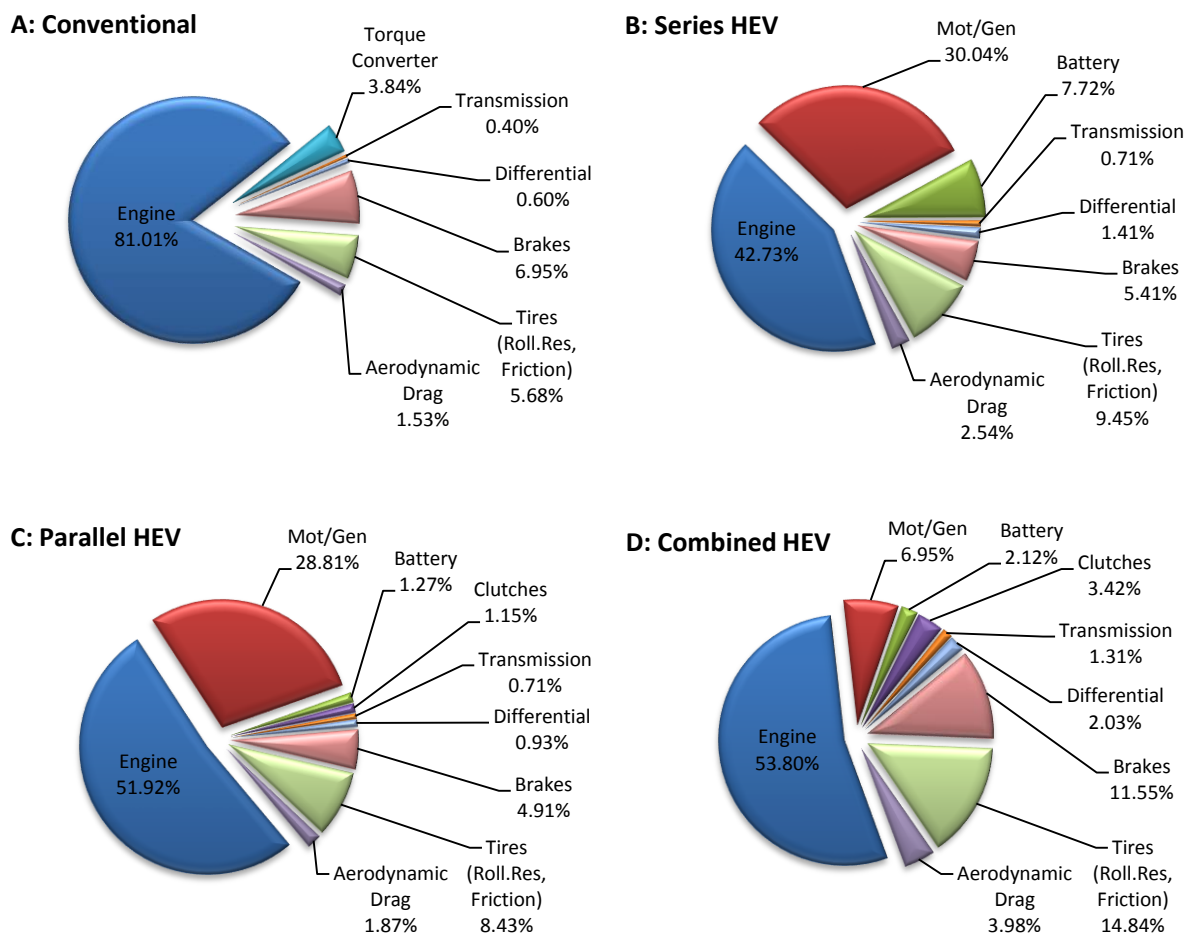


**Figure 73: Energy Losses during NEDC Driving Cycle**

## Chapter 5. University of Idaho FHSAE Case Study

### 5.1 Overview

The previous method of control in the UI-FHSAE based on passive splitting of the torque demanded between the ICE and the EM during hybrid mode. The hybrid mode is used to be activated by turning on a switch. There was no higher level controller to select the proper vehicle mode, and to determine the proper power split between the two power sources while driving on hybrid.

To fully understand the performance of this setup, mock tracks were implanted and used to compare lap times and fuel consumption for different driving modes and styles. These tests involved measuring fuel consumption per lap, the first laps set involved driving at high speeds using ICE only, and then repeated at low speeds. The second set of laps was conducted while the vehicle was in hybrid mode, where both power sources receive the same torque demand from the driver. These tests allowed the team to capture the systems characteristics, as the impact of hybrid mode on fuel consumption and lap times over a certain engine speed range. A detailed description of these tests could be found in [63].

From the gathered data, and the general characteristics of the powertrain components it was noticed that during low speeds, the ICE efficiency is significantly low, so using this source will result in negative effects on fuel consumption. Focusing on this fact, it was recommended to use the EM as the only energy supply when the speed is less than a certain limit, for its higher torque-speed relationship at low rpm, provided that the batteries have enough charge. Also from the data collected during hybrid mode, it was noticed that under certain loads and engine speeds the vehicle's fuel efficiency is raised, but under low speed the vehicle has poor efficiency.

For the 2014 competition the endurance event was increased to 44 km from the previous 22 km. This has led to the necessity to design and implement a supervisory controller to coordinate the overall powertrain & satisfy this target. It also serves as an energy management unit which determines the proper power split during hybrid mode.

## 5.2 Current Developments

There are two main goals in the new Supervisory control system. First is determining the proper driving mode according to the requested demand and the vehicle status. Second is to run the ICE at idling speed during low speeds and low torques while propelling the vehicle by the EM, and to push the ICE operating points to the most efficient points at higher speeds and loads to improve its efficiency. Advancements to the current platform include a vehicle supervisory controller, an EMS, and a Drive-by-Wire (DBW) system. The Supervisory controller is designed to allow for better vehicle mode selection, EMS is integrated to determine how to split the power demand between the available power sources during hybrid mode, and the DBW is implemented to control the ICE through an electronic throttle body, though the ability to idle the engine during low vehicle speeds.

There are several different types of control methods available as mentioned in Chapter 2, however for real time implementation and simplicity, a rule-based EMS was chosen as a start. This system functions by using a predetermined set of rules that dictate the power split between the two available power sources based on the characteristics of the ICE and EM used on the vehicle. The power split during hybrid mode is generated according to the driver's commands through the accelerator and brake pedals, and other operating variables of the vehicle and its components, including vehicle speed, engine speed, throttle position, and battery SOC. Based on some preliminary data, an initial supervisory set of rules was designed. These rules function by allowing the vehicle to switch the drive system into one of three different modes depending on three different parameters. So, the Supervisory controller, depending upon throttle position, wheel speed, and battery SOC will operate the vehicle in electric mode, hybrid mode, or ICE only mode in order to achieve the best possible energy efficiency for a given set of conditions. The power split during hybrid mode between the two power systems, regulated by the EMS, can vary from 0% to 100% and is based on manipulating the torque demand from the driver or splitting it and passing along modified signals to the two power systems controllers. By processing all the received signals, and adhering to the pre-determined set of rules, the

supervisory controller generates control commands and sends them to the corresponding component controllers. The component controllers then generate the proper power split and achieve the required input demands from the driver.

The EM operates during two modes, electric mode, which is low speed-low torque demand while the ICE is idling, and hybrid mode. However during the ICE mode, which is at higher speeds and higher torque demand, the EM is switched off to save the electrical energy. When the vehicle achieves a certain hybrid mode switching speed, the controller will put the vehicle into hybrid mode. The hybrid mode will run until the battery SOC reaches its lower limit and hence the controller will switch into ICE only mode. As a part of this research work, the switching criteria from electric to hybrid and from hybrid to ICE only mode will be optimized to boost the fuel efficiency of the vehicle. The first criterion, hybrid switching speed, is when the Supervisory controller switches the vehicle to hybrid mode over just electric mode. To determine this switching speed, an efficiency map for the EM, and a higher resolution BSFC map for the engine are required to calculate the EM and ICE efficiencies over a range of duty cycles. Once the efficiency maps are determined, a discrete grid optimization method will be used to predict the optimum switching speed for the highest vehicle fuel economy.

### **5.3 Platform Design & Implementation**

The research on the Formula Hybrid vehicle started at the University of Idaho (UI) on 2010 by designing a repacked Yamaha YZ-250F engine to provide a more compact and lighter powertrain configuration. The UI first Hybrid powertrain, shown in Figure 74, featured a unique packaging of a Yamaha YZ-250F engine with a Lynch-D135RAGS electric motor in innovative pre-transmission parallel hybrid architecture. The design included a custom Electronic Fuel Injection (EFI), a repacking of a Torsen differential with an in-house designed planetary gear reduction, and a Rekluse clutch in a custom engine casing to accommodate for the EM coupling. This work was done through several research work that could be found in [64]–[68]. The UI first hybrid vehicle competed and finished 8<sup>th</sup> overall in the 2012 International Formula Hybrid competition.

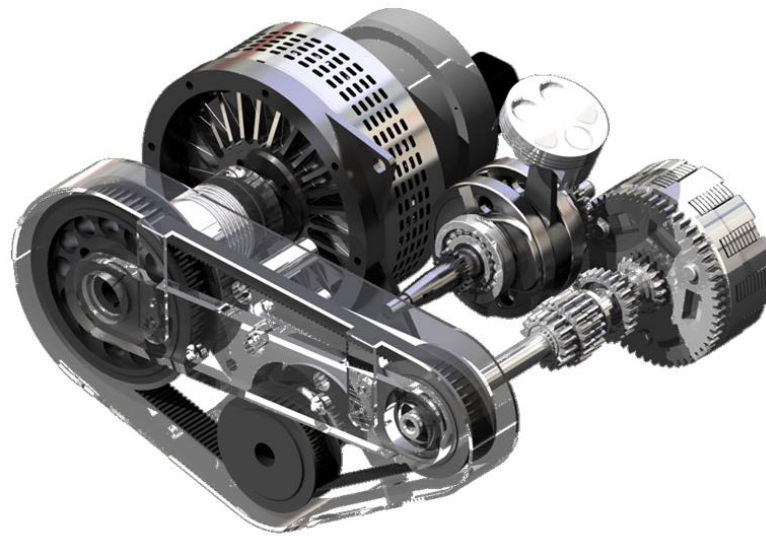


**Figure 74: UI First Pre-transmission Parallel Hybrid Powertrain Render**

### 5.3.1 Current Powertrain Development

In the UI second generation hybrid powertrain, the traction motor-engine coupling location is moved from the countershaft to the output shaft to eliminate time spent on shifting. So, to utilize the electric motor's efficiency range, the EM was moved to the side of the ICE enabling the armature to be directly coupled to a custom ICE output shaft in a new post-transmission design. The custom output shaft incorporates a one way clutch and an R+W flex-coupler. A render of the new pre-transmission powertrain is shown in Figure 75.

The new per-transmission powertrain along with the developed supervisory controller are implemented in a compact, lightweight, mass-centralized, and an innovative designed platform which won the title at the 2014 International Formula Hybrid competition.

The coupling of the engine and motor to provide the tractive force requested by the driver results in an advantage over using one or the other because, while the engine can provide greater torque at high speeds, the traction motor produces more torque at lower speeds.

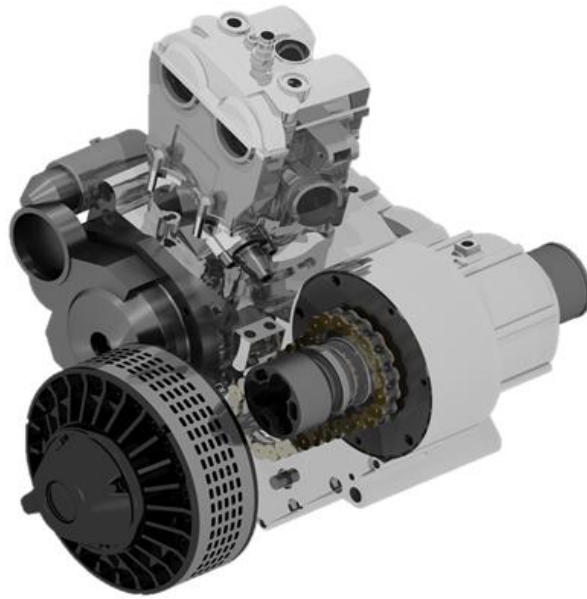


**Figure 75: UI New Post-transmission Parallel Hybrid Powertrain Render**

### **5.3.2 High Voltage Battery Pack**

The EM used in the new platform has a rated voltage of 107.3 [V], and a peak current of 400[A]. Thought in order to utilize the motor's high torque and speed range, the battery capacity was chosen to be 6 [Ah], using 29 Lithium polymer Haiyin pouch cells at a nominal voltage of 3.7 [V]. The battery pack has a total electrical energy of 1.85 [MJ]. The method of selecting the battery cells and determining the battery pack capacity as well as the battery design can be found in [63]. The assembled battery pack is shown in Figure 76.

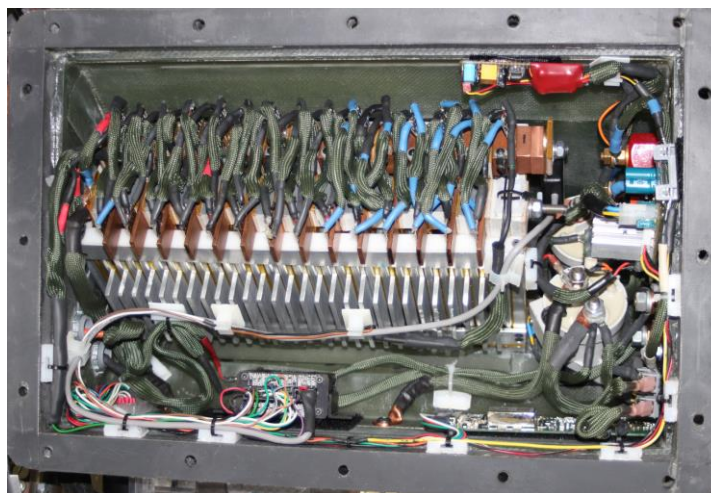


**Figure 76: The Battery Pack**

The Battery Management System (BMS) consists of an EMUS master module and 29 slave modules. Measured voltage and temperature readings are compared to configurable operating limits which can be set by the user in the EMUS software. If the maximum limits are exceeded or communication is lost, a MOSFET will open and inline relays will open, so power to the BMS and high voltage relays are turned off.

SOC is one of the several variables that dictate the operation of the Supervisory controller and the EMS, and to capture the SOC an EMUS current sensor, shown in Figure 77, is included in the battery pack to allow the BMS to determine the SOC and the draw on the system by monitoring the current draw by the EM. The BMS will send the SOC to the supervisory controller so that the system will know the available energy left in the pack and aid in mode selection and determining the most efficient power split between the two power systems based on the predetermined rules. The EMUS current sensor position in the battery pack can be seen in Figure 78.



**Figure 77: EMUS Current Sensor**



**Figure 78: Current Sensor Location in the Battery Box**



### 5.3.3 Supervisory Controller Implementation

A custom Printed Circuit Board (PCB) inside a waterproof container houses a Microchip™ PIC32 microprocessor packaged on a Digilent™ MAX32™ prototyping platform along with isolation and latching circuitry. This makes up the Supervisory Controller System. The processor simultaneously manages vehicle mode, data storage, user interface, fault checking, energy management, and data acquisition. The inputs to the controller are also important. The inputs should be measurable or predictable inputs. For example road load which is the required propulsion power cannot be input for control system, because road load depends on the slope of the road, rolling resistance (depends on the tire pressure and speed), drag forces (depends on the shape of the car and vehicle speed) and also the traction power required for acceleration (depends on the mass of the car, friction coefficient between tire and road). Instead, the microcontroller reads driver input from the throttle, brake, and shift buttons. These input data are then added to current state data to include battery SOC, gear number, vehicle and engine speeds. These parameters dictate the requested throttle output to the ICE and EM controllers.

There are three possible modes of operation: electric only, ICE only and hybrid.

- i. As its name implies, the ICE only propulsion state uses only the ICE to provide the requested road load. The vehicle will run in this mode if the battery SOC is below a desired minimum threshold where the efficiency of the EM is such that it would hurt the vehicle's overall efficiency, though switching off the EM to save energy.
- ii. For electric propulsion, the EM is the only component that is used to provide the requested road load. This state is utilized when the battery SOC is within its acceptable limits and the vehicle speed is low. At this speed, the EM can operate in its most efficient region while the engine would have to idle at its inefficient region.

- iii. In hybrid propulsion mode, the ICE and the EM are used in some combination that provides the requested road load. This is the state that allows the HEV to display its greatest benefits in regard to efficiency. If the battery SOC is acceptable, the two components may be used to provide the tractive power requested. Although the combined output torque of the two components is coupled to the vehicle speed, the component speeds are not coupled to the vehicle speed and therefore all components can be controlled to run at their most efficient operating speeds.

The supervisory controller scheme uses a state machine to determine throttle parameters. The controller rules analyze the throttle request and the current state of the vehicle and determine which mode is best under these conditions according to the layout shown in **Error! Reference source not found.**. The calculated throttle position outputs are then sent to the EM controller, Kelly controller, and the ICE controller, MOTEC M-800, over a 0-5V analog line.

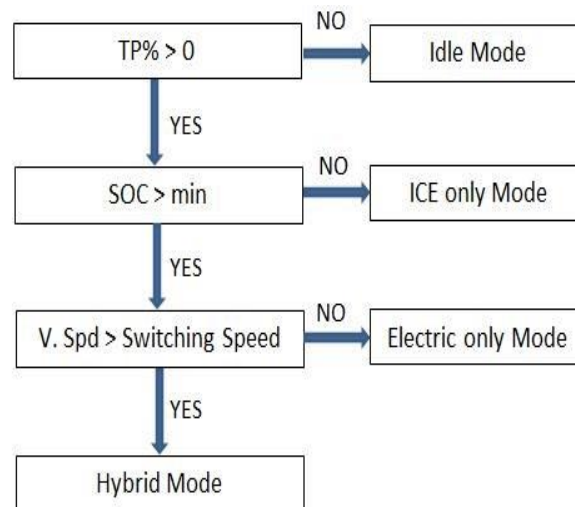


**Figure 79: Supervisory Controller / Vehicle Mode Selection Layout**

For electric mode operation, the control strategy operates such that the ICE runs at a constant fuel throttle angle which has the minimum BSFC; for the lack of a motor/starter integrated system, and the EM makes up the difference between the torque requested by the driver and the torque produced by the ICE. This scheme aims to minimize the amount of

fuel the ICE use by fixing the speed at which the ICE is running to the minimum BSFC speed until the vehicle reaches the hybrid mode switching speed threshold. After reaching this speed and ensuring that the battery SOC is still within its limits the hybrid mode is activated and the vehicle is controlled according to the rule-based EMS. If the battery SOC is no longer within its limits, the ICE only mode is activated and the EM is switched off. The overall control layout is shown in Figure 80.

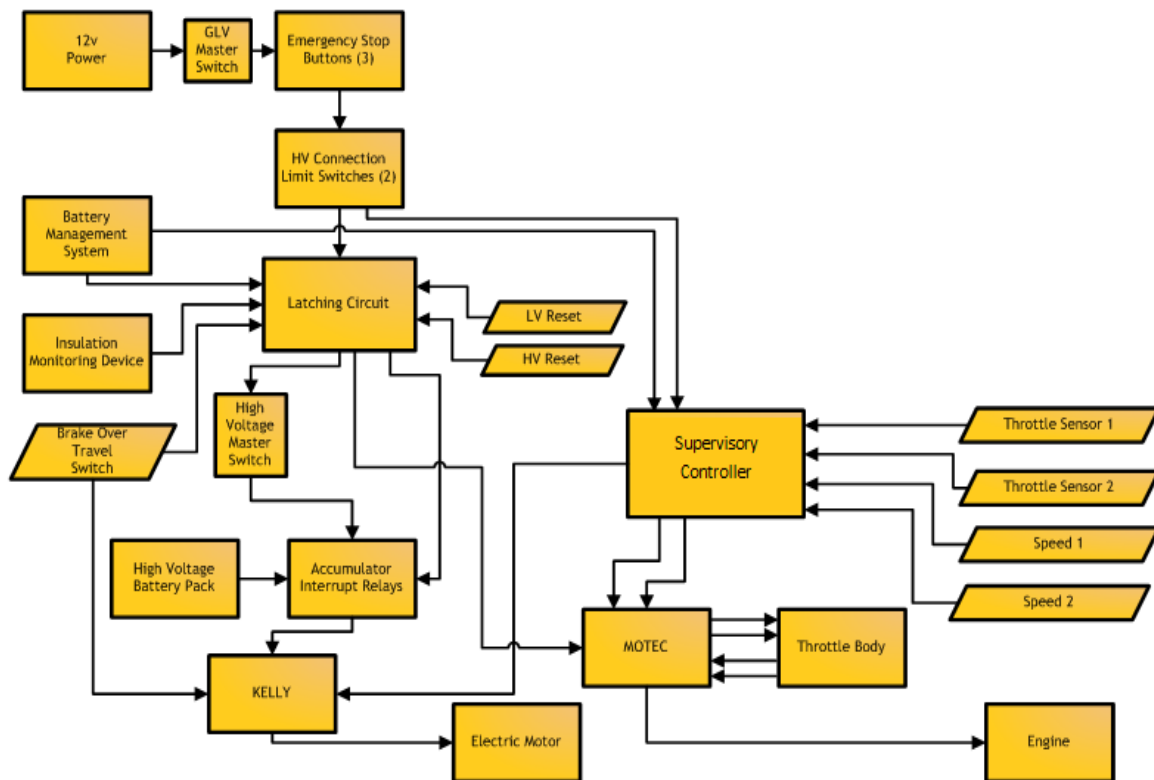


**Figure 80: Overall Supervisory Controller Layout**

### 5.3.4 Hybrid Mode Energy Management

The 2014 Formula Hybrid SAE rules allowed 35.5 [MJ] of energy to be stored on the vehicle during the endurance event. This includes a 27% efficiency consideration for ICE and 80% efficiency consideration for electric systems. [69]

The implemented battery pack in the new platform has a total nominal voltage of 107.3 [V] and a cell capacity of 6 [Ah], though according to equation (5.1) of the Formula

Hybrid SAE rules, the available electrical energy is 1.85 [MJ]. This represents 5% of the amount of energy allowed, leaving 95% or 33.65 [MJ] on the fuel side. According to the fuel energy equivalencies given by the rules, regular gasoline has 2,414 [Wh/L] which is equivalent to 8.69 [MJ/L] considering 27% efficiency. Though, the amount of available fuel is 1.02 [gal].

$$\text{Electric Energy [MJ]} = 0.8 * \text{Voltage}_{Nom}[V] * \text{Capacity}[Ah] * 0.0036 \left[ \frac{MJ}{V * Ah} \right] \quad (5.1)$$

An In house rule-based EMS is designed to control power split between high voltage system and the ICE during hybrid mode. This strategy operates such that the ICE runs over its entire speed range and makes the throttle angle a function of speed to meet a certain percentage of the steady-state road load, while the EM provide the additional percentage. The general principle behind this strategy is that the EM provides power for propulsion during the transients, acceleration to deceleration, and the ICE provides propulsion during higher speeds.

### 5.3.5 Drive-by-Wire

To maximize the benefit of the Supervisory controller, a DBW system is integrated into the vehicle. The DBW uses a potentiometer on the accelerator that sends a signal to the controller which in turn sends a corresponding signal to a servo motor on a Bosch 32 [mm] throttle body to put the engine into the correct torque output required by the driver. Advantages that DBW delivers include more consistent control, safe operation and greater efficiency of the vehicle while also enabling the use of the Supervisory controller to control the throttle position via an electronic signal.

By using the DBW it is possible to idle the engine during low demand periods and thereby improving fuel consumption. Additionally, active control of the throttle response for individual drivers and events can be effective. The DBW system's response can be modified by changing the coefficients used in the DBW control algorithms. This control ensures that during the endurance event for example the engine will not see a rapid change in throttle position. By smoothing out the changes in throttle position, the engine can be

kept from accidentally running into a region of poor efficiency that was not intended by the driver. Figure 81 shows some renders for the accelerator with the DBW potentiometers.

As a failsafe mode, this system uses two potentiometers on the accelerator pedal pivot shaft. The voltages are sent to the controller where the difference between the signals is checked first and if the difference is greater than 10%, the outputs to the ICE and EM controllers are set to null until the input signals regain appropriate coherence. Then these signals are processed and sent to the ICE, and the EM controllers. Should an implausible signal arise, the Supervisory controller and the MOTEC will both terminate the signals until the signals return to a plausible state.

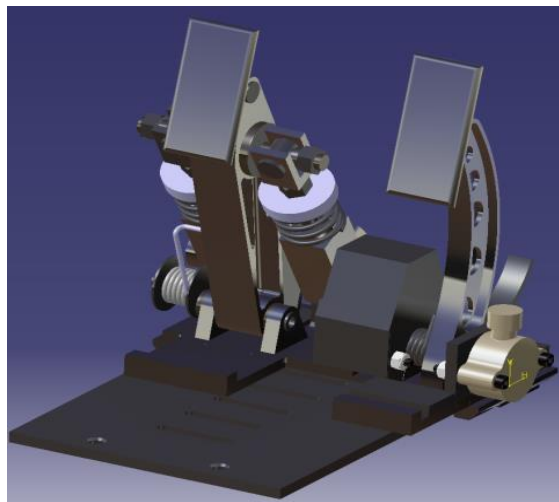


**Figure 81: Throttle Pedal Potentiometers Render**

The DBW has high and low limits. In the event of an open or short circuit, the controller will shut down the output, until the issue is resolved. In addition, the engine controller requires the signals coming from the Supervisory controller be within a very tight tolerance and again within a certain range. This ensures that the outputs from the Supervisory controller are plausible, and prevents any loss of control due to short or open circuited connections.

## 5.4 Case Study Model

The case study powertrain is a torque coupling post-transmission parallel HEV type. A DC permanent magnet EM is coupled to the output shaft of an YZ-250F engine. The EM is intended to propel the vehicle at low speed and load and to assist the ICE in mid-range operations boosting the vehicle efficiency. In this hybrid configuration the EM propels the vehicle during the aforementioned modes. On the other side, the ICE delivers power during hybrid mode and high speed-high torque demand periods.

Performance maps play a significant role in predicting powertrain performance. In the proposed HEV model, the ICE fuel consumption map, the ICE output mechanical map at different loads and speeds, the EM torque characteristics, the driving cycle of the vehicle, and the battery SOC are essential factors to predict the overall powertrain performance and implementing the best required control strategy. The post-transmission powertrain is modeled as a forward facing model in GT-Suite as shown in Figure 82. An YZ-250F engine is modeled as a map-based engine using efficiency maps already generated by a two-zone numerical model. An ICE controller was used to simulate engine control functions such as idling for maximizing fuel economy.

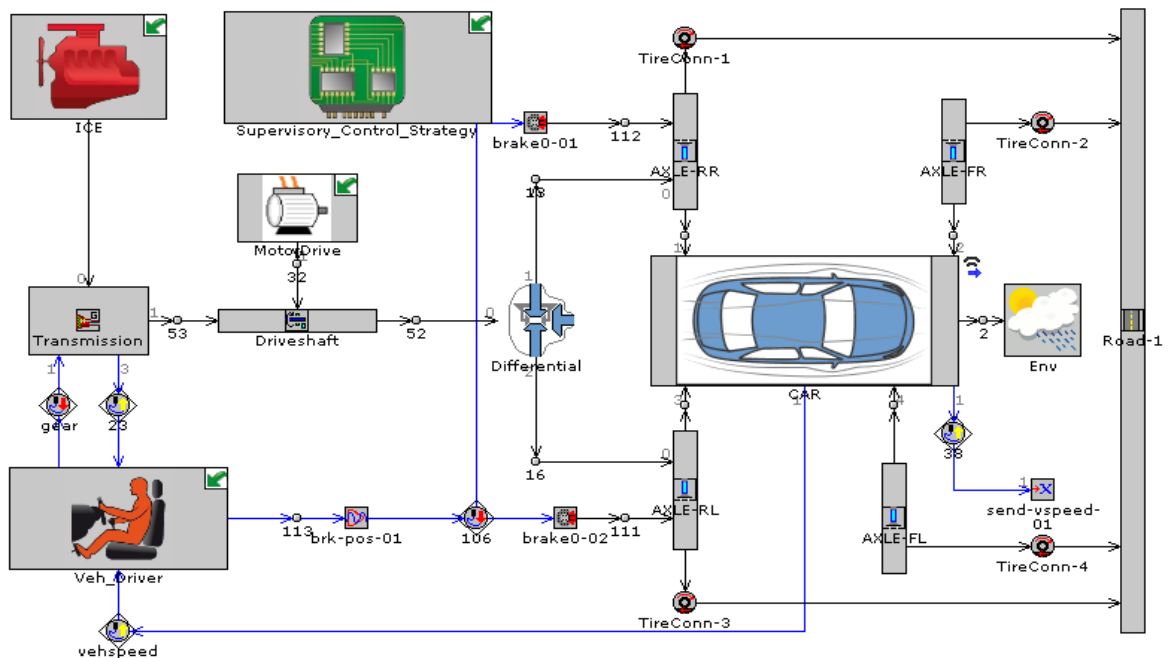
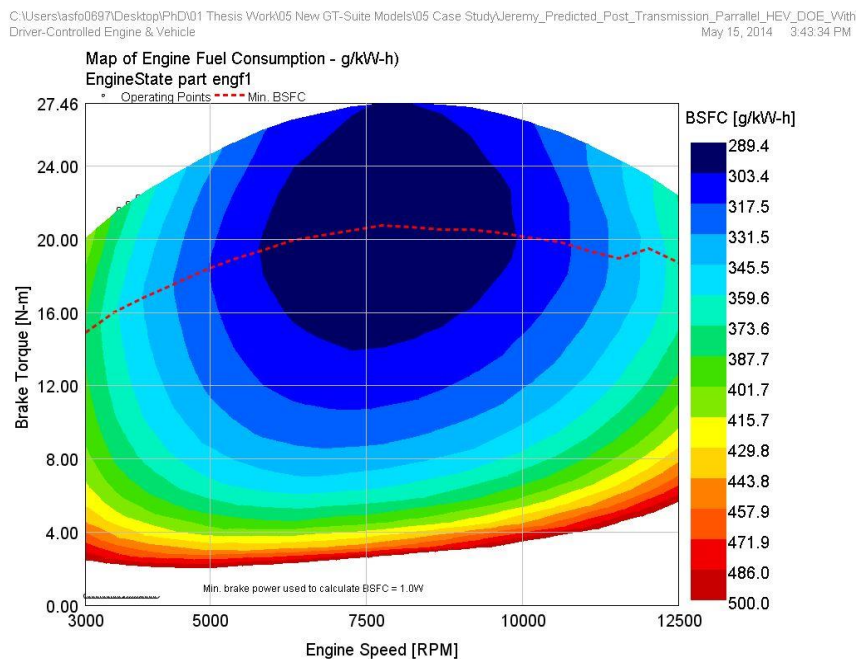


Figure 82: Post-transmission Powertrain Model

### 5.4.1 Engine Performance Map

A two-zone numerical model developed at the University of Idaho is used to predict performance characteristics of the YZ250F engine. This model employed temperature-dependent specific heat ratios, optimized spark timing, sources of inefficiencies, and valve effects. Mechanical efficiencies were calculated using a linear relationship between engine speed and friction losses, while volumetric efficiencies were fluctuated as a function of engine speed. Based on model predictions, specific fuel consumption maps were developed by running simulations at varying engine operating points. It was found that the YZ-250F engine operated most efficiently at an engine speed of 8000 [rpm] at a load of approximately 70%. Figure 83 shows the predicted BSFC map for the YZ-250F engine with the minimum BSFC line in red. [70]

A higher resolution BSFC map was created using the eddy current dynamometer as a backup to validate the predicted maps to be used in forecasting the fuel consumption of the vehicle with the proposed Supervisory controller using the developed GT-Suite model. It was found that the model accurately predicted outputs at different operating throttle positions, and the maximum relative error was 8.61% of the compared data points.



**Figure 83: YZ250F Predicted BSFC map**

### 5.4.2 Traction Motor Torque Characteristics

In addition to the YZ-250F engine performance map, a MotorDrive template is used to define the EM using its torque characteristics, considering the specification of electrical power request, plus an electrical-to-mechanical power conversion efficiency and mechanical friction characteristic. The EM is controlled via an electro-mechanical controller which is programmed to follow a certain control strategy rules. This MotorDrive template calculates a torque based on a power request using the EM torque characteristics.

The current EM on the Formula Hybrid vehicle is a DC motor, Lynch D135RAGS, and its speed, torque, and no load amperage constants have been provided by the manufacturer as shown in Table 7. The EM torque curve based on manufacturer specifications is shown in Figure 84.

**Table 7: Lynch D135RAGS DC Traction Motor Specifications**

No load current [A]	torque constant [Nm/A]	speed constant [rpm/V]	peak power [KW]	peak efficiency %	peak current [A]	rated power [KW]	rated speed [rpm]	rated voltage [V]	rated current [A]	rated torque [Nm]
7.45	0.21	40	36	91	400	18	4400	110	200	42

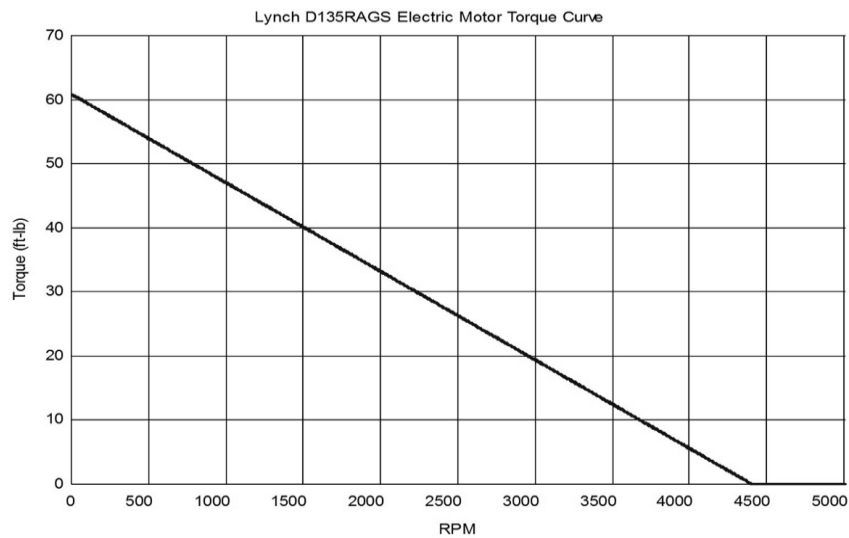


**Figure 84: Traction Motor Torque Curve**



The brake power necessary to follow a certain driving cycle is calculated by a power demand template that calculates the necessary tractive power required for a targeted vehicle speed including tire rolling resistance, aerodynamic drag, road curvature and road grade effects according to equation (3.2). The vehicle design specs are given in Appendix A.

### 5.4.3 Battery Pack Model

A model for the battery pack of a capacity of 6 Ah is developed and represented by lookup maps for internal resistance and open-circuit voltage. The battery model calculates the battery SOC. The SOC is calculated based on the power being drawn from the electric circuit. An inverter is used in conjunction with the battery pack template to ensure the maximum discharge power limit of the battery is not exceeded when it is connected to the electrical or electromagnetic component(s).

### 5.4.4 Supervisory Control Strategy

The supervisory control strategy model shown in Figure 85 is setup using a HEV Controller template, mode selector template, and component controllers.

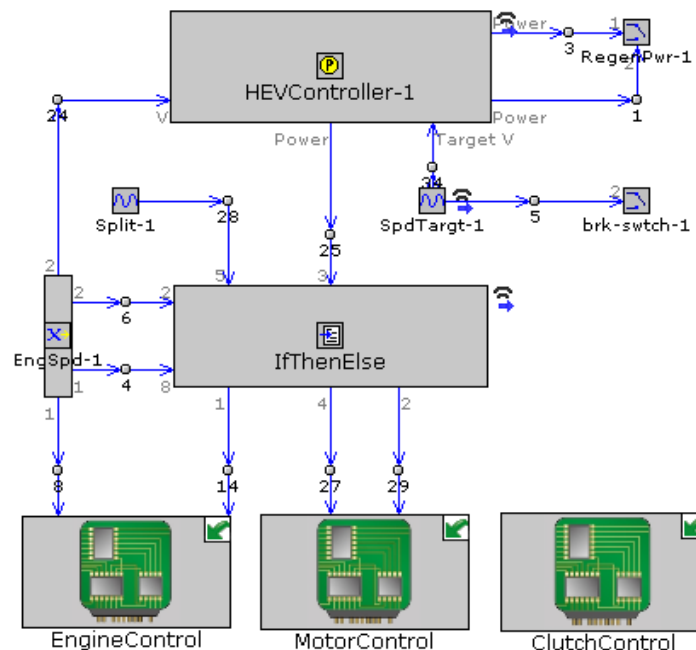


**Figure 85: Supervisory Control Strategy Model**

The HEV controller template determines the required power to meet the target vehicle speed. The IfThenElse template is used as a mode selector to determine what operating mode the vehicle is in by implementing conditional programming into the model.

The Inputs to the mode selector are the battery SOC, actual vehicle speed, tractive power, engine state, torque split, target vehicle speed, and engine speed. While the outputs are the engine power, motor power, engine state, and vehicle mode as shown in Figure 86.

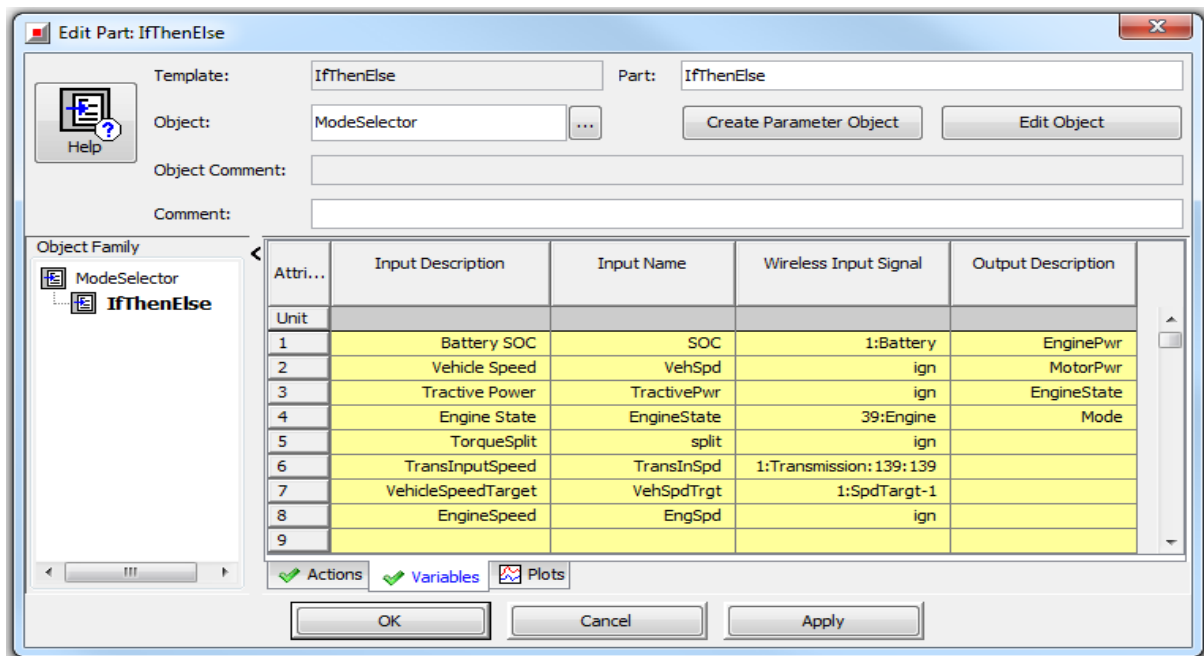


**Figure 86: Mode Selector Inputs/Outputs Variables**

An infinite number of conditional statements that determine a particular output can be created using this template as shown in Figure 87. The conditional statement could be a logical expression, or a combination of logical expressions, that will cause the corresponding action to be active when the condition is met. As mentioned before there are three main modes, electric only, hybrid, and ICE only modes. These modes are described in the model template as actions, which are activated under certain condition(s). These conditions are the Microchip™ PIC32 microprocessor programmed code, which is packaged on the Digilent™ MAX32™ prototyping platform PCB. The Supervisory controller algorithm developed by the team is given in Appendix B.

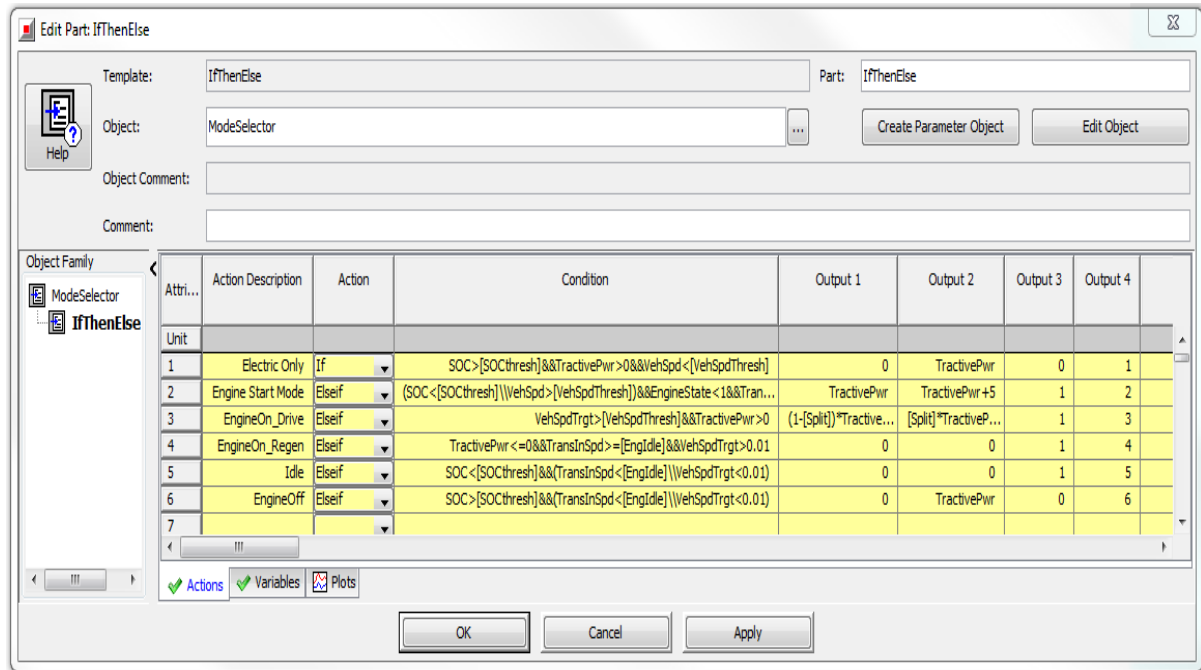


**Figure 87: Mode Selector Actions and Conditions**

The mode is determined by evaluating the battery SOC and the actual vehicle speed. The vehicle will operate in electric mode if the battery SOC is above a certain limit and the vehicle speed is below a certain speed, though output 1 which is the engine power is set to zero, while output 2 which is the required EM power is set to 100% of the tractive power.

If the vehicle speed becomes higher than a certain threshold, the EngineOn\_Drive which is the Hybrid mode is activated and outputs 1 & 2 are sent according to an optimized power split percentages which will be determined in the next chapter. When the vehicle needs to decelerate, should the SOC be low, EngineOn\_Regen (an option regenerative mode) will be used. If the vehicle needs to come to rest and the SOC is low, the controls will select 'Idle' mode and leave the engine running. If the SOC is above the threshold, the controls will select 'Engine Off' as the vehicle comes to rest.

#### 5.4.5 Model Driving Cycle

The driving pattern, driver style, surrounding weather, and powertrain type are some of the several parameters the vehicle fuel economy depends on. The GT-Suite model uses a model based controller that is typically used when performing dynamic driving cycle

analysis with hybrid vehicles. This model consists of a feed forward component to calculate the necessary tractive power required for a targeted vehicle speed or acceleration. It extracts key information from the drivetrain model to define the model basic and advanced parameters.

In GT-Suite, the vehicle controller will work to maintain a minimal error between the model's speed and the actual drive cycle speed. This is done by calculating the error in actual and model speed then calculating the anticipated acceleration, and thus powertrain torque required to meet the actual speed for the future time step.

To validate the case study model, the ARTEMIS Urban driving cycle shown in Figure 88 is used. The speed profile is already provided by GT-Suite. The reason behind choosing this specific driving cycle is its varying speeds, though validate the supervisory controller decisions and the EMS, having several accelerating and braking events allowing the prediction of fuel consumption and predicting the potential energy saved by incorporating a regenerative system. The driving cycle characteristics are given in Table 8.

**Table 8: Model Driving Cycle Characteristics**

Time [sec]	Distance [mile]	Average Speed [Km/hr.]	Max Speed [Km/hr.]	Average/Maximum Acceleration [ $m/s^2$ ]	Average/Maximum Deceleration [ $m/s^2$ ]
993	3.4	18	58	0.67/22.5	-0.7/-20.7

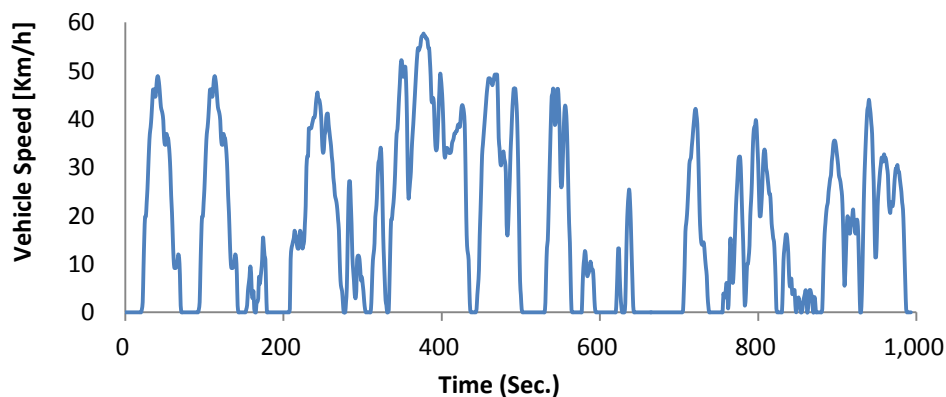


**Figure 88: ARTEMIS Urban Driving Cycle**

## Chapter 6. Supervisory Controller Optimization

### 6.1 GT-Suite Optimization Tools

There are two different tools available within GT-Suite to determine the optimal value of one or more input parameters that produce a desired response of a result variable, Direct Optimization tool and Design of Experiments tool.

#### 6.1.1 Direct Optimization Tool

The direct optimization tool is used to find the values of one or more parameters that produce the desired result of a single result variable. The desired result can be a maximum, minimum, or a specific target value for the selected result variable. The criteria for the optimization are set up prior to running the simulation. This method is called the direct optimizer because the optimization logic is built directly into the GT-Suite solver executable, and the solver will iterate logically through combinations of input parameters until it determines that the optimization criteria have been met (or until it is determined that they are impossible to meet). During this type of optimization, the input values for the next iteration of the solver are determined based on the inputs and corresponding results of previous iterations. The result of this optimization is a single set of parameter values that best meet the optimization criteria. This method is ideally suited for a situation where the optimization task is well defined and involves only a single result variable that can be optimized independently for each simulation case. The reason that this method is preferred for such situation is that it will generally result in the minimum number of solver iterations to produce the desired response. This is because the solver uses an algorithm to determine the input values for the next iteration based on feedback from results of prior iterations. However, this algorithm doesn't make the direct optimizer a good selection when the overall shape of the response surface is of interest. The feedback algorithm that is used for the direct optimizer also has other implications to consider. If the setup criteria for the optimization must be changed, or if it is necessary to optimize a different result variable, it is necessary with the direct optimization method to set up and run a new optimization. [71]

### 6.1.2 Design of Experiments Tool

The design of experiments tool is a more comprehensive and flexible method that allows the user to perform a variety of optimization tasks, but that typically requires more points to be run than in the direct optimizer case and involves post-processing of data to obtain results. In this tool, the user sets up a matrix of experiments to be run by the solver covering the desired ranges of one or more input parameters. After running the matrix of experiments, the resulting data can then be loaded into a post-processing environment to fit a mathematical response surface through the data for one or more result variables. Once this response surface has been established, it is possible to quickly and easily perform optimizations on this surface. The criteria for the optimization are entered into the post-processing environment where the optimization will take place. The GT-Suite solver in this case has no knowledge of the eventual optimization task, and simply runs a predefined set of experiments. The purpose of the solver is simply to generate the data over the complete range of inputs that will be used to define the response surface in the post processor. This method requires more points to be run, and requires post processing of results to perform the actual optimization. However, this method has several benefits that are gained because there is no feedback mechanism within the runs as in the direct optimizer. First, because each experiment is a separate independent case, it is possible to use the distributed computing feature to divide up the runs among different processors. This can actually make the total runtime for this method less than the total runtime for the direct method, even though more points may need to be run. Second, multiple different optimizations may be run in the post-processing environment without re-running any simulations. This is because the original set of experiments that were run covered the whole input design space. Once the resulting result data is loaded into the post-processor and the response surface created, it is possible to run as many different optimizations on the surface as desired, including different result variables. It is also possible to load in multiple result variables to the post-processor at the same time if the optimization task requires the optimization of an objective function that is a combination of two or more result variables. [71]

## 6.2 Case Study Optimization

Since GT-Suite Direct Optimizer is used to find the values of one or more independent parameters that produce a single desired dependent variable result, though it'll be used for the purpose of optimizing the parameters involved in the case study for designing the EMS.

A direct optimizer is set up and run to determine the effect of power split percentages, minimum battery SOC, and hybrid mode switching speed as input parameters on the total fuel consumption as a result quantity. This optimizer works by varying one or more independent parameters to optimize the dependent variable result, then running the simulation and resetting one or more parameters and running again. This process is repeated until the optimal or target value is found or until the maximum number of iterations specified has been run. The optimizer is designed such that it can only properly find a solution if the solution is unique. The optimization algorithm uses the discrete-grid method for optimum search, which reduces the search range into smaller ranges by  $\frac{1}{2}$  until the optimum is found. It is a very robust method and it will always find an optimum within the range tested.

### 6.2.1 Discrete-Grid Optimization Set-up

To set-up the optimization problem, the goal of optimization is chosen from between a target optimization, OptimumMin, or OptimumMax. Since, fuel economy is the main goal behind hybridization of vehicles, though minimizing fuel consumption is the goal behind applying optimization techniques to our case study. The different result variables to be optimized are available and could be easily accessed using a value selector. In this case the ICE fuel consumption is the required result variable as shown in Figure 89. The maximum number of iterations that the optimizer should run before the simulation is terminated is calculated internally, and it will be set to the required number of iterations automatically. The initial iteration state is set to Previous-iteration, where the algorithm uses the last state of the previous iteration as the initial value of the current iteration.

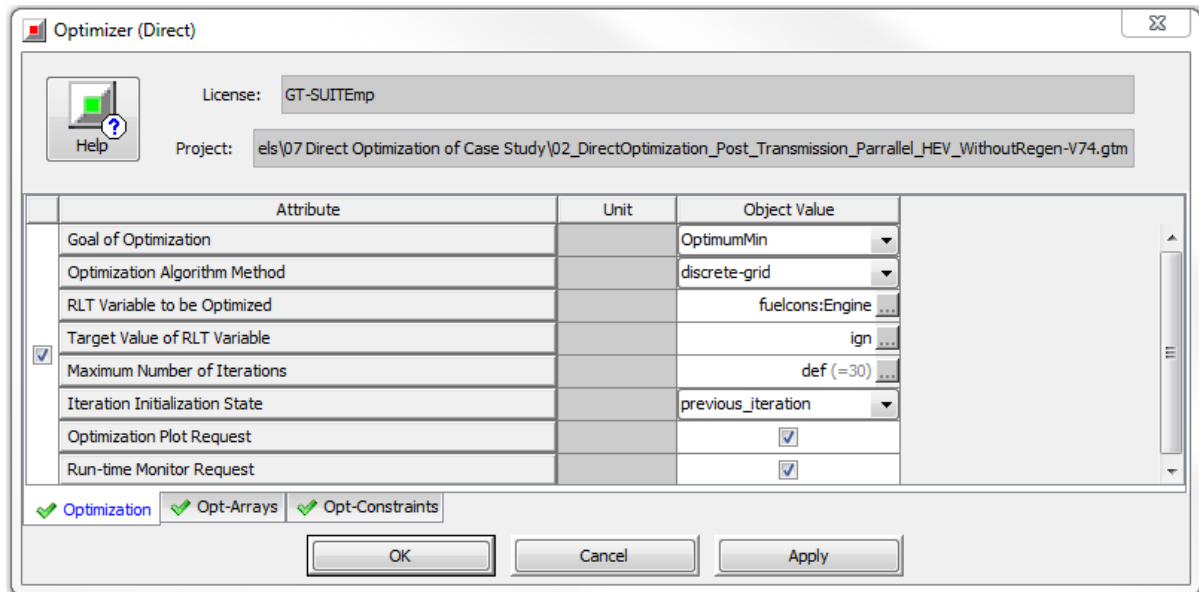


**Figure 89: Discrete-Grid Optimization Method Set-up**

The parameters to be varied during the optimization are selected as shown in Figure 90. The upper and lower ranges over which the parameters should be varied are specified in the same units given to the parameters. The precision of the solution depends on the selected resolution, which is the minimum difference between parameter values, as a percentage of the parameter range that will be evaluated when the parameter is being varied. This value determines the convergence criterion of the optimization problem.

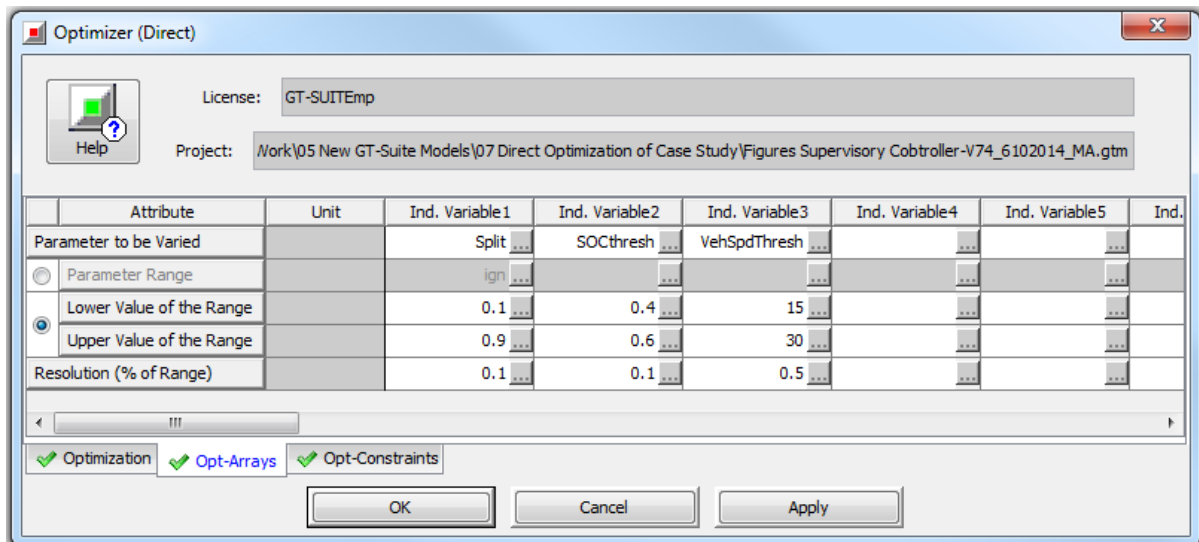


**Figure 90: Independent Variable Parameters Ranges**



The final step is to add the problem constraints. Two major constraints in this case study, the battery SOC range, and the EM maximum speed. These two constraints are added to the optimization problem as shown in Figure 91.

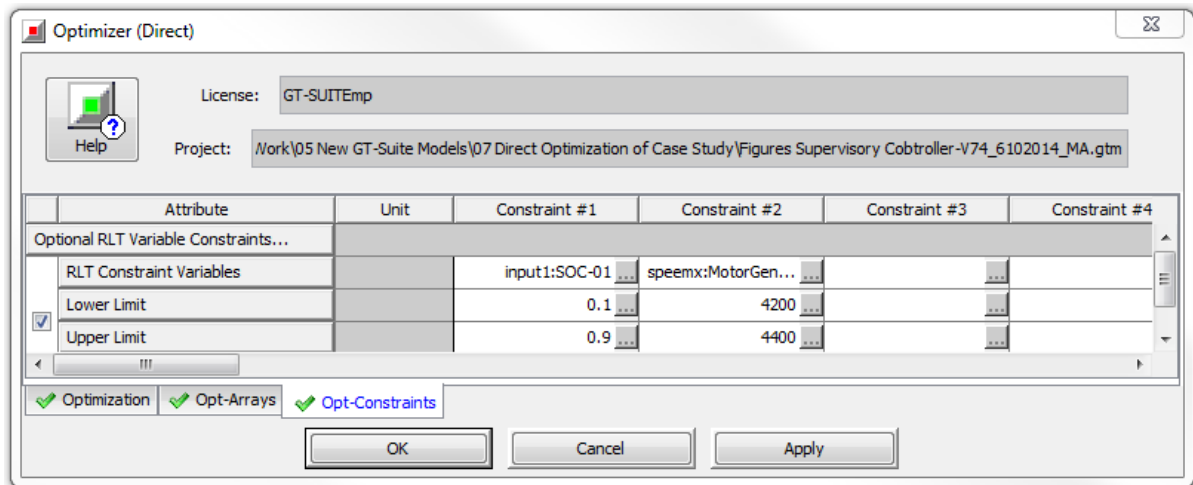


**Figure 91: Optimization Problem Constraints Set-up**

The optimization problem could be formulated as:

min: Fuel Consumption =  $f([\text{Split}], [\text{VehSpdThresh}], [\text{SOCThresh}])$

Subjected to:

$$10 \% \leq \text{Split} \leq 90 \%$$

$$15 [\text{Km/h}] \leq \text{VehSpdThresh} \leq 30 [\text{Km/h}]$$

$$0.4 \leq \text{SOCThresh} \leq 0.6$$

Where:

[Split]: is the power split percentage of the EM to ICE during hybrid mode.

[VehSpdThresh]: is the hybrid mode switching speed.

[SOCThresh]: is the minimum battery SOC to switch to ICE only mode.

Now the optimization problem is ready to run. The next section will highlight the optimization outputs.

## 6.2.2 Optimization Problem Outputs

The number of iterations that the optimizer should run before the simulation termination is calculated internally and it is set to the required number of iterations automatically as mentioned before. For this specific optimization problem, the optimum values of the parameters were found in 272 iterations, where the convergence criteria were satisfied. Figure 92 shows the convergence of the switching speed factor. It could be seen that the optimum switching speed to hybrid converges towards 17.9 [Km/h], 11.25 [mph].

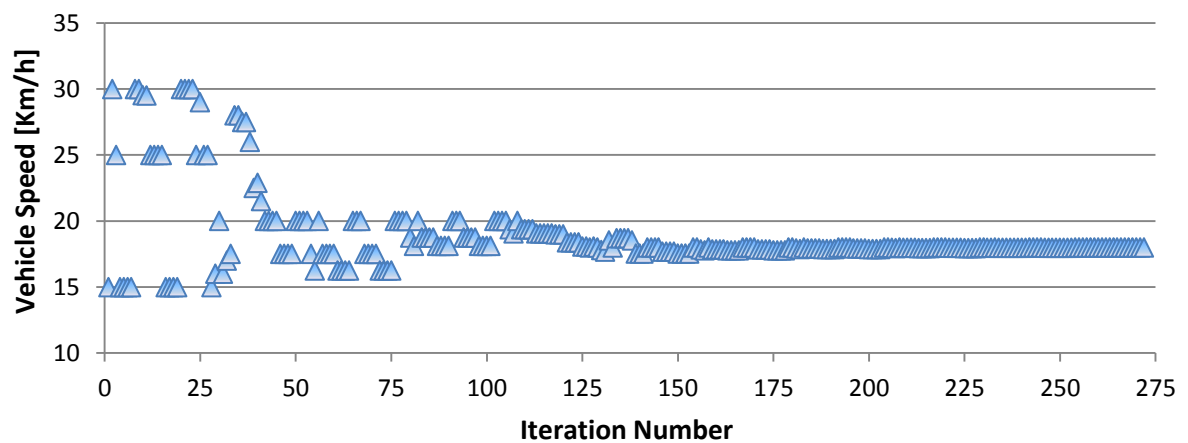


Figure 92: Optimum VehSpdThresh Parameter Value

Figure 93 shows the iterations done to find the optimal power split percentages. This value, 24.5% represents the optimum electric motor power percentage of the required tractive power during hybrid mode.

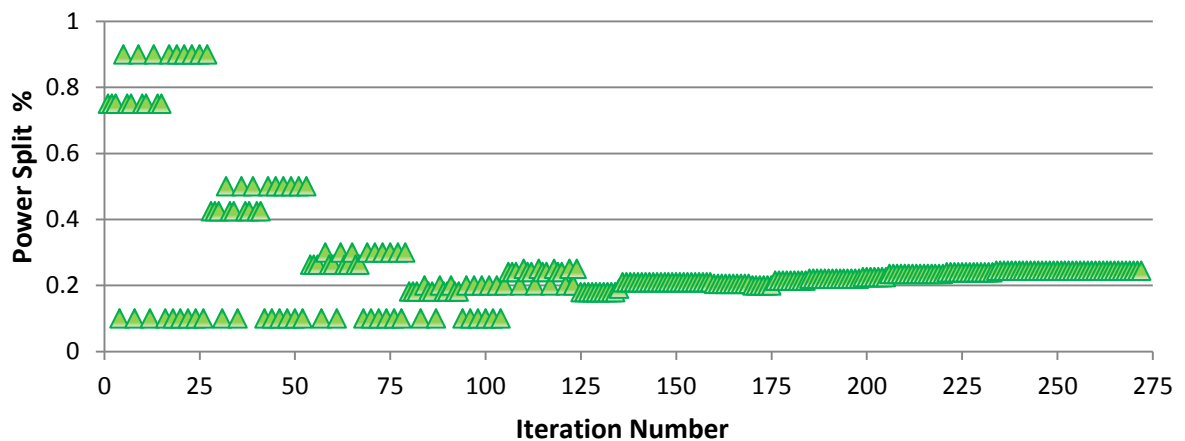
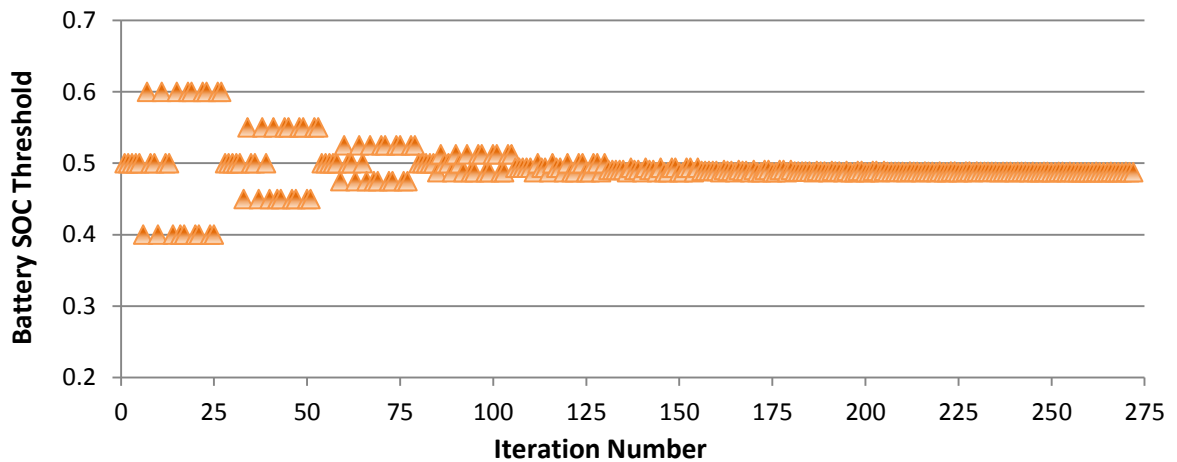


Figure 93: Optimum Power Split % Parameter Value

The iterations of the third and last factor in this optimization problem are shown in Figure 94. The optimal minimum battery SOC value is predicted to be 0.49, at which the supervisory control will switch the vehicle into ICE only mode. The EM will be switched off and the required tractive power will be supplied by the ICE.



**Figure 94: Optimum Min. Battery SOC Parameter Value**

The objective of the optimization problem was to minimize the amount of fuel consumed of the case study vehicle model while performing a specific driving cycle. The outputs of the iterations predict the minimum amount of fuel consumed during the aforementioned driving cycle to be 320.4 [g] as shown in Figure 95, which implies a fuel economy of 29[mpg].

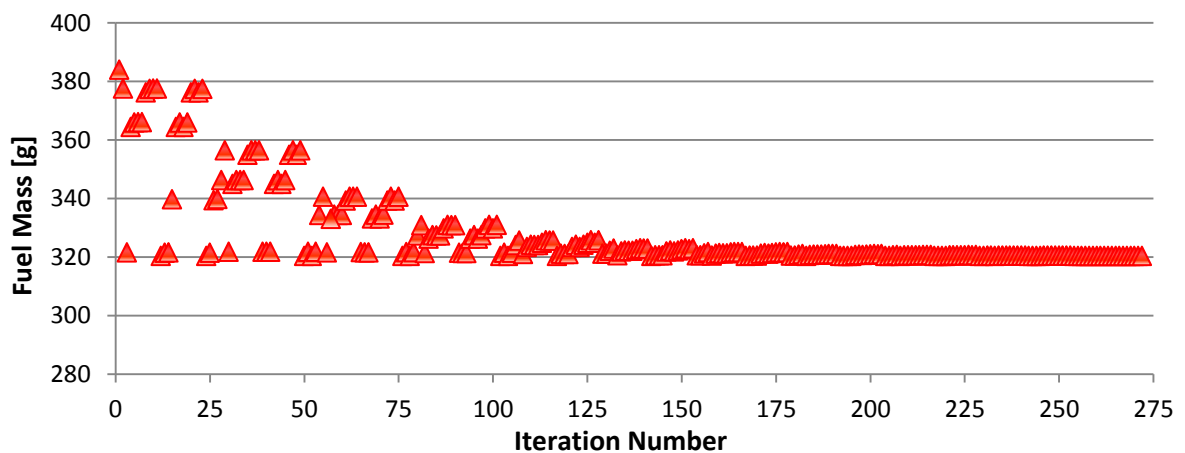


**Figure 95: Optimum Fuel Consumption Amount**

## 6.3 Model Outputs

In this section, some results from the GT-Suite models will be displayed and discussed in order to demonstrate the validity of the models created for this research. Each plot of results will display both the vehicle speed and the performance characteristic of interest versus time unless otherwise noted. This will allow for a quick reference to vehicle speed and a visual approximation of vehicle acceleration so that the effect of these on the characteristic plotted can be seen.

Three model output sets will be displayed. The first set of results to be discussed concerns the model outputs without a supervisory controller and an EMS. The second set shows the model results using the optimized values of the supervisory controller factors, and the final set will display the output with a regenerative energy capturing. Each of these sets will display the required tractive power to follow the prescribed speed profile, the supplied ICE & EM power, average fuel consumption rate and average battery SOC during the driving cycle. Some of the model results are gathered in a comparative analysis given in Table 9.

### 6.3.1 Without A Supervisory Controller

This model sends the same exact power request signal to both power sources, so that a 50% of the required power is requested and supplied from each of the sources. The model doesn't use a supervisory controller, meaning that there is no mode selection and thus both sources will supply power over the entire driving cycle until the battery is out of energy.

Figure 96 shows the vehicle speed profile along with the required tractive power and the power supplied from both power sources. To be able to have a better vision, the outputs of the model during the first 200 seconds are displayed in Figure 97. It can be seen that the ICE and the EM delivers the exact same amount of power during the entire driving cycle, which has a bad effect on the overall energy consumption and fuel economy due to engine operation at low speed-low load. The average fuel consumption rate and the average battery SOC are plotted together in Figure 98.

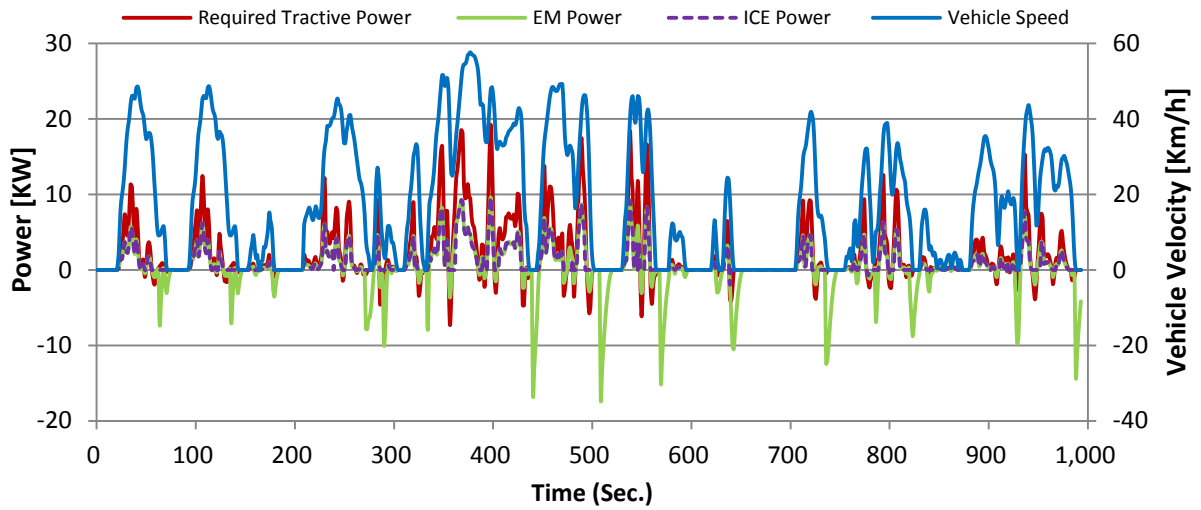


Figure 96: Power Required & Supplied Without EMS

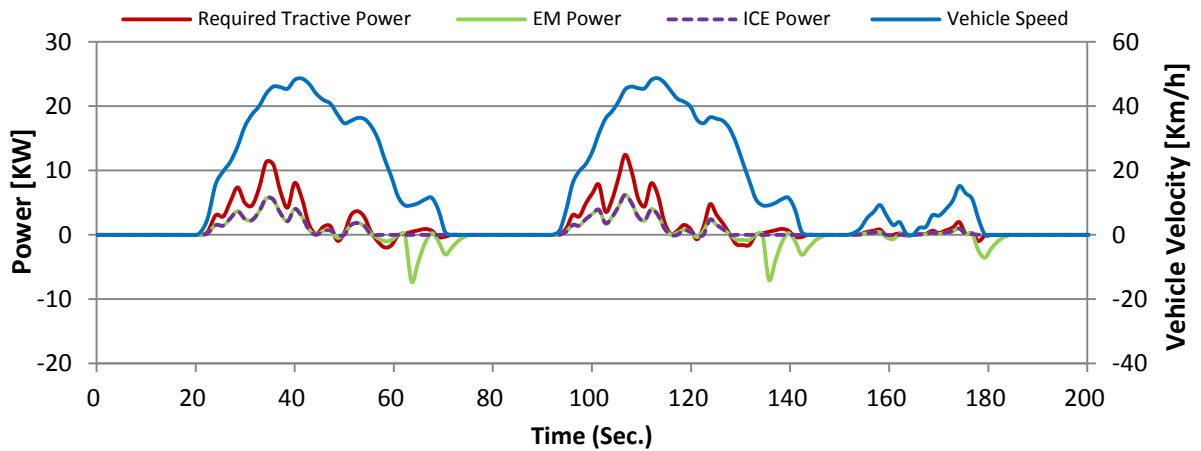


Figure 97: Power Supplied During the First 200 sec. Without EMS

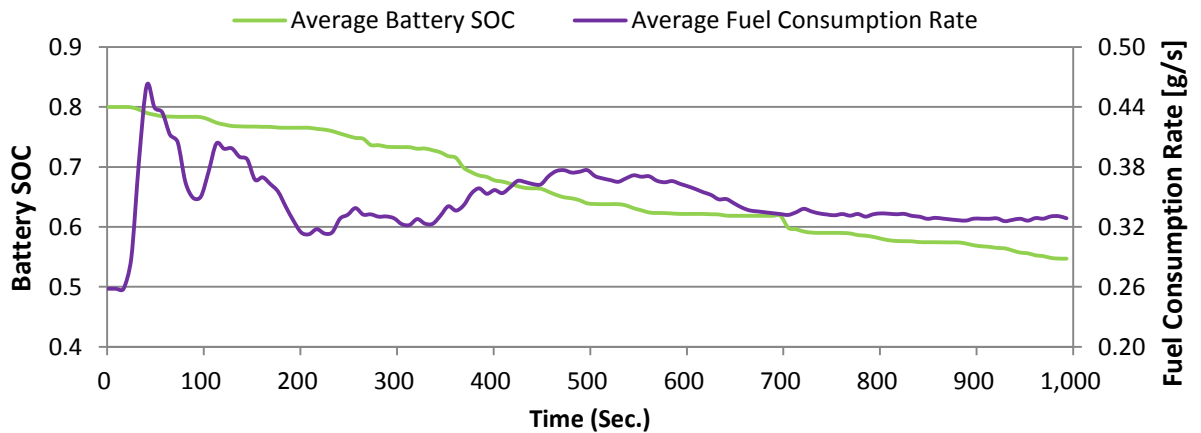
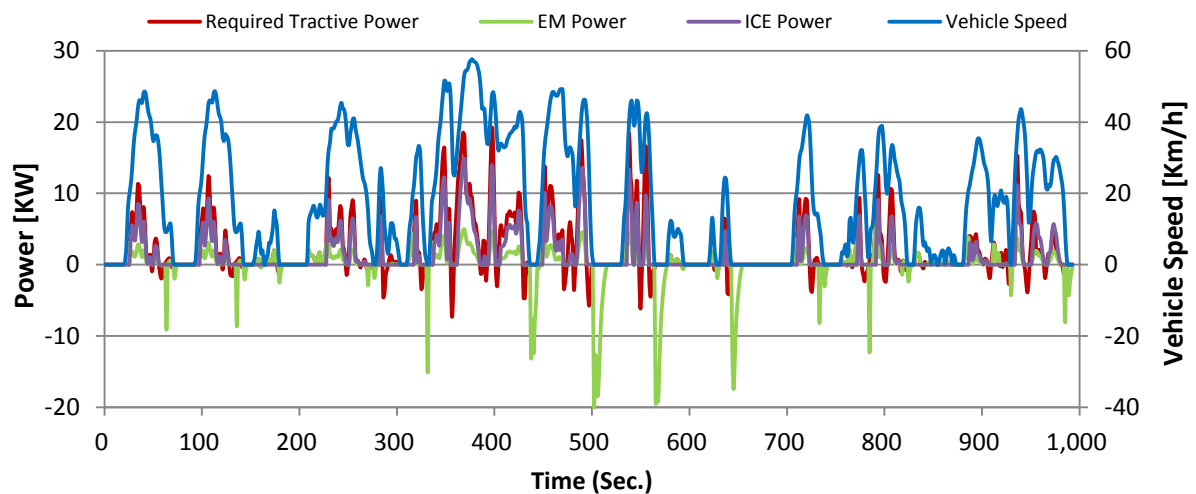


Figure 98: Avg. Fuel Consumption Rate & Avg. Battery SOC, Without EMS

### 6.3.2 With Optimized EMS

In this model the supervisory controller decides the appropriate vehicle mode according to the operating parameters. Then by using the optimized values obtained before, the controller sends the splitted power signals to the power sources, so that a 24.5% & 75.5% of the required power are requested and supplied from the EM & ICE respectively. Figure 99 shows the vehicle speed profile along with the required tractive power and the power supplied from both power sources. Figure 100 shows the outputs of the model during the first 200 seconds. It can be seen that the ICE and the EM don't deliver the same amount of power during the entire driving cycle, which has a better effect on the overall energy consumption due to operation of the ICE at higher speed-higher load region.



**Figure 99: Power Required & Supplied Using Optimized EMS Factors**

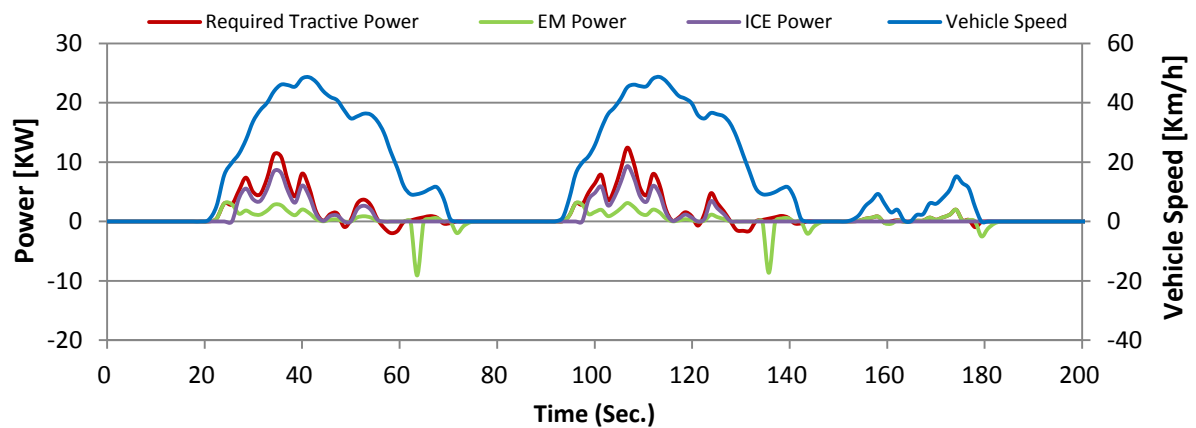


**Figure 100: Power Supplied During the First 200 sec., Optimized EMS**

Figure 101 shows the average fuel consumption rate, and the average battery SOC for the optimized EMS model. It can be noted that there is a decrease in average fuel consumption rate from 0.35 [g/s] to 0.32 [g/s], and an increase in the overall battery SOC from 0.54 to 0.61. That is for using the supervisory controller and the EMS during this driving cycle.

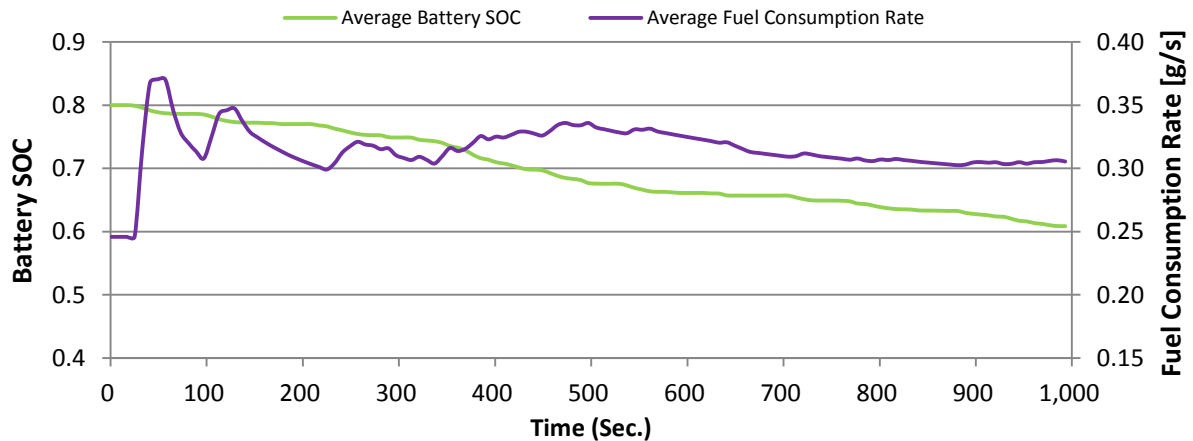


**Figure 101: Avg. Fuel Consumption Rate & Avg. Battery SOC , Optimized EMS**

### 6.3.3 With EMS & Regenerative Energy

After running the model using the optimized EMS factors, it is realized that there is a good opportunity to capture energy during deceleration periods, which could be seen in the huge EM negative power losses in Figure 99. The controller is modified to allow for regenerative energy capturing. By capturing some of this energy, the battery energy might last longer, thus raising the overall fuel economy. The model is run with the same parameters; the only difference is feeding the regenerated energy back to the battery.

Comparing the second and third model results by the end of the driving cycle, Figure 102 shows a reasonable decrease in the EM losses over the entire driving cycle due to regeneration, which can be noticed in the difference between average battery SOC in Figure 101 and Figure 104. The second case the battery SOC starts at 0.8 and ends at 0.61, but with regeneration the SOC starts at 0.8 and ends at 0.64, which means that the captured energy during deceleration periods regains about 15% of the electrical energy spend during the entire driving cycle.

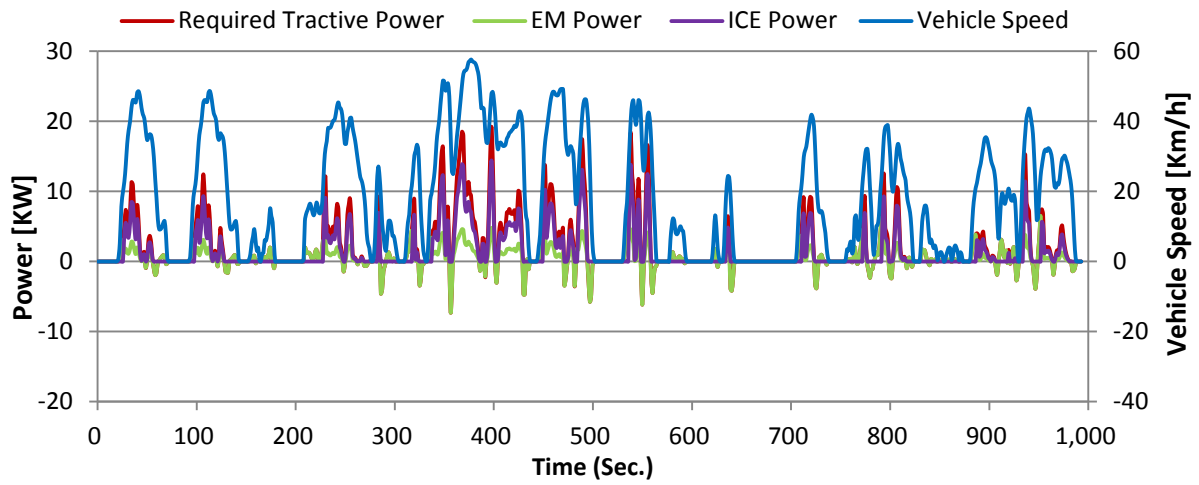


Figure 102: Power Required, Supplied, & Regenerated in Optimized EMS & Regen

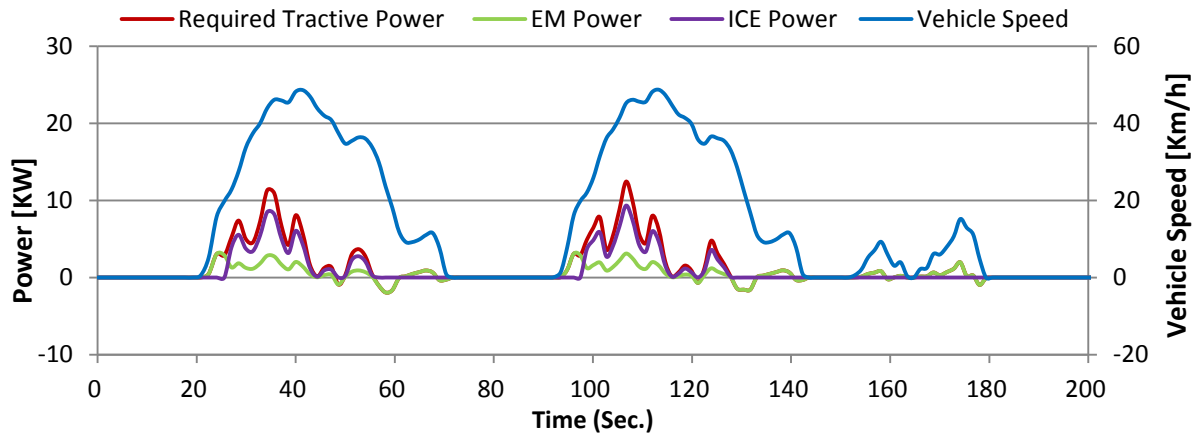


Figure 103: Power Supplied During the First 200 sec., Optimized EMS & Regen

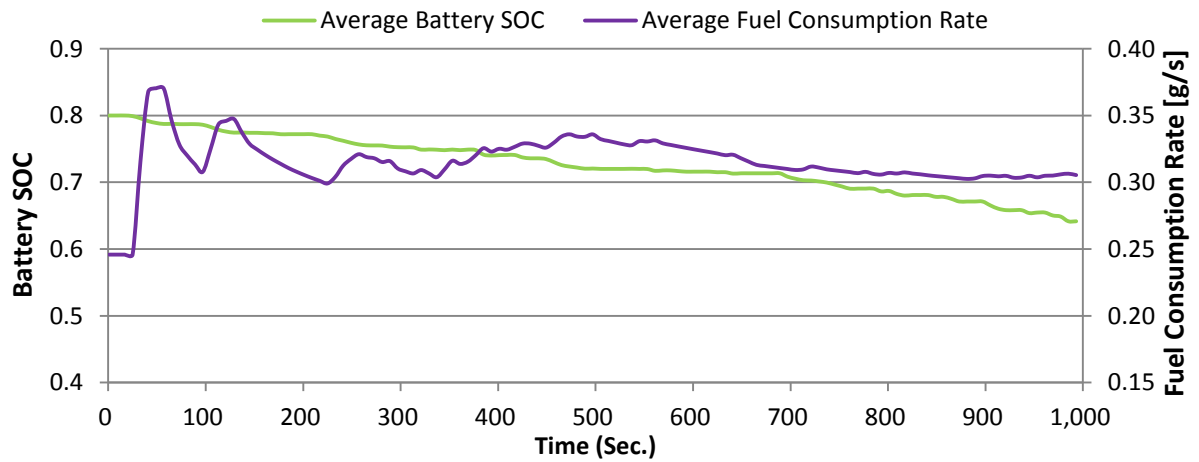


Figure 104: Avg. Fuel Consumption Rate & Avg. Battery SOC, Optimized EMS & Regen



### 6.3.4 Model Results Comparative Analysis

Some of the model performance results are given in Table 9, in a comparative analysis to explore the benefits behind using a vehicle supervisory controller, and the potential energy savings acquired using an EMS and regenerative braking.

**Table 9: Comparative Analysis of Model Results**

Model	Without EMS	With Optimized EMS	With EMS & Regen.	Comments
<b>Avg. /Max. Vehicle Speed [mph]</b>	11.5 35.9	10.94 34.92	11.01 35.7	The differences in the predicted speeds are due to the switching between modes.
<b>Total Distance Traveled [mile]</b>	3.43			All cases run the same driving cycle.
<b>Avg. /Max. Acceleration [m/s<sup>2</sup>]</b>	0.67 14.12	0.60 12.92	0.61 12.91	Lower accelerations in cases using EMS due to operation on different vehicle modes. Higher deceleration in third case due to EM regenerative braking.
<b>Avg. /Max. Deceleration [m/s<sup>2</sup>]</b>	-0.44 -13.74	-0.50 -14.87	-0.71 -16.07	
<b>Avg. BSFC [g/kW-h]</b>	340.7	305.4	305.4	The ICE runs at a better BSFC using the supervisory controller, leading to a better average fuel consumption rate.
<b>Avg. Fuel Consumption Rate[g/s]</b>	0.35	0.32	0.32	
<b>Total Fuel Mass [g]</b>	372.8	320.4	320.4	Lowering the amount of fuel used during for the same driving cycle using controller optimized factors.
<b>Total Fuel Volume [gal]</b>	0.137	0.117	0.117	
<b>Combined Gas Mileage [mpg]</b>	25	29	31	Higher fuel economy achievement using EMS, even higher with Regen.
<b>Fuel Energy Depleted [MJ/ mile]</b>	-4.706	-4.044	-4.044	Potential energy savings through certain supervisory control commands for traction power supply.
<b>Electrical Energy Depleted [MJ/ mile]</b>	-0.416	-0.375	-0.375	
<b>Regenerated Energy [MJ/mile]</b>	0	0	0.051	Earning energy recapturing through regenerative braking.
<b>Total Energy Used [MJ/ mile]</b>	-5.122	-4.419	-4.368	Acquiring lower total energy usage for the same driving cycle and surrounding situation.

### 6.3.5 Energy Analysis

As a further predictions of the models, energy losses in each of the previous simulated cases are presented in pie charts, normalized to the distance.

Figure 105 shows the different amounts of energy losses per mile during the driving cycle for the first case, hybrid without a supervisory controller.

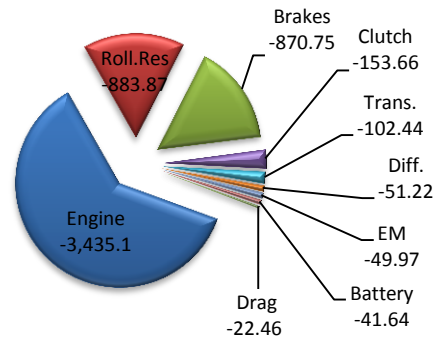


Figure 105: Without EMS

The second case energy losses per mile are given in Figure 106. Using the optimized controller factors values previously found reduces the amount of fuel energy losses due to reduction in the total amount of fuel energy used during the entire driving cycle.

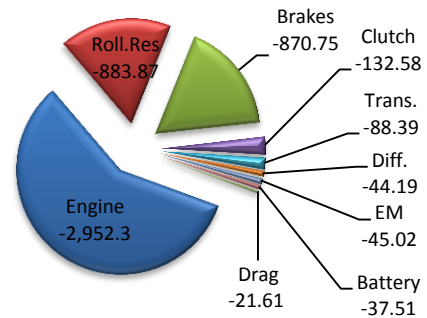


Figure 106: With Optimized EMS

Figure 107 shows the normalized energy losses for the third case, using the optimized factors along with the regenerative braking capability. The amount of fuel energy losses is lowered due to engine operation in higher efficiency region. The braking energy losses are lowered due to braking by the EM and recapturing of a portion of the braking losses.

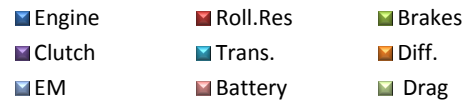
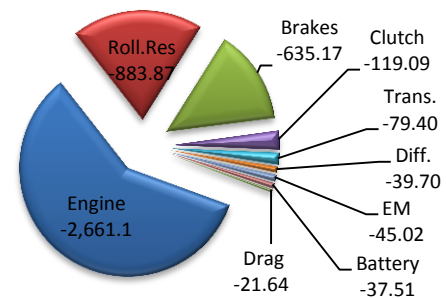
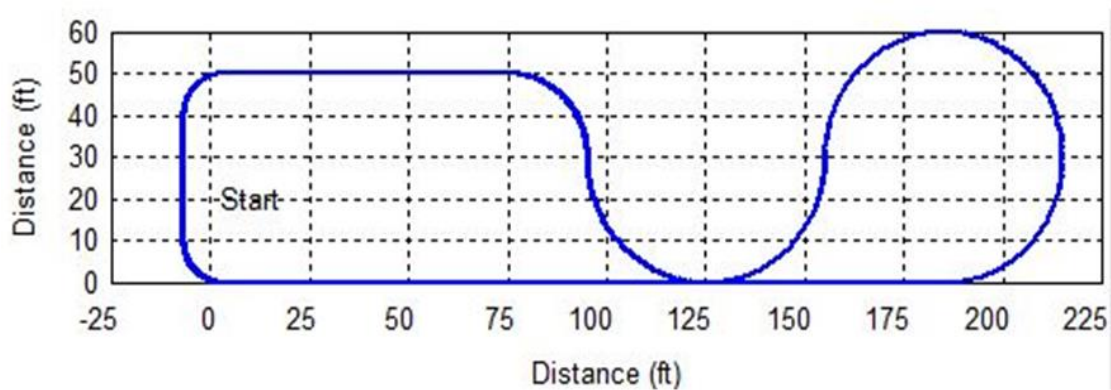


Figure 107: With EMS & Regen

For the second and third cases, the battery energy losses are lower than the first case due to reduction in the EM power output during hybrid mode according to the optimized split percentage.

## 6.4 Testing

In order to perform a comparison between the former vehicle and the new developed systems, testing had to be undertaken. In an attempt to achieve consistent results across the various tests, the track designed and used in [63] is chosen for testing for several reasons. First being that the information on fuel economy of this platform without the new developed systems were obtained using this track, so using the same track will limit the number of variables for a true comparison. Also, this track, shown in Figure 108, allows monitoring vehicle performance under dynamic events such as acceleration, cornering, and deceleration, testing out the vehicle for reliability issues with the new controller and many other sub systems such as braking, suspension, and handling.



**Figure 108: Testing Track**

The first primary validation test was to ensure the proper design and implementation of the drive-by-wire system that was integrated for the purpose of providing the supervisory controller with the driver accelerator pedal commands. The vehicle was tested on ICE only for several runs to ensure the stability of the system. Some of these runs were at full race speed and some were at more conservative speeds. The track was designed to resemble a one mile autocross track. With a known amount of fuel in the fuel system, and due to the lack of an accurate fuel consumption measurement method, every run the fuel system is emptied and the amount of fuel consumed is calculated.

For validation purposes, the results of the same tests of the mechanically actuated throttle given in [63] are compared to the drive-by-wire system test results in Table 10.

**Table 10: Comparison of ICE only Test Results With and Without DBW System**

	Average Lap Time [s]	Fastest Lap time [s]	Total Distance [mile]	Avg. Speed [mph]	Fuel Efficiency [MPG]	Fuel Energy Used [MJ]
<b>ICE only/Autocross fast run</b>						
<b>Without DBW</b>	20.4	19.4	1	19.55	17.6	1.9
<b>With DBW</b>	19.22	18.8	1.12	20.22	17	2.1
<b>ICE only/Conservative Slow run</b>						
<b>Without DBW</b>	24.12	22.5	1	16.54	21.6	1.52
<b>With DBW</b>	21.9	19.95	1.19	17.73	19.5	1.99

It is clear from the test results that the new electronically controlled throttle body via the DBW system hasn't affected the engine performance for both fast and slow runs. Even though, there is a decrease of 3% and 9.6% in the fuel efficiency during the fast and slow runs respectively, but this is because the relative increase in vehicle speed by 3.4% and 7.2% respectively.

The values that might have significant impressions on the engine speed during these runs are the amounts of energy used in [MJ]. The fuel energy used is calculated for the measured used gas during each run using a gasoline energy content of 2414[Wh/L] given in [69]. The new test shows an increase in the fuel energy used by 10% and 30% during the fast and slow runs respectively, which is an indication of engine operation at relatively higher speeds and loads, thus consuming more fuel.

Finally, For the purpose of predicting the vehicle fuel economy and performance during hybrid mode using the model, a desired vehicle speed profile should be used. Though, using the designed track to capture real vehicle speed and importing the vehicle speed profile into the model for different performance parameters prediction and testing. Unfortunately, no physical track test data currently exists as the physical vehicle faced data acquisition, and EM mechanical coupling issues.

## Chapter 7. Conclusions and Recommendations

In this dissertation, a wide range of HEV architectures have been characterized and compared. Advanced models for different layouts in modern hybrid electric vehicles were created using GT-Suite software. Detailed comparisons were undertaken to assess fuel consumption rates and energy dissipation associated with four standard driving cycles. The model was then used to design an optimized rule-based supervisory controller for the University of Idaho Formula Hybrid Vehicle.

### 7.1 Conclusions

The GT-Suite model replicated hybrid vehicle performance found in other studies with an ICE only vehicle model yielding the lowest fuel economy in all kinds of driving situations, city and highway, as shown in Table 4. The series HEV had poor fuel economy for highway driving patterns where regeneration is insignificant. Similarly, the series HEV had moderate fuel economy for city driving cycles. The parallel and the series-parallel HEV model showed the best fuel economy for both city and highway driving scenarios as shown in Figure 53.

A comprehensive energy analysis considering energy depleted from various sources and energy added from regeneration was summarized in Table 5. For the city driving cycles the three different hybrid drivetrains showed a significant energy saving even after adding the amount of energy required to recover the battery charge at the end of the cycle, while during highway driving both parallel and combined hybrids were superior. To identify and quantify the reasons for fuel economy changes energy losses are attributed to all powertrain components as shown in Table 6.

Another aspect considered in this work concerns the control system of hybrid vehicles to regulate the power split between the ICE and electric motor. Among the control strategies covered in the literature, dynamic programming is the only one that guarantees global optimality if the driving cycle is known in prior. However, it is not practical for real-time application due to computational complexity and uncertainty about the driving trajectory before the trip starts. On the other hand, control rules written in fuzzy logic, rule-

based and neural network controllers are generally not optimized, but these can integrate heuristic reasoning based on expert knowledge. These algorithms do require some information to perform off line optimization or tuning of the parameters but it is typically less than that required by dynamic programming.

An important outcome of this dissertation is specifying a supervisory control strategy that minimizes fuel use through a rule-based energy management strategy. This was done with a GT-Suite model that incorporated a predicted YZ-250F performance map, a Lynch electric motor torque curve, vehicle geometry, and experimentally determined roll down parameters. The resulting supervisory control algorithm layout is shown in Figure 79, and its design/implementation process was discussed in Chapter 5. The supervisory controller parameters also were optimized using discrete grid optimization method to minimize fuel consumption as described in Chapter 6.

Three case scenarios, without EMS, with EMS, and with EMS as well as energy regeneration, were run to investigate the benefits behind using the optimized energy management system, and the potential energy regeneration. The ARTEMIS Urban driving cycle, shown in Figure 88, was used during the simulations due to inaccessibility of a competition driving cycle. A comparative analysis of the performance results of the three cases was done and summarized in Table 9. The model results shows a significant improvement in fuel economy using the optimized EMS parameters from 25 [mpg] to 29 [mpg], even higher using rear regeneration, but is not as significant as just implementing the EMS.

The GT-Suite model was also able to predict the amount of energy needed to complete the endurance event for the three case studies. Table 11 gives the energy allotment allowed on the competition regarding the endurance event, and Table 12 gives rough calculations for the amount of energy required to complete the event for each of the three different cases.

For the first time at the University of Idaho, an optimized supervisory controller is designed and implemented in the Formula Hybrid vehicle incorporating a rule-based energy management strategy that accounts for the proper power split between the power sources of a parallel hybrid powertrain in a compact, lightweight, mass-centralized platform.

**Table 11: Endurance Event Energy Allotment**

Fuel Energy Available considering Efficiency [MJ]	Engine Efficiency	Fuel Energy Available before Efficiency [MJ]	Electric Energy Available considering Efficiency [MJ]	High Voltage System Efficiency	Electric Energy Available before Efficiency [MJ]	Total Energy Available before Efficiency [MJ]
33.65	0.27	124.630	1.85	0.8	2.318	126.95

**Table 12: Endurance Event Energy Predictions**

	Total Chemical Energy Depleted [MJ/mile]	Endurance Event Distance [mile]	Total Amount of Energy Required [MJ]	Comments
<b>Without EMS</b>	5.122	27.34	140.035	The vehicle will not be able to complete the event.
<b>With EMS</b>	4.419	27.34	120.815	The vehicle will be able to complete the event with just enough energy.
<b>With EMS &amp; Regen</b>	4.368	27.34	119.42	The vehicle will complete the event, but there will be excess energy onboard.

## 7.2 Recommendations

Future work should be undertaken in three different areas: (1) UI-FHSAE platform design, (2) parametric studies with the GT-Suite model, and (3) vehicle performance testing under competition-specific driving cycles.

Adoption of light-weight, regenerative braking for the UI-FHSAE platform is needed to provide adequate margin for completing the endurance event. One option is adding a new front powertrain that is capable of front electric drive and energy regeneration during braking. This is attractive because more than 60% of the braking energy is dissipated in the front wheels, but this could add more than 75 lbs. to vehicle weight. The other, more preferred option is recapturing energy from the rear wheels using the current powertrain setup. This would not add any extra mass but would not yield as much energy recovery. Addition of energy regeneration systems further underscores the importance of a supervisory controller. Methods outlined in this dissertation could be reprogrammed to determine more dynamic rule-based parameters.

The GT-Suite model could also support sensitivity studies that could document of different design changes in future vehicle configurations. The energy impact of reducing vehicle mass would be fairly easy to obtain, as would benefits of reduced rolling resistance, and addition of aerodynamic features. With some additional effort, elevation changes in the road course could be added and different vehicle handling behaviors associated with different weight distribution schemes could be quantified.

Finally, much work is needed to characterize driver behavior on simulated track environments. This would help define realistic driving cycles with different average speeds and different overall fuel economy. These driving cycles could then be used to refine the optimized parameters referenced by the rule-based supervisory controller. The TK Solver model developed by Wos [68], and refined by Rinker [63] is anticipated to be very helpful in prescribing driving cycles with different levels of aggressiveness and average speed. Synthesizing outputs of the GT-Suite model described here with such a track-side tool could provide significant competitive advantage under different event conditions where on-board energy storage is limited.



## References

- [1] L. Serrao, S. Onori, and G. Rizzoni, "A Comparative Analysis of Energy Management Strategies for Hybrid Electric Vehicles," *Journal of Dynamic Systems, Measurement, and Control*, vol. 133, no. 3, p. 031012, 2011.
- [2] X. Zhang and C. Mi, "Vehicle Power Management: Modeling, Control and Optimization," First Edition. Springer, 2011.
- [3] M. Ehsani, Y. Gao., and A. Emadi, "Modern Electric, Hybrid Electric, and Fuel Cell Vehicles: Fundamentals, Theory, and Design," CRC Press, 2010.
- [4] "The 1899 Lohner Porsche, the first Hybrid Vehicle," Available: <http://www.hybrid-vehicle.org/hybrid-vehicle-porsche.html>.
- [5] K. Chau and Y. Wong, "Overview of Power Management in Hybrid Electric Vehicles," *Energy Conversion and Management*, vol. 43, no. 15, pp. 1953–1968, Oct. 2002.
- [6] C. C. Lin, H. Peng, J. W. Grizzle, J. Liu, and M. Busdiecker, "Control System Development for an Advanced-Technology Medium-Duty Hybrid Electric Truck," *SAE International*, Warrendale, PA, 2003-01-3369, Nov. 2003.
- [7] N. Jalil, N. A. Kheir, and M. Salman, "A rule-based energy management strategy for a series hybrid vehicle," presented at the *Proceedings of the American Control Conference*, 1997, vol. 1, pp. 689–693.
- [8] B. M. Baumann, G. Washington, B. C. Glenn, and G. Rizzoni, "Mechatronic design and control of hybrid electric vehicles," *IEEE/ASME Transactions on Mechatronics*, vol. 5, no. 1, pp. 58–72, Mar. 2000.
- [9] C. C. Lin, J. M. Kang, J. W. Grizzle, and H. Peng, "Energy management strategy for a parallel hybrid electric truck," presented at the *Proceedings of the American Control Conference*, 2001, vol. 4, pp. 2878–2883.
- [10] C. C. Lin, H. Peng, J. W. Grizzle, and J. M. Kang, "Power management strategy for a parallel hybrid electric truck," *IEEE Transactions on Control Systems Technology*, vol. 11, no. 6, pp. 839–849, Nov. 2003.

- [11] Z. Han, Z. Yuan, T. Guangyu, C. Quanshi, and C. Yaobin, "Optimal Energy Management Strategy for Hybrid Electric Vehicles," *SAE International*, Warrendale, PA, 2004-01-0576, Mar. 2004.
- [12] Y. Zhu, Y. Chen, G. Tian, H. Wu, and Q. Chen, "A four-step method to design an energy management strategy for hybrid vehicles," in *Proceedings of the 2004 American Control Conference*, vol. 1, pp. 156–161.
- [13] A. Sciarretta and L. Guzzella, "Control of hybrid electric vehicles," *IEEE Control Systems*, vol. 27, no. 2, pp. 60–70, Apr. 2007.
- [14] C. Desai and S. S. Williamson, "Comparative study of hybrid electric vehicle control strategies for improved drivetrain efficiency analysis," *IEEE Electrical Power Energy Conference (EPEC)*, 2009, pp. 1–6.
- [15] F. R. Salmasi, "Control Strategies for Hybrid Electric Vehicles: Evolution, Classification, Comparison, and Future Trends," *IEEE Transactions on Vehicular Technology*, vol. 56, no. 5, pp. 2393–2404, Sep. 2007.
- [16] H. Khayyam, A. Kouzani, S. Nahavandi, V. Marano, and G. Rizzoni, "Intelligent Energy Management in Hybrid Electric Vehicles," in *Energy Management*, F. Macia, Ed. InTech, 2010.
- [17] P. Caratozzolo, M. Serra, and J. Riera, "Energy management strategies for hybrid electric vehicles," in *Electric Machines and Drives Conference, IEMDC'03. IEEE International*, 2003, vol. 1, pp. 241–248.
- [18] T. Hofman, M. Steinbuch, R. V. Druten, and A. Serrarens, "Rule-based energy management strategies for hybrid vehicles," *International Journal of Electric and Hybrid Vehicles*, vol. 1, no. 1, p. 71, 2007.
- [19] N. J. Schouten, M. A. Salman, and N. A. Kheir, "Fuzzy logic control for parallel hybrid vehicles," *IEEE Transactions on Control Systems Technology*, vol. 10, no. 3, pp. 460–468, May 2002.
- [20] N. J. Schouten, M. A. Salman, and N. A. Kheir, "Energy management strategies for parallel hybrid vehicles using fuzzy logic," *Control Engineering Practice*, vol. 11, no. 2, pp. 171–177, Feb. 2003.

- [21] X. He, M. Parten, and T. Maxwell, "Energy Management Strategies for a Hybrid Electric Vehicle," in *Vehicle Power and Propulsion, IEEE Conference, 2005*, pp. 536 – 540.
- [22] G. Shi, Y. Jing, A. Xu, and J. Ma, "Study and Simulation of Based-fuzzy-logic Parallel Hybrid Electric Vehicles Control Strategy," in *Sixth International Conference on Intelligent Systems Design and Applications, ISDA 2006, vol. 1*, pp. 280 –284.
- [23] S. Wahsh, H. G. Hamed, M. N. F. Nashed, and T. Dakrory, "Fuzzy logic based Control strategy for parallel Hybrid Electric Vehicle," in *Power Systems Conference, MEPCON 2006. Eleventh International Middle East, 2006, vol. 1*, pp. 30 –34.
- [24] X. Liu, Y. Wu, and J. Duan, "Power split control strategy for a series Hybrid Electric Vehicle using fuzzy logic," in *IEEE International Conference on Automation and Logistics, ICAL 2008*, pp. 481 –486.
- [25] E. T. Stephen and S. P. Boyd, "Finding Ultimate Limits of Performance for Hybrid Electric Vehicles," *SAE Paper*, 2000.
- [26] S. Delprat, J. Lauber, T. M. Guerra, and J. Rimaux, "Control of a parallel hybrid powertrain: optimal control," *IEEE Transactions on Vehicular Technology*, vol. 53, no. 3, pp. 872 – 881, May 2004.
- [27] A. Sciarretta, M. Back, and L. Guzzella, "Optimal control of parallel hybrid electric vehicles," *IEEE Transactions on Control Systems Technology*, vol. 12, no. 3, pp. 352 – 363, May 2004.
- [28] M. Koot, J. T. B. A. Kessels, B. de Jager, W. P. M. H. Heemels, P. P. J. van den Bosch, and M. Steinbuch, "Energy management strategies for vehicular electric power systems," *IEEE Transactions on Vehicular Technology*, vol. 54, no. 3, pp. 771 – 782, May 2005.
- [29] B. Wu, C. Lin, Z. Filipi, and H. Peng, "Optimal power management for a hydraulic hybrid delivery truck," *Vehicle System Dynamics*, pp. 1–2, 2004.
- [30] V. H. Johnson, K. B. Wipke, and D. J. Rausen, "HEV Control Strategy for Real-Time Optimization of Fuel Economy and Emissions," *SAE International, Warrendale, PA, 2000-01-1543*, Apr. 2000.

- [31] J. S. Chen and M. Salman, "Learning energy management strategy for hybrid electric vehicles," in *Vehicle Power and Propulsion, IEEE Conference*, 2005, pp. 68 – 73.
- [32] J. S. Won, R. Langari, and M. Ehsani, "An energy management and charge sustaining strategy for a parallel hybrid vehicle with CVT," *IEEE Transactions on Control Systems Technology*, vol. 13, no. 2, pp. 313 – 320, Mar. 2005.
- [33] I. Kolmanovsky, I. Siverguina, and B. Lygoe, "Optimization of powertrain operating policy for feasibility assessment and calibration: stochastic dynamic programming approach," in *Proceedings of the 2005 American Control Conference*, vol. 2, pp. 1425 – 1430.
- [34] C. C. Lin, H. Peng, and J. W. Grizzle, "A stochastic control strategy for hybrid electric vehicles," in *Proceedings of the 2004 American Control Conference*, vol. 5, pp. 4710 – 4715.
- [35] E. D. Tate, J. W. Grizzle, and H. Peng, "Shortest path stochastic control for hybrid electric vehicles," *International Journal of Robust and Nonlinear Control*, vol. 18, no. 14, pp. 1409–1429, Sep. 2008.
- [36] C. Musardo, G. Rizzoni, and B. Staccia, "A-ECMS: An Adaptive Algorithm for Hybrid Electric Vehicle Energy Management," in *44th IEEE Conference on Decision and Control, and 2005 European Control Conference*, pp. 1816 – 1823.
- [37] P. Pisu and G. Rizzoni, "A Comparative Study Of Supervisory Control Strategies for Hybrid Electric Vehicles," *IEEE Transactions on Control Systems Technology*, vol. 15, no. 3, pp. 506 – 518, May 2007.
- [38] C. C. Lin, Z. Filipi, L. Louca, H. Peng, D. Assanis, and J. Stein, "Modeling and control of a medium-duty hybrid electric truck," *International Journal of Heavy Vehicle Systems*, vol. 11, no. 3/4, p. 349, 2004.
- [39] B. Wu, C. Lin, Z. Filipi, H. Peng, and D. Assanis, "Optimization of Power Management Strategies for a Hydraulic Hybrid Medium Truck," *Proceedings of the 2002 Advanced Vehicle Control Conference, Hiroshima, Japan, Sep. 2002*.
- [40] B. Bates, "Getting a Ford HEV on the road," *IEEE Spectrum*, vol. 32, no. 7, pp. 22 – 25, Jul. 1995.

- [41] T. Markel, A. Brooker, T. Hendricks, V. Johnson, K. Kelly, B. Kramer, M. O'Keefe, S. Sprik, and K. Wipke, "ADVISOR: a systems analysis tool for advanced vehicle modeling," *Journal of Power Sources*, vol. 110, no. 2, pp. 255–266, Aug. 2002.
- [42] J. R. Bumby, P. H. Clarke, and I. Forster, "Computer modeling of the automotive energy requirements for internal combustion engine and battery electric-powered vehicles," *Physical Science, Measurement and Instrumentation, Management and Education, IEE Proceedings A*, vol. 132, no. 5, pp. 265–279, Sep. 1985.
- [43] K. B. Wipke, M. R. Cuddy, and S. D. Burch, "ADVISOR 2.1: a user-friendly advanced powertrain simulation using a combined backward/forward approach," *IEEE Transactions on Vehicular Technology*, vol. 48, no. 6, pp. 1751–1761, Nov. 1999.
- [44] K. B. Wipke and M. R. Cuddy, "Using an advanced vehicle simulator (ADVISOR) to guide hybrid vehicle propulsion system development," presented at the NESEA sustainable transportation and S/EV symposium, New York City, United States, 1996.
- [45] N. Kim and A. P. Rousseau, "Comparison between Rule-Based and Instantaneous Optimization for a Single-Mode, Power-Split HEV," *SAE International*, Warrendale, PA, 2011-01-0873, Apr. 2011.
- [46] J. Zeman, I. Papadimitriou, K. Watanabe, M. Kubo, and T. Kumagai, "Modeling and Optimization of Plug-In Hybrid Electric Vehicle Fuel Economy," *SAE International*, Warrendale, PA, SAE Technical Paper 2012-01-1018, Apr. 2012.
- [47] K. L. Butler, M. Ehsani, and P. Kamath, "A Matlab-based modeling and simulation package for electric and hybrid electric vehicle design," *IEEE Transactions on Vehicular Technology*, vol. 48, no. 6, pp. 1770–1778, Nov. 1999.
- [48] F. U. Syed, M. L. Kuang, J. Czubay, and H. Ying, "Derivation and Experimental Validation of a Power-Split Hybrid Electric Vehicle Model," *IEEE Transactions on Vehicular Technology*, vol. 55, no. 6, pp. 1731–1747, Nov. 2006.
- [49] C. C. Lin, Z. Filipi, Y. Wang, L. Louca, H. Peng, D. Assanis, and J. Stein, "Integrated, Feed-Forward Hybrid Electric Vehicle Simulation in SIMULINK and its Use for Power Management Studies," *SAE International*, Warrendale, PA, 2001-01-1334, Mar. 2001.

- [50] M. Ehsani, K. M. Rahman, and H. A. Toliyat, "Propulsion system design of electric and hybrid vehicles," *IEEE Transactions on Industrial Electronics*, vol. 44, no. 1, pp. 19 – 27, Feb. 1997.
- [51] Z. Rahman, K. L. Butler, and M. Ehsani, "Designing parallel hybrid electric vehicles using V-ELPH 2.01," presented at the *Proceedings of the American Control Conference*, 1999, vol. 4, pp. 2693 –2697.
- [52] A. Singer-Englar, R. Kamisky, P. Erickson, A. Frank, W. Allan, C. Bangar, C. Carde, A. Dalal, D. Garas, J. Holdener, N. Meyr, and C. Nitta, "Design and Development of a Parallel Hybrid Powertrain for a High Performance Sport Utility Vehicle," *SAE International*, Warrendale, PA, 2005-01-3827, Oct. 2005.
- [53] W. Liu, *Introduction to Hybrid Vehicle System Modeling and Control*. John Wiley & Sons, 2013.
- [54] J. M. Miller, *Propulsion Systems for Hybrid Vehicles, 2nd Edition*, Barnes & Noble, 2010. .
- [55] C. Mi, M. A. Masrur, and D. W. Gao, *Hybrid Electric Vehicles: Principles and Applications with Practical Perspectives*. John Wiley & Sons, 2011.
- [56] L. Guzzella and A. Sciarretta, *Vehicle Propulsion Systems: Introduction to Modeling and Optimization, Second Edition*. Springer, 2010.
- [57] D. Prokhorov, *Computational Intelligence in Automotive Applications*. Springer Berlin Heidelberg, 2008.
- [58] X. Wei, "Modeling and control of a hybrid electric drivetrain for optimum fuel economy, performance and driveability," PhD dissertation, The Ohio State University, 2004.
- [59] K. Koprubasi, "Modeling and Control of a Hybrid-Electric Vehicle for Drivability and Fuel Economy Improvements," PhD dissertation, The Ohio State University, 2008.
- [60] L. Serrao, "A comparative analysis of energy management strategies for hybrid electric vehicles," PhD dissertation, The Ohio State University, 2009.

- [61] M. Asfoor, A. M. Sharaf, and S. Beyerlein, "Use of GT-Suite to Study Performance Differences between Internal Combustion Engine (ICE) and Hybrid Electric Vehicle (HEV) Powertrains," presented at the AMME-16, Military Technical College, Cairo, Egypt, 2014.
- [62] A. R. Ogilvie, "GT Suite simulation of a power split hybrid electric vehicle," MS thesis, University of Alabama, 2011.
- [63] D. Rinker, "Use of a TK Solver Performance Model in the Design and Testing of a Formula Hybrid Racecar," MS thesis, University of Idaho, 2013.
- [64] R. T. Storms, "Fuel injection and intake/exhaust sizing of a YZ250F engine for a formula hybrid vehicle," MS thesis, University of Idaho, 2009.
- [65] B. P. Butsick, "Design and mathematical modeling of a hybrid FSAE drivetrain," MS thesis, University of Idaho, 2011.
- [66] B. Bashford, "Electric propulsion subsystem for a parallel-drive formula hybrid vehicle," MS thesis, University of Idaho, 2012.
- [67] D. Cordon, S. Wos, S. Beyerlein, and E. Odom, "Highly Integrated Parallel Hybrid Powertrain," SAE International, Warrendale, PA, SAE Technical Paper 2012-32-0026, Oct. 2012.
- [68] S. H. Wos, "Hybrid vehicle mathematical modeling & drive cycle simulation," MS thesis, University of Idaho, 2013.
- [69] "Formula-Hybrid-2014-Rules." SAE International.
- [70] J. Cuddihy, "A User-Friendly, Two-Zone Heat Release Model for Predicting Spark-Ignition Engine Performance and Emissions," MS thesis, University of Idaho, 2014.
- [71] "GT-Suite General and Advanced Simulation Application Manual." Gamma Technologies.

## **Appendix A: Vehicle Specifications**



Dimensions	Front	Rear
Overall Length, Width, Height	102inches x 60 inches x 44 inches	
Wheelbase	61 inches	
Track	60.5 inches	60 inches
Weight (empty)	165 lbs.	385 lbs.
Weight with 150lb driver	240 lbs.	460 lbs.

**Ergonomics**

Driver Size Adjustments	Foam Seat Inserts, Adjustable Peal Assembly
Seat (materials, padding)	Aluminum w/ Insert Padding
Driver Visibility (angle of side view, mirrors?)	200 degrees
Instrumentation	Electronic Button Shifting

**Drivetrain**

Type	Parallel Post-Transmission
Architecture	Coupled at the output-shaft of the Drivetrain

**I.C. Engine**

Manufacture / Model	Yamaha YZ250F
No. of Cylinders	1
Bore	77 mm
Stroke	53.6 mm
Displacement	249 cc
Muffler	FMF Q4
Max. rated Hp @ RPM	42 hp @ 11,500 RPM
Max. rated torque @ RPM	21.5 ft.-lbs.@ 8,500 RPM
Throttle	Bosch 32mm Electronic Throttle Body

**Accumulator / Batteries**

Type	Ultra-Power Lithium Ion Polymer Cell
Manufacturer	Haiyin Technology Co. Ltd
Model No.	P68100120F
Capacity (Nameplate Rating)	6 Ah
Nominal Voltage	3.7V
Quantity	29
Total battery voltage	110V
Total capacity (Wh)	720 Wh
Protection / Fuses	Little Fuse FLNR 125V
Protection / Relays	Kilovac EV200

**Drive Motor(s)**

Manufacturer	Lynch
Type	DC/PM motor
Model Number	LEM 200 - D135RAGS
Hp (max) @ RPM	48.3 hp @ 2300 rpm
Torque (max) @ RPM	31 ft. lbs. @ 2400 rpm
Maximum voltage	110V (rated)
Maximum current	400A

<b>Motor Controller</b>		
Manufacturer	Kelly Controller	
Model Number	KDH12601E	
Maximum voltage in	18V	
Maximum voltage out	136	
Maximum current in	600 A	
Maximum current out	600 A	
Suspension Parameters	Front	Rear
Suspension Type	Unequal Length Double Wishbone Suspension	Trailing Arm Suspension
Tire Size and Compound Type	20.5x6x13 R23B	20.5x6x13 R23B
Wheels	Keizer Aluminum Wheels w/ Custom Centers	Keizer Aluminum Wheels w/ Custom Centers
Design ride height (chassis to ground)	4.25 inches	4.35 inches
Center of Gravity Design Height	10 inches	
Suspension design travel	2.25 inches	2.25 inches
Static Toe and adjustment method	Turnbuckle	Turnbuckle
Static camber and adjustment method	Turnbuckle Adjustable A-arms	Turnbuckle Adjustable A-arms
Front Caster and adjustment method	Adjustable A-arms	
Static Ackermann and adjustment method	N/A	
Anti-dive / Anti Squat	N/A	N/A
Roll center position static	0"X by 0" Y by 1.2" Z	0"X by 0" Y by 1.4" Z
Steer location, Gear ratio, Steer Arm Length	Lower Rear / 8.2:1	
Mechanical Brake System / Hub & Axle	Front	Rear
Brake Rotors	8 inch A2 Floating Rotors	8 inch A2 Rotor
Master Cylinder	Repackaged Willwod Compact Master Cylinders with Remote Reservoirs	
Calipers	Wilwood Kart Calipers	Wilwood Kart Calipers
Hub Bearings	Timken Wheel Bearings	Timken Wheel Bearings
Upright Assembly	14 Gauge Box Steel	14 Gauge Box Steel
Axle type, size, and material	N/A	3/4 in Dia./ 4130 Chromalloy w/ Taylor Racing Tripod

**Frame**

Frame Construction	Tubular Space Frame
Material	4130 Chromoly Steel
Joining method and material	Professionally TIG Welded
Bare frame weight with brackets and paint	90 lbs.
Crush zone material	5052 extruded Aluminum Honeycomb
Crush zone length	9.5"
Crush zone energy capacity	1.6 MJ

## **Appendix B: Supervisory Controller Code**

```

/* ===== EnergyMan.c =====
 * Created: 19 December 2013
 * Last Mod: 12 April 2014
 * Data Acquisition added 26 June 2014
 */

/* Included files for system */
#include <plib.h>

/* Included files for platform */
#include "config_bits.h"
#include "MAX32.h"
#include "sw_timer.h"
#include "Compiler.h"
#include "HardwareProfile.h"

/* Included files for application */
#include "EnergyMan.h"
#include "DataDefs.h"
#include "FSIO.h"

/////////////////////////////////////////////////////////////////
// Globals to record necessary variables:
// RPM - Rotations Per Minute
// GEAR - Current gear of the tranny
// TPS - Throttle Position Sensor
// SPD - Vehicle speed
// SOC - State Of Charge of the battery
// left_WSS - Left Wheel Speed Sensor
// right_WSS - Right Wheel Speed Sensor
// x,y,zAccel- Data from the accelerometer
// state - State of the engine (combustion, electric, hybrid, idle)

// The following buttons must be powered, pullup pins disabled for CN in code
// brake - State of the brake (applied/not applied)
// - C doesn't do bool, so this will only be 1 or 0
// record - Button to start/stop recording (bool, 1 or 0)
// Replaced by DATA_BTN
// new_file - Button for USB thingy (bool, 1 or 0)
// No longer needed
/////////////////////////////////////////////////////////////////
unsigned short int RPM = 0, GEAR = 1;
unsigned int TPSA = TPS_INIT, TPS1 = TPS_INIT, TPS2 = TPS_INIT;
unsigned int SPD = 0, SOC = 300, offset, WSSL = 0, WSSR = 0;
unsigned int xAccel, yAccel, zAccel;
short int state = IDL, brake = NOT_PRESSED, record = NOT_PRESSED, new_file =
NOT_PRESSED;
short int EMS_Status = 0, TSPU_Status = 0;

unsigned short int GetDataFlag = 0;

//PWM interrupt capture values
unsigned short int TPS_width = 0, TPS_period = 0,
WSS_width = 0, WSS_period = 0,
SOC_width = 0, SOC_period = 0;

int main(void) {

    FSFILE *pData;
    FSFILE *pTest;
    FSFILE *pError;

    char temp[10];
    char cData[33];
    char FileName[] = "DatSet00.txt";
    char ErrorFile[] = "Errors.txt";

```

```

char ErrorMessage[] = "File already exists: ";
char writeArg = 'w';
char readArg = 'r';
char appendArg = 'a';
char NewLine = '\n';
char cChar;
char HorizontalTab = 9;

int bytesWritten;
unsigned int length = 0;
int Normalizer = 0;
unsigned short int TimerON = 0;
unsigned short int Button = 0;
unsigned short int count = 0;
unsigned short int WriteData = 0;
unsigned int nDataSets = 0;
int i = 0, y = 0, c = 0, c0 = 0, c10 = 0;

system_initialize(); /* Hardware setup */

INTEnableSystemMultiVectoredInt();

// Must initialize the FAT16/FAT32 library. It also initializes SPI and other
related pins.
while( !FSInit() )
{
    // Failed to initialize FAT16/FAT32 signal the users

    PORTSetBits(IOPORT_A, BIT_3);
    DelayMs(5);
    PORTClearBits(IOPORT_A, BIT_3);
    DelayMs(5);
    PORTSetBits(IOPORT_A, BIT_3);
    DelayMs(20);
    PORTClearBits(IOPORT_A, BIT_3);
}

//Loop to check and keep track of button push events for dataAq.
while( count < 3 )
{
    Button = PORTReadBits( IOPORT_F, BIT_3 );

    if( Button != 0 )
    {
        PORTClearBits(IOPORT_F, BIT_3);
        DelayMs( 5 );
        Button = PORTReadBits( IOPORT_F, BIT_3 );
    }

    if( Button == 0 )
    {
        PORTClearBits(IOPORT_F, BIT_3);
    }
    if( Button != 0 && TimerON == 0 && count == 0 )
    {
        TimerON = 1;
        OpenTimer4( T4_ON | T4_SOURCE_INT | T4_PS_1_256 , Period );
        ConfigIntTimer4( T4_INT_ON | T4_INT_PRIOR_3 );
        PORTClearBits(IOPORT_F, BIT_3);
        Button = 0;
        count++;
        DelayMs( 5 );
    }
    if( Button != 0 && TimerON == 1 && count == 1 )
    {

```

```

    TimerON = 0;
    CloseTimer4();
    PORTClearBits(IOPORT_F, BIT_3);
    GetDataFlag = 0;
    Button = 0;
    count++;
}
if( Button != 0 && count == 2 )
{
    WriteData = 1;
    count++;
    GetDataFlag = 0;
}

//Check flag for DataAq, if flag is set store data in 2D array.
if( GetDataFlag != 0 )
{
    if( nDataSets < DataSets )
    {
        Data[nDataSets][0] = ReadCoreTimer();

        Data[nDataSets][1] = RPM;

        Data[nDataSets][2] = GEAR;

        Data[nDataSets][3] = TPS1;

        Data[nDataSets][4] = TPS2;

        Data[nDataSets][5] = TPSA;

        Data[nDataSets][6] = SPD;

        Data[nDataSets][7] = SOC;

        Data[nDataSets][8] = WSSL;

        Data[nDataSets][9] = WSSR;

        Data[nDataSets][10] = xAccel;

        Data[nDataSets][11] = yAccel;

        Data[nDataSets][12] = zAccel;

        Data[nDataSets][13] = state;

        Data[nDataSets][14] = brake;

        Data[nDataSets][15] = EMS_Status;

        Data[nDataSets][16] = TSPU_Status;

        nDataSets++;

        GetDataFlag --;
    }
    else
    {
        TimerON = 0;
        CloseTimer4();
        PORTClearBits(IOPORT_F, BIT_3);
        GetDataFlag = 0;
        Button = 0;
    }
}

```

```

        count++;
    }

}

}

//WriteData flag has been set so write data to SD card.
while( WriteData == 1 )
{
    //Test file -- if it exists increment the number and try again.

    pTest = FSfopen( FileName, &readArg );

    while( pTest != NULL )
    {
        pError = FSfopen( ErrorFile, &appendArg );

        length = strlen( ErrorMessage );

        bytesWritten = FSfwrite ( (void *) ErrorMessage, length, 1, pError );

        length = strlen( FileName );

        bytesWritten = FSfwrite ( (void *) FileName, length, 1, pError );

        bytesWritten = FSfwrite ( (void *) &NewLine, 1, 1, pError );

        FSfclose( pError );

        FSfclose( pTest );

        c++;

        if( c < 10)
        {
            c0 = c;

            cChar = '0' + c0;

            FileName[7] = cChar;
        }
        else if( c < 100 )
        {
            c0 = c % 10;

            c10 = c / 10;

            cChar = '0' + c0;

            FileName[7] = cChar;

            cChar = '0' + c10;

            FileName[6] = cChar;
        }

        pTest = FSfopen( FileName, &readArg );
    }

    // Create new file.
    pData = FSfopen( FileName, &writeArg );

    // Write data to file.

```

```

for( i = 0; i < DataCat; i++ )
{
    switch( i )
    {
        case 0:
            strcpy( temp, DataLabel00 );
            break;
        case 1:
            strcpy( temp, DataLabel01 );
            break;
        case 2:
            strcpy( temp, DataLabel02 );
            break;
        case 3:
            strcpy( temp, DataLabel03 );
            break;
        case 4:
            strcpy( temp, DataLabel04 );
            break;
        case 5:
            strcpy( temp, DataLabel05 );
            break;
        case 6:
            strcpy( temp, DataLabel06 );
            break;
        case 7:
            strcpy( temp, DataLabel07 );
            break;
        case 8:
            strcpy( temp, DataLabel08 );
            break;
        case 9:
            strcpy( temp, DataLabel09 );
            break;
        case 10:
            strcpy( temp, DataLabel10 );
            break;
        case 11:
            strcpy( temp, DataLabel11 );
            break;
        case 12:
            strcpy( temp, DataLabel12 );
            break;
        case 13:
            strcpy( temp, DataLabel13 );
            break;
        case 14:
            strcpy( temp, DataLabel14 );
            break;
        case 15:
            strcpy( temp, DataLabel15 );
            break;
        case 16:
            strcpy( temp, DataLabel16 );
            break;
        default:
            strcpy( temp, DataLabel99 );
            break;
    }

    length = strlen( temp );

    bytesWritten = FSfwrite ( (void *) temp, length, 1, pData );

    bytesWritten = FSfwrite ( (void *) &HorizontalTab, 1, 1, pData );

```



```

    }

    bytesWritten = FSfwrite ( (void *) &NewLine, 1, 1, pData );
    Normalizer = Data[0][0];

    for( i = 0; i < nDataSets; i++ )
    {
        for( y = 0; y < DataCat; y++ )
        {
            Data[i][0] = ( (Data[i][0] - Normalizer) / 2052 );

            itoa( cData, Data[i][y], 10 );

            length = strlen( cData );

            bytesWritten = FSfwrite ( (void *) cData, length, 1, pData );

            bytesWritten = FSfwrite ( (void *) &HorizontalTab, 1, 1, pData );

        }

        bytesWritten = FSfwrite ( (void *) &NewLine, 1, 1, pData );

    }

    // After writing, close the file.
    FSfclose( pData );

    //Signal that data writing is done.
    while( MDD_SDSPI_MediaDetect() != 0 )
    {
        PORTSetBits(IOPORT_A, BIT_3);
        DelayMs(20);
        PORTClearBits(IOPORT_A, BIT_3);
        DelayMs(20);
        PORTSetBits(IOPORT_A, BIT_3);
        DelayMs(20);
        PORTClearBits(IOPORT_A, BIT_3);
        DelayMs(20);
        PORTSetBits(IOPORT_A, BIT_3);
        DelayMs(20);
        PORTClearBits(IOPORT_A, BIT_3);
        DelayMs(20);
    }

}

} /* End of main */

void system_initialize(void) {
    /* Configure CHIPKIT board */
    MAX32_setup();

    //Configure Pins for ANALOG output
    mPORTBSetPinsAnalogIn(BIT_0);
    mPORTBSetPinsAnalogIn(BIT_1);
    mPORTBSetPinsAnalogIn(BIT_2);
    mPORTBSetPinsAnalogIn(BIT_3);

    mPORTCSetPinsDigitalIn(TSPU_PWR);
    mPORTDSetPinsDigitalOut(SPEAKER);
    mPORTDClearBits(SPEAKER);

```

```

mPORTGSetPinsDigitalOut( DATA_LED );
mPORTFSetPinsDigitalIn( DATA_BTN );
mPORTFClearBits( DATA_BTN );

// ----- configure and enable the ADC -----//

// ensure the ADC is off before setting the configuration
CloseADC10();

// define setup parameters for OpenADC10
//          Turn module on | ouput in integer | trigger mode auto | enable
autosample
#define PARAM1  ADC_MODULE_ON | ADC_FORMAT_INTG | ADC_CLK_AUTO | ADC_AUTO_SAMPLING_ON

// ADC ref external      | disable offset test      | enable scan mode | perform 4
samples | use dual buffers | use only mux A
#define PARAM2  ADC_VREF_AVDD_AVSS | ADC_OFFSET_CAL_DISABLE | ADC_SCAN_ON |
ADC_SAMPLES_PER_INT_4 | ADC_ALT_BUF_ON | ADC_ALT_INPUT_OFF

//          use ADC internal clock | set sample time
#define PARAM3  ADC_CONV_CLK_INTERNAL_RC | ADC_SAMPLE_TIME_15

// set inputs to analog
#define PARAM4  ENABLE_AN0_ANA | ENABLE_AN3_ANA | ENABLE_AN4_ANA

// only scan An0 to An3
#define PARAM5  SKIP_SCAN_AN1 | SKIP_SCAN_AN2 | SKIP_SCAN_AN5 |SKIP_SCAN_AN6
|SKIP_SCAN_AN7 | \
                SKIP_SCAN_AN8 |SKIP_SCAN_AN9 |SKIP_SCAN_AN10 |SKIP_SCAN_AN11 | \
                SKIP_SCAN_AN12 |SKIP_SCAN_AN13 |SKIP_SCAN_AN14 |SKIP_SCAN_AN15

// set negative reference to Vref for Mux A
SetChanADC10(ADC_CHO_NEG_SAMPLEA_NVREF);

// open the ADC
OpenADC10(PARAM1, PARAM2, PARAM3, PARAM4, PARAM5);

// -- configure the ADC interrupt, priority level 2 --
// NOTE: the C32 compiler manual uses ADC_INT_ENABLE for the enable flag
// this is wrong, use ADC_INT_ON / ADC_INT_OFF
ConfigIntADC10(ADC_INT_PRI_2 | ADC_INT_SUB_PRI_1 | ADC_INT_ON);

// clear the interrupt flag
mAD1ClearIntFlag();

// Enable the ADC
EnableADC10();

/* Configure Timers for PWM using internal clock, 1:1 prescale */
OpenTimer1(T1_ON | T1_SOURCE_INT | T2_PS_1_32, 20000); //
OpenTimer2(T2_ON | T2_SOURCE_INT | T2_PS_1_1, 1000);
OpenTimer3(T3_ON | T3_SOURCE_INT | T3_PS_1_4, 0xFFFFFFFF); //Input capture

/*configure timer interupts for output changes and state machine*/
mT1SetIntPriority(2);
mT1SetIntSubPriority(1);
mT1IntEnable(1);

/*Open the output compare (PWM) funtions*/
OpenOC1(OC_ON | OC_TIMER_MODE16 | OC_TIMER2_SRC | OC_PWM_FAULT_PIN_DISABLE, 0,
1000);
OpenOC2(OC_ON | OC_TIMER_MODE16 | OC_TIMER2_SRC | OC_PWM_FAULT_PIN_DISABLE, 0,
1000);
OpenOC3(OC_ON | OC_TIMER_MODE16 | OC_TIMER2_SRC | OC_PWM_FAULT_PIN_DISABLE, 0,
1000);

```

```

/*Input Capture Setup for Frequency calc of Left Wheel speed*/
mIC3ClearIntFlag();
OpenCapture3(IC_ON | IC_IDLE_STOP | IC_FEDGE_RISE | IC_TIMER3_SRC | IC_INT_1CAPTURE
| IC_EVERY_RISE_EDGE);
ConfigIntCapture3(IC_INT_ON | IC_INT_PRIOR_3 | IC_INT_SUB_PRIOR_0);

/*Input Capture Setup for Frequency calc of Right Wheel speed*/
mIC5ClearIntFlag();
OpenCapture5(IC_ON | IC_IDLE_STOP | IC_FEDGE_RISE | IC_TIMER3_SRC | IC_INT_1CAPTURE
| IC_EVERY_RISE_EDGE);
ConfigIntCapture5(IC_INT_ON | IC_INT_PRIOR_3 | IC_INT_SUB_PRIOR_0);

// CloseCapture3();
// OpenCapture3(IC_INT_1CAPTURE | IC_TIMER2_SRC | IC_FEDGE_RISE | IC_ON |
IC_EVERY_RISE_EDGE);
// ConfigIntCapture3(IC_INT_ON | IC_INT_PRIOR_1 | IC_INT_SUB_PRIOR_1);
// mIC3ClearIntFlag();
// EnableIntIC3;

//Change notice ISR for brake, record, and new file signals
mCNOpen(CN_ON, CN14_ENABLE | CN15_ENABLE | CN16_ENABLE, CN_PULLUP_DISABLE_ALL);
mCNSetIntPriority(1);
mCNIntEnable(1);
mCNClearIntFlag();

} /*End of system_initialize */

void __ISR(_INPUT_CAPTURE_3_VECTOR, IPL3) LeftWheelSpeed(void) {

static unsigned short int curr_time = 0, prev_time = 0, period = 0;
static float per_ave = 0;
static unsigned int time_buf[32];

ReadCapture3(time_buf);
curr_time = time_buf[0];

period = curr_time - prev_time;
per_ave = (99 * per_ave + (float) period) / 100;
if (per_ave > 0) {
WSSL = SPD_MUL / ((float) per_ave); //T2_ticks/(32*per_ave) rev/sec* 3600 s/hr *
20pi in/rev /12/5280
}
prev_time = curr_time;
mIC3ClearIntFlag();
}

void __ISR(_INPUT_CAPTURE_5_VECTOR, IPL3) RightWheelSpeed(void) {

static unsigned short int curr_time = 0, prev_time = 0, period = 0;
static float per_ave = 0;
static unsigned int time_buf[32];

ReadCapture5(time_buf);
curr_time = time_buf[0];

period = curr_time - prev_time;
per_ave = (99 * per_ave + (float) period) / 100;
if (per_ave > 0) {
WSSR = SPD_MUL / ((float) per_ave); //T2_ticks/(32*per_ave) rev/sec* 3600 s/hr *
20pi in/rev /12/5280
}
}

```

```

    }
    prev_time = curr_time;
    mIC5ClearIntFlag();
}

void __ISR( _TIMER_4_VECTOR, ipl3 ) _Timer1Handler( void )
{
    mPORTASetBits( LED4 );
    DelayMs(5);
    mPORTAClearBits( LED4 );

    GetDataFlag = 1;

    mT1ClearIntFlag();
}

void __ISR( _TIMER_1_VECTOR, ipl2 ) MachineHandler(void) {

    static unsigned short int speaker_pwr = 0, check = 0;
    state_machine();
    output();

    if (check == 0) {
        TSPU_Status = mPORTCReadBits(TSPU_PWR);
        if (TSPU_Status != 0) speaker_pwr = 1;
    }
    if (speaker_pwr != 0) {

        mPORTDSetBits(SPEAKER);
        DelayMs(5);
        mPORTDClearBits(SPEAKER);
        DelayMs(5);
        mPORTDSetBits(SPEAKER);
        DelayMs(5);
        mPORTDClearBits(SPEAKER);
        DelayMs(5);
        speaker_pwr = 0;
        check = 1;
    }

    TSPU_Status = mPORTCReadBits(TSPU_PWR);
    if (TSPU_Status == 0) check = 0;

    mT1ClearIntFlag();
}

void __ISR( _ADC_VECTOR, ipl2 ) AdcHandler(void) {

    // determine which buffer is idle and create an offset
    offset = 8 * ((~ReadActiveBufferADC10() &0x01));
    // read the result of each channel conversion from the idle buffe
    TPS1 = ((99 * TPS1)+(3 * ReadADC10(offset + 2))) / 100;
    TPS2 = ((99 * TPS2)+(2930 - 3 * ReadADC10(offset + 1))) / 100;
    //TPS1 = ((99 * TPS1)+(150+ 275/100 * ReadADC10(offset + 2))) / 100;
    //TPS2 = ((99 * TPS2)+(2080 - 275/100 * ReadADC10(offset + 1))) / 100;
    //TPS1 = (99*TPS1+ReadADC10(offset + 2))/100;
    //TPS2 = (99*TPS2+ReadADC10(offset + 1))/100;

    //SOC = ReadADC10(offset);
    TPSA = (TPS1 + TPS2) / 2;
    mAD1ClearIntFlag();
}

void __ISR( _CHANGE_NOTICE_VECTOR, ipl1 ) brakes(void) {
    brake = PORTD & BRAKE;
}

```

```

    mCNClearIntFlag();
}

void output(void) {
    //toggle LED

    EMS_Status = mPORTEReadBits(EMS_PWR);

    if (EMS_Status == 0) {
        SetDCOC1PWM(TPS1);
        SetDCOC2PWM(TPS2);
        SetDCOC3PWM(TPSA);
    } else if (state == HEV) {
        SetDCOC1PWM(TPS1);
        SetDCOC2PWM(TPS2);
        // if (brake == 1) {
            SetDCOC3PWM(TPSA);
        //} else {
            //SetDCOC3PWM(0);
        //}
    } else if (state == ICE) {
        SetDCOC1PWM(TPS1);
        SetDCOC2PWM(TPS2);
        SetDCOC3PWM(0);
    } else if (state == ELE) {
        SetDCOC1PWM(0);
        SetDCOC2PWM(0);
        //if (brake == 1) {
            SetDCOC3PWM(TPSA);
        // } else {
            // SetDCOC3PWM(0);
        // }
    } else if (state == IDL) {
        SetDCOC1PWM(TP_IDL);
        SetDCOC2PWM(TP_IDL);
        // SetDCOC3PWM(0);
    } else {
        SetDCOC1PWM(0);
        SetDCOC2PWM(0);
        SetDCOC3PWM(0);
    }
}

void state_machine() {
    SPD = ((WSSL + WSSR) / 2);
    if (TPSA > TPS_MIN) {
        if (SOC > SOC_MIN) {
            if (SPD > SPD_CUTOFF || TPSA >= 300) {
                state = HEV;
            } else {
                state = ELE;
            }
        } else {
            state = ICE;
        }
    } else {
        state = IDL;
    }
}

/* End of EnergyMan.c */

```